



5-1999

The design and testing of a centrifugal controlled variable camshaft phasing device for small-block Chevrolet engines

John C. McCracken

Follow this and additional works at: https://trace.tennessee.edu/utk_gradthes

Recommended Citation

McCracken, John C., "The design and testing of a centrifugal controlled variable camshaft phasing device for small-block Chevrolet engines. " Master's Thesis, University of Tennessee, 1999.
https://trace.tennessee.edu/utk_gradthes/9905

This Thesis is brought to you for free and open access by the Graduate School at TRACE: Tennessee Research and Creative Exchange. It has been accepted for inclusion in Masters Theses by an authorized administrator of TRACE: Tennessee Research and Creative Exchange. For more information, please contact trace@utk.edu.

To the Graduate Council:

I am submitting herewith a thesis written by John C. McCracken entitled "The design and testing of a centrifugal controlled variable camshaft phasing device for small-block Chevrolet engines." I have examined the final electronic copy of this thesis for form and content and recommend that it be accepted in partial fulfillment of the requirements for the degree of Master of Science, with a major in Mechanical Engineering.

Frank H. Speckhart, Major Professor

We have read this thesis and recommend its acceptance:

Jeffery W. Hodgson, William R. Hamel

Accepted for the Council:

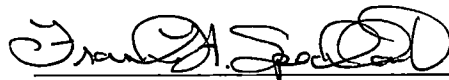
Carolyn R. Hodges

Vice Provost and Dean of the Graduate School

(Original signatures are on file with official student records.)

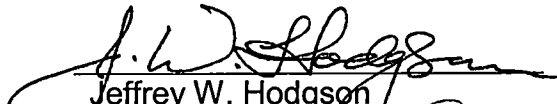
To the Graduate Council:

I am submitting herewith a thesis written by John C. McCracken entitled "The Design and Testing of a Centrifugal Controlled Variable Camshaft Phasing Device for Small-Block Chevrolet Engines." I have examined the final copy of this thesis for form and content and recommend that it be accepted in partial fulfillment of the requirements for the degree of Master of Science, with a major in Mechanical Engineering.

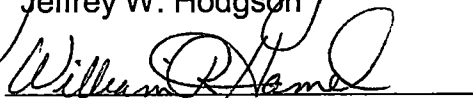


Frank H. Speckhart
Professor

We have read this thesis and
recommend its acceptance:

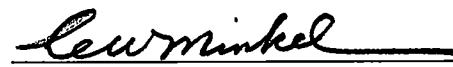


Jeffrey W. Hodgson



William R. Hamel

Accepted for the Council:



Associate Vice Chancellor and
Dean of The Graduate School

THE DESIGN AND TESTING
OF A
CENTRIFUGAL CONTROLLED VARIABLE CAMSHAFT PHASING DEVICE
FOR
SMALL-BLOCK CHEVROLET ENGINES

A Thesis Presented for the Master of Science Degree
The University of Tennessee, Knoxville

John C. McCracken
May, 1999

Tell me if anything is ever done.

- Leonardo DaVinci

ACKNOWLEDGEMENTS

I am grateful to many people in the Mechanical Engineering Department for making my six years (and two degrees) at the University of Tennessee so rewarding. I am particularly grateful to Dr. Frank Speckhart, my major professor, for his support, encouragement, and advice. Also to Dr. William Hamel and Dr. Jeff Hodgson, both of who served on my graduate committee. This project would not have been a success without the advice, suggestions, and top-notch work of Danny Gramm, Steve Hunley, and Gary Hatmaker, in the Mechanical Engineering machine shop. I also owe a debt of gratitude to some of my fellow graduate students who have been a sounding board for ideas, made themselves available when I needed help, and have been good friends. These include Craig Rutherford, Andrew Ridnour, and Jim McDonald. Most importantly, I thank my parents, Larry and Carolyn McCracken, who have been a constant source of love and support. Without them, I would never have reached this moment.

ABSTRACT

One method of improving performance and efficiency of internal combustion engines is to vary the timing of the valve opening and closure while leaving the lift and duration constant. This is called variable camshaft phasing and, generally, the camshaft should be advanced at low engine RPM and retarded as engine speed increases. The purpose of this project was to design and test a mechanically variable camshaft phasing device that retards the camshaft continuously over a given engine speed range as a function of engine speed.

It was desired to design a device that would fit on an unmodified engine block utilizing an unmodified camshaft that could fit under a slightly modified timing cover. A conceptual design was developed based on analysis of various geometries. Computer simulations were employed to search for the optimal kinematic configuration that would give the device a minimal torque dependency. Several different types of springs were then analyzed using both computer models and static testing that would allow the device to operate over the desired range of engine speeds.

A prototype variable cam phasing device was built and tested in a 1970's model Chevrolet small-block V8 driven by the Mechanical Engineering Department's engine dynamometer. The device exhibited unacceptable wear and fatigue characteristics in some areas of the device. However, the data that was gathered is encouraging and indicates that the prototype device represents a viable design.

TABLE OF CONTENTS

Chapter	Page
1. Introduction	1
Background	1
Problem Statement	3
Procedure of Study	4
2. Design Approach	6
Survey of Previous Work	6
Mathematical Modeling of the Mechanism	10
Spring Considerations and Analysis	14
Computer Simulation of the Mechanism	17
3. Final Design Concept	18
Selection of Design Concept	18
Optimum Geometry	19
Finalizing the Design Concept	22
4. Component Design	24
Stock Timing Gear	24
Cam Extension Design	25
Balancing Springs	26
Sprocket Design	30
Centrifugal Weight Design	32
Cam Button	35
5. Prototype Design	36
6. Device Testing and Results	40
Static Testing and Results	40
Dynamic Testing	46
Dynamic Testing Procedure	47
Dynamic Testing Results and Analysis	49
7. Conclusions and Recommendations	54
References	56
Appendices	58
Appendix A. Mathematical Models of the Device and Its Systems	59
Appendix B. Spring Analysis	69
Appendix C. Computer Programs	78
Appendix D. Machine Drawings	96
Vita	108

LIST OF TABLES

Table	Page
1. Categories of VVA Mechanisms	2
2. Maximum Design Stresses as a Percentage of Tensile Strength for Carbon Steel Cantilever Springs in Cyclical Applications	17
3. Bill of Materials for Centrifugal Weight Assembly	37
4. Bill of Materials for Prototype VCP Mechanism	38
5. Length and Position of Spring Leaves in the Spring Pack Used in Both Static and Dynamic Testing	42

LIST OF FIGURES

Figure	Page
1. Generalized Concept of Backdriving Torque	4
2. Design of Cam Retarding Mechanism by Dr. F.H. Speckhart	7
3. Cam Retarder Mechanism by Richard Moissan	8
4. Torque Dependency of a Cam Retarder Mechanism by Richard Moissan	8
5. Assembly Drawing of a Variable Cam Phasing Device by David Connor	9
6. Hysteresis of a Variable Cam Phasing Device by David Connor	9
7. Torque Dependency of a Variable Cam Phasing Device by David Connor	10
8. Generalized Representation of a Linear Centrifugal Weight	11
9. Generalized Representation of Pivoting Centrifugal Weight	12
10. Generalized Representation of Four-bar Linkage	13
11. Generalized Representation of a Slot and Pin Arrangement	13
12. Generalized Representation of Coil Spring Arrangement	14
13. Concept of Leaf Springs Arrangement	15
14. Tensile Strength versus Rockwell Hardness for Quenched and Tempered Spring Steel	16
15. Final Design Geometry	20

16. Camshaft Retard Angle vs. Centrifugal Weight Pivot Angle	21
17. Percentage of Torque Required to Drive the Valve Train that Backdrives the Mechanism vs. Centrifugal Weight Rotation Angle	21
18. Schematic of Final Design Concept	23
19. Chevrolet Small-Block Timing Sprocket, 1987 to Present	25
20. Isometric Drawing of the Cam Extension	26
21. Balancing Spring Geometry	27
22. Balancing Spring Dimensions	28
23. Theoretical Torque Dependency with and without Four Balancing Springs	28
24. Theoretical Torque Dependency with and without Eight Balancing Springs	29
25. Sprocket Interior	30
26. Sprocket Exterior	31
27. Alignment Angles of the Two Sprocket Components and the Cam Extension	32
28. Isometric Drawing of the Centrifugal Weight	33
29. Detail Drawing of Weight Cap	34
30. Detail Drawing of Cam Button	35
31. Exploded Assembly View of the Centrifugal Weight	37
32. Exploded Assembly View of the Prototype VCP Mechanism	38
33. Timing Cover Used in Prototype Testing	39

34. Static Testing Weight	41
35. Static Testing Fixture	41
36. Experimental Leaf Spring Torque Data and Curve Fit	43
37. Predicted Operation Curves for a System Using 8 Balancing Springs	43
38. Predicted Operation Curves for a System Using 6 Balancing Springs	44
39. Predicted Operation Curves for a System Using 4 Balancing Springs	44
40. Predicted Operation Curves for a System Using 2 Balancing Springs	45
41. Setup for Fatigue Testing Leaf Springs	46
42. Dynamic Testing, Engine of Test Stand	47
43. Dynamic Testing, Device and Modified Timing Cover Installed on Test Engine	48
44. Dynamic Testing, Close-up of Device and Modified Timing Cover Installed on Test Engine	48
45. Dynamic Results for a System with 8 Balancing Springs	50
46. Dynamic Results for a System with 6 Balancing Springs	50
47. Dynamic Results for a System with 4 Balancing Springs	51
48. Dynamic Results for a System with 2 Balancing Springs	51

CHAPTER ONE

INTRODUCTION

Background

In four-cycle internal combustion engines, either spark or diesel engines, precise timing of both the intake of fresh charge (or just fresh air, as diesels require) and the release of exhaust are required. These steps are accomplished through the opening and closing of valves. The most common type of valves in four-cycle engines, "poppet" valves, are opened and closed in a reciprocating motion and are almost exclusively actuated mechanically by a camshaft.

Engines that function at continuous speeds or that operate over a small range of speeds, such as industrial generators engines, can be optimized to run at much higher efficiencies than engines required to perform over wide speed and power bands. Automotive and other such applications that are required to operate over wide speed ranges are compelled to sacrifice efficiency because designers of these engines have been forced to seek a compromise among power output, fuel consumption, reliability, idle quality, and, since the 1970's, emission standards.

In recent years, some manufacturers have attempted to circumvent these compromises by employing variable valve actuation (VVA) and/or variable valve phasing (VVP) devices on engines [1]. In the latter method, fixed duration and lift are employed, but the phase angle relationship between crank position and cam position is varied. This can also be referred to as variable cam phasing (VCP) since the camshaft phase angle relationship with the crank is varied. In the former method, the lift and/or duration of the intake or exhaust valves is altered, and VVP may also be employed.

Such devices are categorized into one of fifteen general VVA types [2], which are given in table 1.

Table 1 – Categories of VVA Mechanisms	
Category	Description
1	Electrically actuated valves, usually solenoids. Allows complete freedom of lift, duration, and phasing.
2	Hydraulically actuated valves, hydraulic or pneumatic cylinders. Allows complete freedom of lift, duration, and phasing.
3	Valve actuated through variable characteristic hydraulic lifters. Varies lift and duration.
4	Axially varying cam profiles. Cam profile varies continuously along camshaft axis to vary both duration, lift, and phasing. Ferrari uses this type of system on their 3.4L V8.
5	Valves actuated via lost-motion mechanisms. Allows variation in lift and duration.
6	Valve actuated through a variable lever ratio linkage. Allows variation of lift.
7	Valves actuated by two independent cams in series. Output displacement is the sum of the effective displacements of the individual camshafts.
8	Valve actuating cam is varied through a variable-motion drive. Can produce any desired range of duration.
9	Valves actuated via two cams in parallel. Output displacement equals the larger effective displacement of either camshaft.
10	Valves actuated through a standard camshaft with variable advance. Allows phasing variation. This project falls into this category.
11	Valves actuated by multiple discrete cams, one at a time. Allows discrete variations in lift, duration, and phasing. The Honda VTEC system falls into this category.
12	Adjust the valve train tappets transversely relative to the camshaft. Allows variation in the phase angle.
13	Suppressed valve movement. Valves are actuated in the usual manner, but their motion can be suppressed at any time. Some 1981 Cadillacs used this type of system to make a variable displacement engine.
14	Two valves operate in series at each port.
15	Two valves operate in parallel at each port.

Adapted From: Dresner, T. and Barkan, P., "A Review and Classification of Variable Valve Timing Mechanisms," SAE Paper 890674, 1989

There has been demand in the after-market performance industry for a VVA device for implementation on preexisting engines. Because present VVA systems, like those mentioned above, have been exclusive to the manufacturer's engine line, such designs are not easily adjusted for retrofit onto other engine platforms. Systems designed for preexisting engines have met with little success and have all been mechanically actuated and controlled.

Problem Statement

This thesis problem is focused on the design, manufacture, and testing of a mechanically controlled and actuated VCP device that will operate predictably, safely, and durably. There are five requirements to be met in this study.

First, the mechanism will be used on a stock Chevrolet V8 engine. The timing cover can be modified, if necessary, provided that it fit under a stock water pump and harmonic balancer. Because of this space limitation, the mechanism will be limited to the interior and the close proximity of a standard timing sprocket.

Secondly, the phase change between the crank and camshaft will be limited to 4° . This phase lag will be measured at the cam with the cam retarded by this amount.

Third, the working speed of the device will be from 2000 to 3000 engine RPM; and, over this interval, the phase change should be continuous.

Fourth, the torque dependency of the mechanism will be reduced to a minimum. Torque dependency refers to the fact that the device will be "backdrivable" implying that the operation of the mechanism will be dependent, to some extent, on the torque required to drive the cam. This is because the cam is "pulled" by the centrifugal weights and a component of that force "backdrives" the centrifugal weights (see figure 1). This backdriving torque is proportional to the cosine of the angle β . Because the torque required to drive the camshaft will be different on different vehicles, reduction of the torque dependency will be a requirement of a robust design.

Thirdly, and concurrently to the first, the individual parts of the device and the mechanism as a whole was statically tested to verify its operation and illuminate areas where improvements could or should be made.

Lastly, the device was tested and evaluated in an actual engine. From this information, an assessment of the success of the project and a verification of the concept would be made.

CHAPTER TWO

DESIGN APPROACH

Survey of Previous Work

In the undertaking of any large, design project, an obvious starting point is in research of previous design work. As mentioned above, much time and money have been spent studying means of improving the efficiency of reciprocating engines and one area that has received significant attention is VVA. A literature search revealed several sources of information on VVA devices, but very little discussion on mechanical VCP mechanisms was discovered. Only a few references were found for mechanical VCP mechanisms and some of those warrant discussion here.

Dr. Frank Speckhart [3], on sabbatical from the University of Tennessee in 1977, designed and built a VCP system for small-block Chevrolet engines. John Lingenfelter successfully used it for racing that year. Figure 2 shows a schematic of the pin and slot linkage arrangement. It operated via two pivoting centrifugal weights with a pin attached to them. As engine speed increased, these weights pivoted allowing the camshaft, which was rigidly attached to an "end plate" containing slots that corresponded to the aforementioned pins, to retard. As engine speed decreased, the torque generated by the springs about the pivot point would overcome the torque due to centrifugal force. This would cause the weights to return to their original position thus forcing the cam to return also.

Although Dr. Speckhart's design met with some success, there were still problems to overcome. Hysteresis due to friction between the pin and slot was large. The centrifugal and spring forces were required to be large to reduce the relative import of friction and the springs were overstressed thus having a short operating life. This design was also backdrivable, but to what degree is unknown.

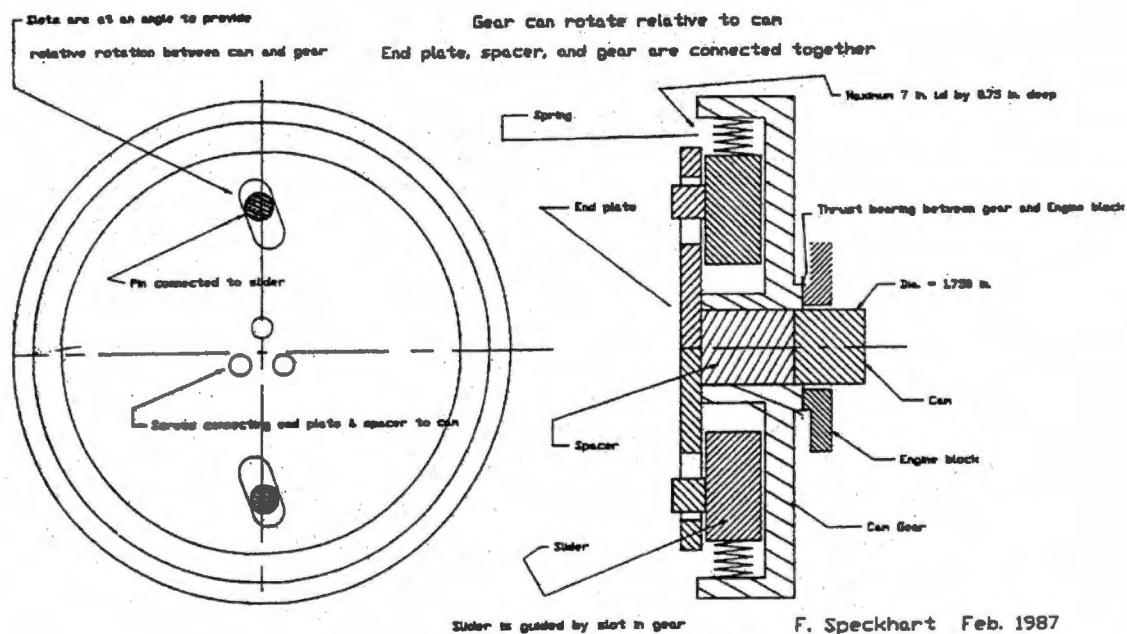


Figure 2 – Design of Cam Retarding Mechanism by Dr. F. H. Speckhart
Source: Dr. F. H. Speckhart

Richard Moisan [4] did an unpublished study entitled "Design of a Camshaft Gear for Variable Valve Timing in a 350 Cubic Inch Chevrolet High Performance Engine" in 1987 at the University of Tennessee. This design (see figure 3) also employed pivoting weights whose centrifugal force, equilibrated by springs, allowed the cam to retard. Unlike Dr. Speckhart's pin and slot approach, Mr. Moisan's design utilized linkage resembling that of a centrifugal advance distributor. This design's major drawback was that it was overly backdrivable. Figure 4 explains that a difference in the torque required to drive the cam of 5 ft-lbf would cause a change in the mechanism's position of 47.4%. Mr. Moisan did not elaborate on hysteresis.

David Connor [5] published his master's thesis in 1989 entitled "The Design and Testing of a Cam Timing Delay Mechanism for High Performance Combustion Engines." He designed, built, and tested a working model. It, like a previous example, employed pivoting centrifugal weights and springs to retard the camshaft by 2° through a pin and slot arrangement. Figure 5 is an exploded view of his device. Mr. Connor extensively studied the hysteresis effects and the torque dependency in his design. They are shown in figures 6 and 7

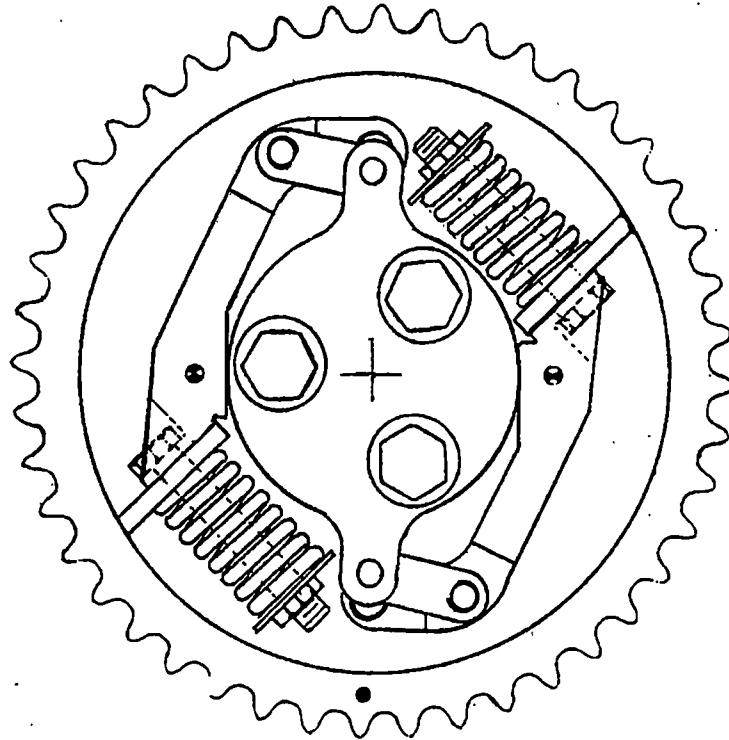


Figure 3 – Cam Retarder Mechanism by Richard Moissan
 Source: Richard Moissan, "Design of a Camshaft Gear for Variable Valve Timing in a 350 Cubic Inch Displacement Chevrolet High Performance Engine," Unpublished design project, University of Tennessee, 1987

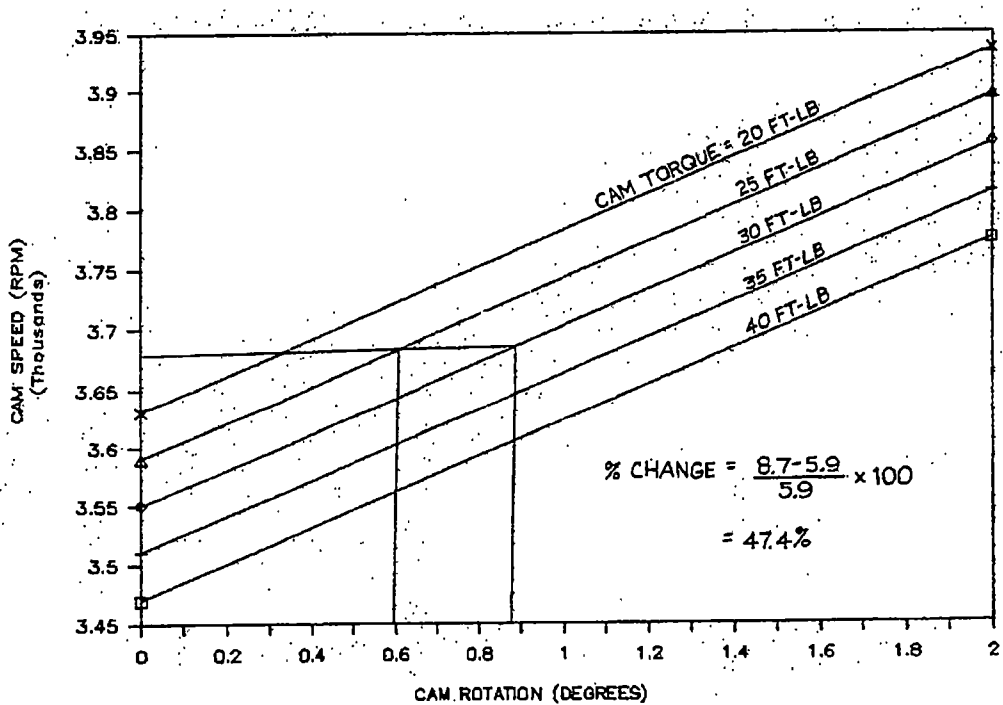


Figure 4 – Torque Dependency of a Cam Retarder Mechanism by Richard Moissan
 Source: Richard Moissan, "Design of a Camshaft Gear for Variable Valve Timing in a 350 Cubic Inch Displacement Chevrolet High Performance Engine," Unpublished design project, University of Tennessee, 1987

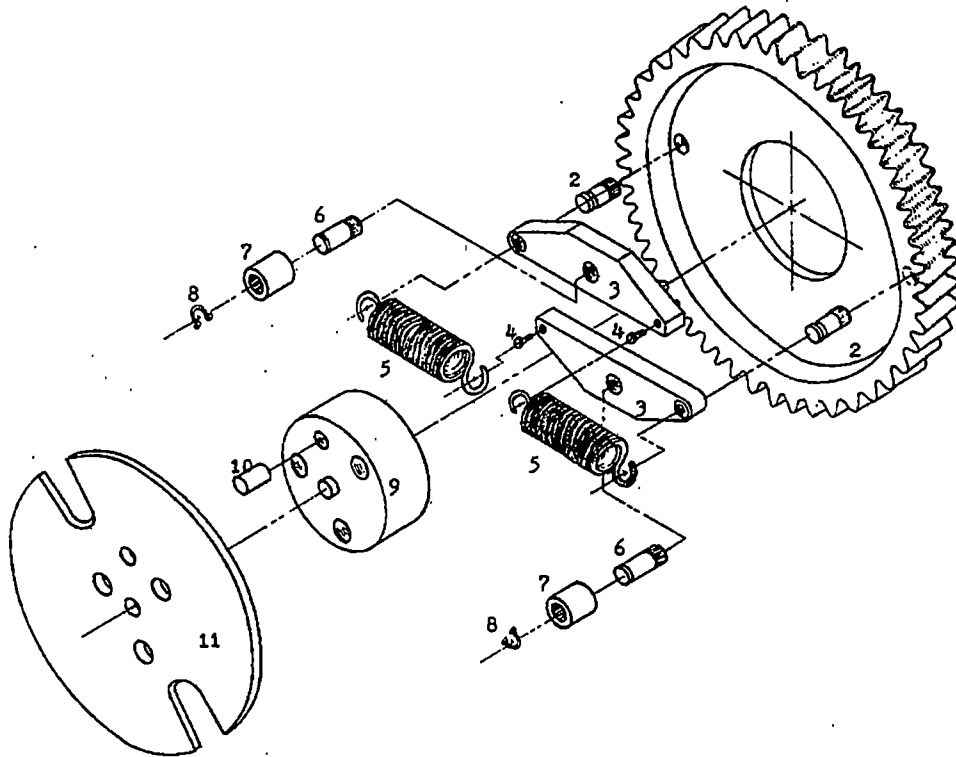


Figure 5 – Assembly Drawing of a Variable Cam Phasing Device by David Connor
 Source: "The Design and Testing of a Cam Timing Delay Mechanism for High Performance

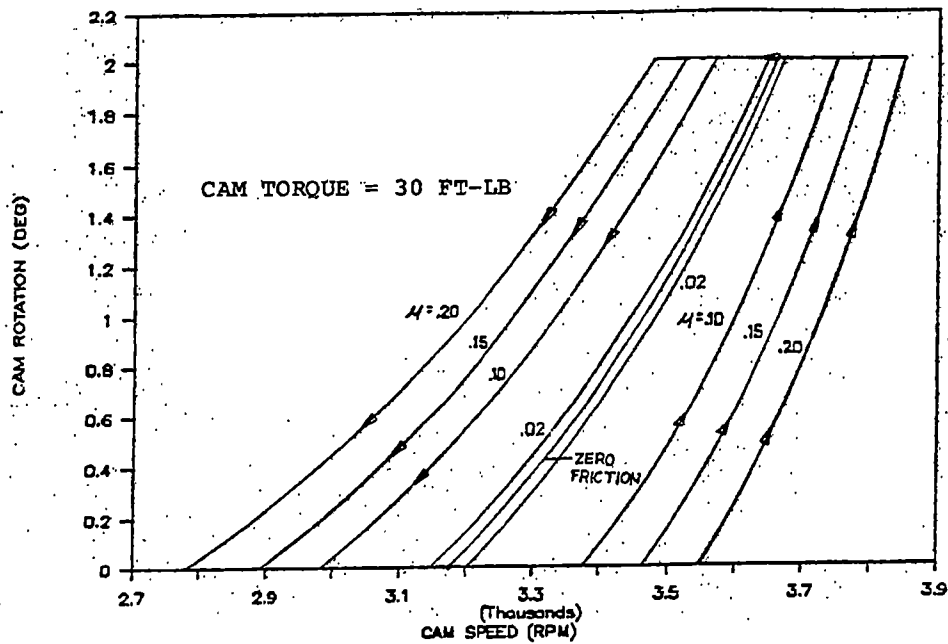


Figure 6 – Hysteresis of a Variable Cam Phasing Device by David Connor
 Source: "The Design and Testing of a Cam Timing Delay Mechanism for High Performance
 Combustion Engines," University of Tennessee, 1989

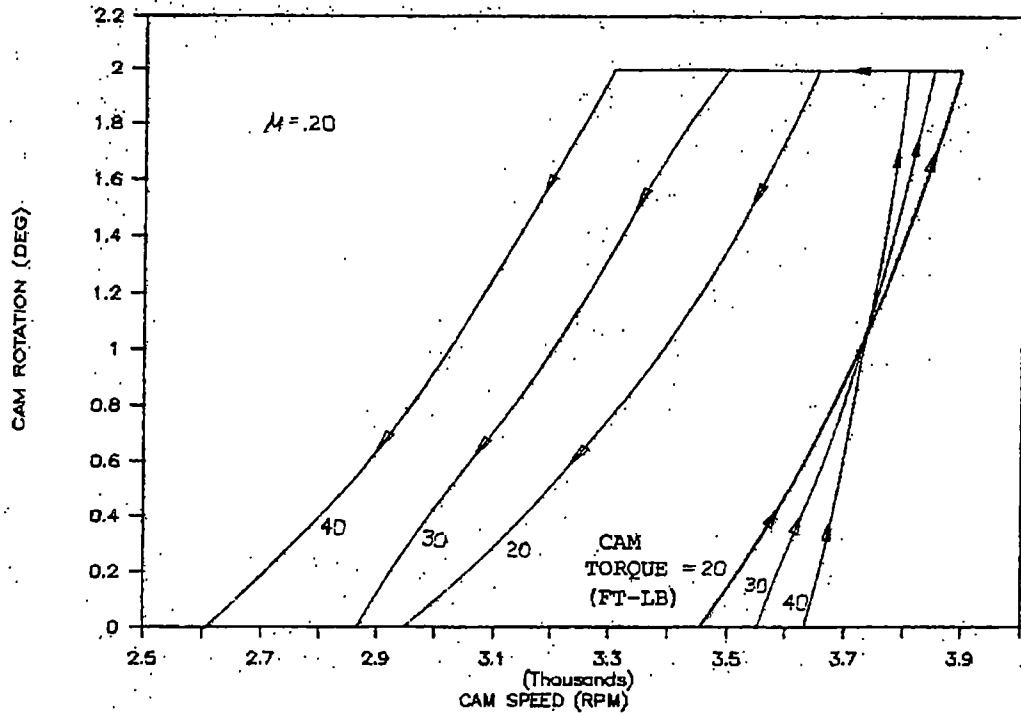


Figure 7 – Torque Dependency of a Variable Cam Phasing Device by David Connor
 Source: "The Design and Testing of a Cam Timing Delay Mechanism for High Performance Combustion Engines," University of Tennessee, 1989

respectively. His design was limited to engine speeds well above those encountered in normal engine operation (7100 – 7800 engine rpm).

Engineers at Competition Cams [6], in Memphis, Tennessee, indicated that they have had several inventors submit mechanical VCP devices. Many of these devices would operate acceptably for short periods of time, but would eventually fail due to spring fatigue. The details of the various designs are unknown.

From these examples it was deduced that the major problems facing the design of a robust VCP mechanism are hysteresis, torque dependency, and spring life.

Mathematical Modeling of the Mechanism

Mathematical models of the various methods of control and actuation of a mechanical VCP device were necessary for both optimization of the mechanism and for eliminating poor alternatives. Three major areas in need of modeling

were the centrifugal forces exerted on the centrifugal weights; the various methods of controlling relative cam rotation; and the various methods of applying spring force. Appendix A contains the mathematical models of all of the various alternatives mentioned below.

Two different types of centrifugal weights were studied, a pivoting weight and a linearly translating weight. A linear centrifugal weight differs from the pivoting type by, as the name implies, moving linearly instead of rotating about a fixed point.

The linearly translating centrifugal weight, shown in figure 8, was much easier to model than the pivoting variety. The analysis of this weight required only five variables. r was the distance from the center of rotation to the mass center of the weight, $\Delta\bar{r}$ was the amount the weight was allowed to travel, the rate of the spring and its initial deflection were needed as well as the mass of the weight.

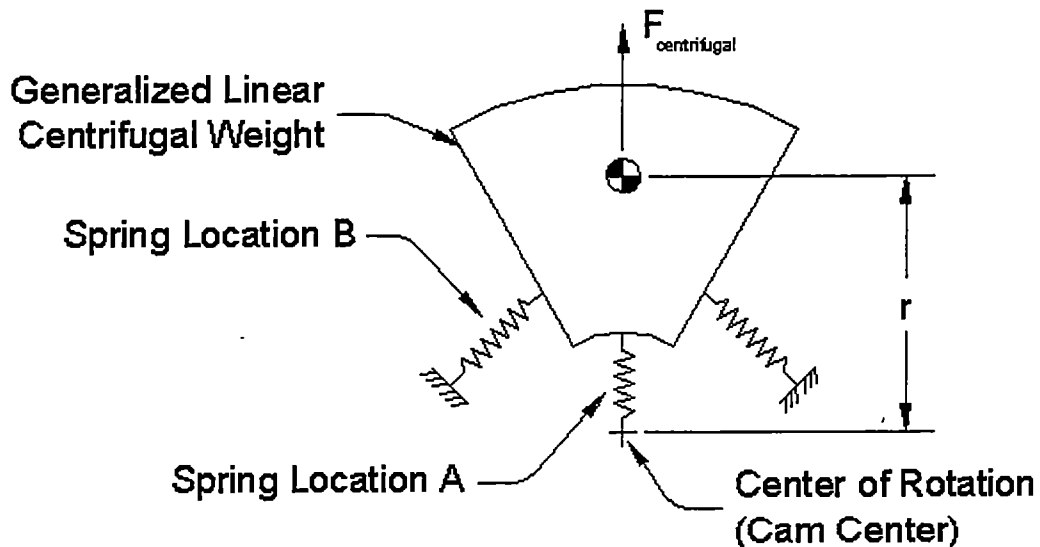


Figure 8 – Generalized Representation of a Linear Centrifugal Weight

The pivoting weight, for which a general representation is shown in figure 9, required more thought and more variables to define it. r_c was the distance from the center of rotation to the mass center of the weight, r_{p1} was the distance from the center of rotation to the pivot point, γ_{init} was the initial angle between r_{p1} and r_c , $\Delta\gamma$ was the angle through which the weight would pivot, and, finally, the mass of the weight. All of the other variables were calculated from those given

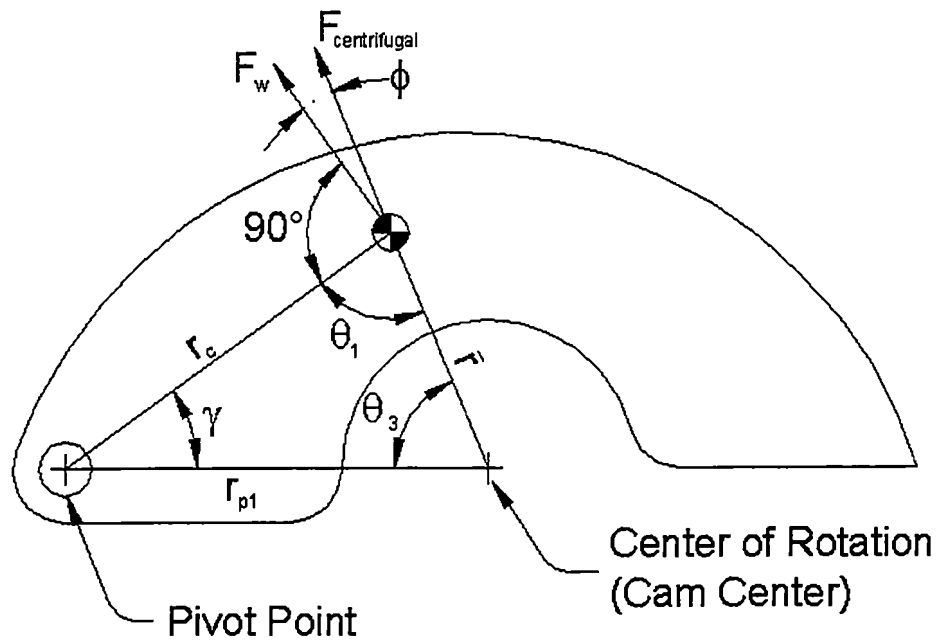


Figure 9 – Generalized Representation of Pivoting Centrifugal Weight

and were necessary to compute the torque generated by the centrifugal acceleration.

Two kinematic methods of controlling the retard angle and rate that were considered were the slot and pin concept and a four-bar linkage method. The four-bar linkage method (see figure 10) required some complex analysis to determine its geometry and force balance for all practical configurations. Link d was to be the distance from the cam center to the centrifugal weight pivot point, link a was to be the link rigidly attached to the camshaft, link c was to be the centrifugal weight, and link b was a free link. Link e was a hypothetical link whose length varied with time and was used for force and torque calculations.

The slot and pin approach shown in figure 11 also demanded considerable thought to produce a model that would compute the geometry of the slot and pin at any time. The pin was assumed to be rigidly connected to the centrifugal weight and was represented by link r_1 . The slot was assumed to be in a member rigidly attached to the camshaft and was represented by link r_2 . Links r_3 and r_4 were used in calculating the slot configuration. The complexity was due to the fact that this model could predict the geometry for a slot whose centerline was not parallel or collinear with a line connecting the center of rotation and the center of the pin.

Spring Considerations and Analysis

Several different types and configurations of springs were envisioned, of which all merited study in the search for an optimal design. Three different types of springs were considered; these included compression, extension, and cantilever springs. All spring analyses are contained in Appendix B.

Extension springs were modeled when anchored to the weight and sprocket or when anchored from weight to weight (see figure 12). Compression springs were considered because, via linkage, they could act like an extension spring (i.e. a drawbar spring) without the disadvantageous hoop stress that plagues extension springs. r_s was the distance from the pivot point of the centrifugal weight to the anchor point of the spring, r_{p1} was the distance from the camshaft center to the center of rotation of the weight, r_{p2} was the distance from the center of rotation of the centrifugal weight to the second anchor point of the spring which could be either on the other weight or on the sprocket. r_{p3} was the distance from the center of rotation of the other centrifugal weight to the second anchor point of the spring and was only used when the second anchor point was on the other weight and β was the angle between r_s and r_{p2} . All other variables were computed from these and were necessary for the calculations.

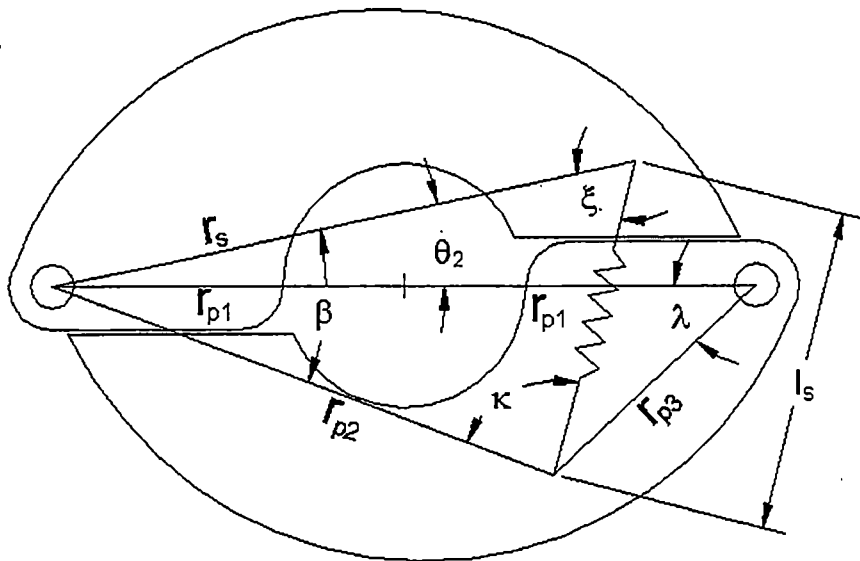


Figure 12 – Generalized Representation of Coil Spring Arrangement

Leaf springs (cantilever springs) also underwent study where they could be attached at one or several points on the centrifugal weight and would be able to slide against the interior of the sprocket (see figure 13). The leaf spring model was more complex and the geometrical calculations were even more difficult. Since testing the device in a static setting was planned, it was decided that a model would be made to experimentally determine the parameters rather than mathematically model a leaf spring system on a pivoting centrifugal weight. The test model would be made so that the optimum location for the attachment point of the spring to the weight could be located with some accuracy and to find the number of springs that would yield the correct torque (see Chapter 6).

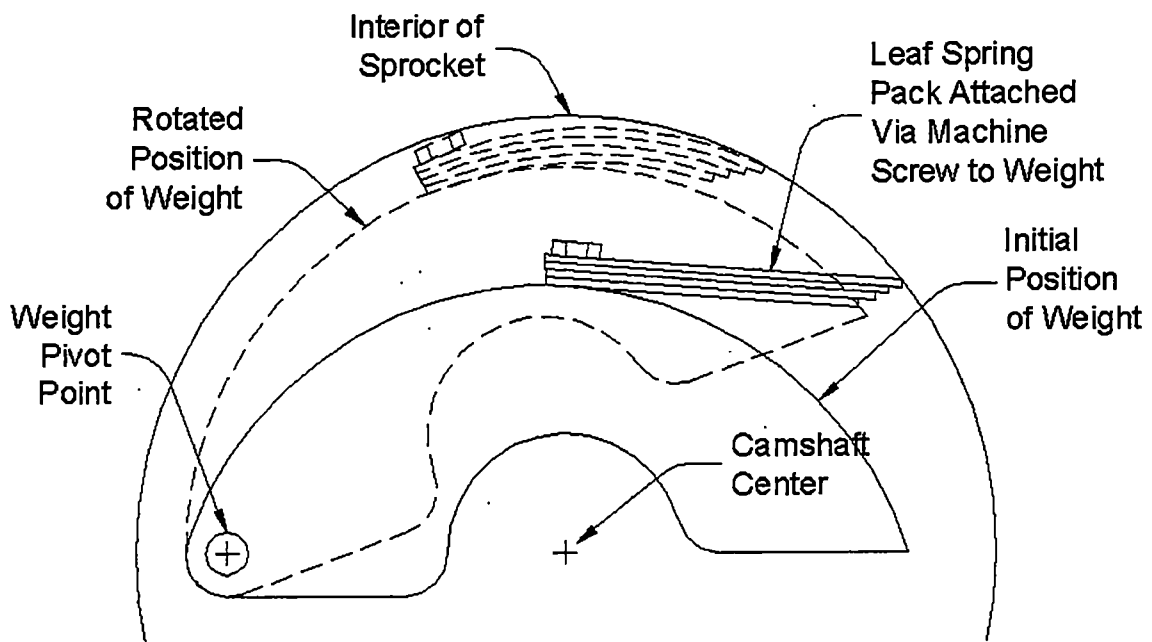


Figure 13 – Concept of Leaf Springs Arrangement

While the overall system was difficult to model, certain aspects of the leaf springs could be predicted. One of them was the maximum stress in each leaf. As previously mentioned, an acceptable fatigue life is a necessary requisite of a successful design. It would be optimal to have the springs “wrap” around the weight on a constant radius thus meaning that the stress is constant throughout the length of the leaf spring. Elementary mechanics theory states that the stress in a cantilever beam bending about a constant radius is given by,

$$\sigma = \frac{E \cdot y}{r} \quad (\text{Equation 2})$$

where σ is stress,
 E is the modulus of elasticity,
 y is half of the thickness of the beam,
 r is the radius of curvature.

Obviously the bottom leaf spring, the leaf spring with the smallest radius of curvature, would be under the highest stress. Since this leaf would fail first, it is the one that had to be in mind during design. The spring material chosen was shim or feeler gage stock. It is inexpensively available in a variety of thicknesses in strips that are generally 0.500-inches wide. The major industrial catalogs (MSC, McMaster-Carr, etc.) list shim and feeler gage stock as having a Rockwell hardness between C48 and C60. Associated Spring [7] publishes a chart giving the tensile strength of steel based on its Rockwell hardness (see figure 14). From the chart, steel having a hardness of Rockwell C54, the midpoint of the range, would have a tensile strength of 300,000-psi.

The cyclical fatigue life for cantilever springs is given in Table 2 [7]. According to this table, a 1,000,000-cycle life is attainable if the maximum stress

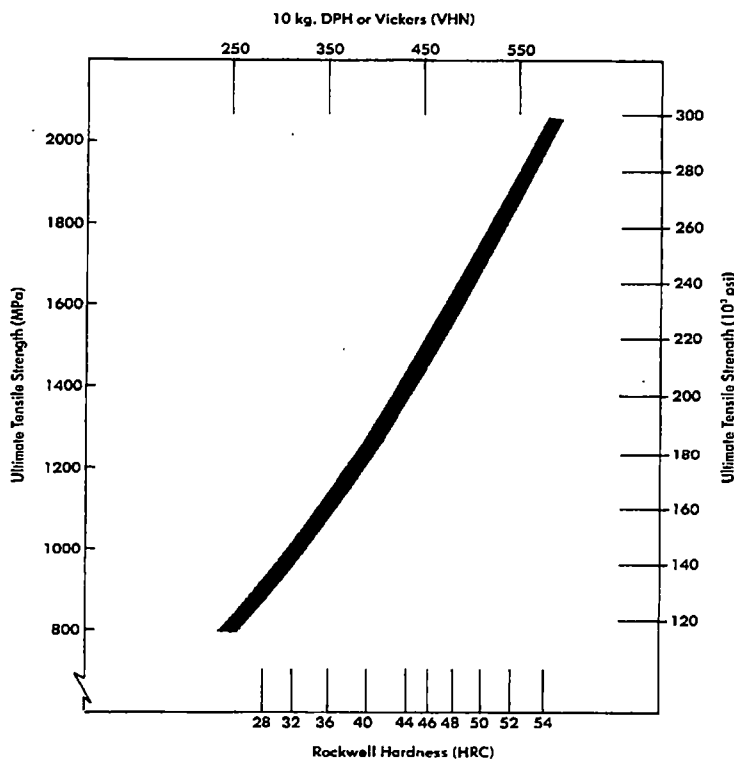


Figure 14 – Tensile Strength versus Rockwell Hardness for Quenched and Tempered Spring Steel
 Source: Associated Spring, *Design Handbook*, Barnes Group, 1981

Number of Cycles	Not Shot-Peened	Shot-Peened
10^5	53%	62%
10^6	50%	60%
10^7	48%	58%

Source: Associated Spring, *Design Handbook*, Barnes Group, 1981

in the spring does not exceed 50% of its ultimate tensile strength (feeler gage stock is not shot-peened).

The challenge in the selection of a spring type (coil or leaf) was to maximize the mass of the centrifugal weight while still being able to restrain the weight over the operating speed range and to not exceed the stress limits prescribed for an acceptable operating life. The major consideration here was the pivot angle of the centrifugal weight since a weight with a small rotation angle would require a stiffer spring that would have less deflection. A weight with a larger rotation angle would need a spring with a lower spring rate but would have a greater deflection.

Added to this was space consideration. Helical springs inherently use space more inefficiently than do leaf springs. These springs have no material in the middle and between the coils whether initially, as compression springs do, or during deflection, as extension springs do. This problem can be somewhat alleviated by using nested spring combinations, but, at best, they do not use space as efficiently as leaf springs.

Computer Simulation of the Mechanism

In order to optimize the kinematics of the mechanism, computers were employed to simulate individual parts or the performance of the device as a whole. The simulations were written in MATLAB (see Appendix C for program listings and descriptions) and were based on the mathematical models of the device and/or on analytical data (see Chapter 6).

CHAPTER 3

FINAL DESIGN CONCEPT

Selection of Design Concept

From the computer simulation studies several conclusions were reached and, from these, a decision was made to move forward with one concept.

The first decision was to use a pivoting centrifugal weight instead of a linearly translating variety. This conclusion was reached because centrifugal force is quadratic whereas spring force is linear. This is true for both spring locations, A and B, shown in figure 8 above. The result is that the motion of the weight is predictable for only a short period of time since the system quickly becomes unstable (see Appendix A1 for proof). A pivoting centrifugal weight did not share this problem because both the centrifugal torque and the spring torque about its pivot point are quadratic (see Appendix B2).

The next alternative to be eliminated from consideration was retard by four-bar linkage. This decision was more difficult to make than that of the type of weights to use. The four-bar linkage approach differs significantly with that of the slot and pin method, but both require a pivoting centrifugal weight. Both the slot and pin method and the four-bar linkage approach performed adequately in simulations meaning that both schemes would accurately and predictably retard the cam by the specified amount. Four-bar linkage showed itself to be more adaptable to operation in different position around the weight. The slot and pin, conversely, would function properly at only one place on the weight.

However, because of the restrictive space requirements and the obvious need to avoid overly complex solutions, the four-bar method was abandoned. The method required an additional member (an extra link, link b) over that of the slot and pin approach. It also required at least three places where members would need to pivot on or about other members. In comparison, the slot and pin approach required only one pivoting joint and one sliding that, unlike the four-bar method, could all be incorporated into existing members.

The decision to use leaf springs was also made based on the limits imposed by the space requirements. Leaf springs make use of the space that they occupied more efficiently than their coil spring counterparts thus allowing the centrifugal weights to be more massive.

Optimum Geometry

The first step in a prototype design was to take the basic design concept of a pivoting centrifugal weight retarding the cam through pin and slot linkage and determine the best basic geometry in which the parts should operate. The best geometry was subjective to several criteria. First and foremost, was operation: it was necessary to rotate the cam 4° when both opening (retarding the cam) and closing (advancing the cam) the centrifugal weights. Secondly, the torque dependency over the operating range should be reduced to a minimum. Third, and to a lesser degree, manufacturing concerns were a consideration.

Since this device has only one degree-of-freedom, the most important variable considered during design was the angle through which the centrifugal weights rotate. Also, as mentioned earlier, some of the major considerations facing this project were torque dependency and hysteresis. Hysteresis would be directly affected by the magnitude of friction relative to spring and centrifugal forces. Torque dependency would be proportional to the angle through which the centrifugal weights rotated. All things being equal, a weight that rotates 20° would have less mass and less torque dependency than one that rotates only 10° ; however, the 10° weight would have more torque dependency than the 20° weight and would have greater mass.

Much deliberation went into making a final decision for the geometry of the mechanism shown in figure 15. It was found that the compromises mentioned above were already made because, above all, space was the main consideration – the device had to fit under a stock or slightly modified timing cover. The length of the slot increases as the pivot angle increases, and, conversely, the distance from the slot's initial position to the cam center

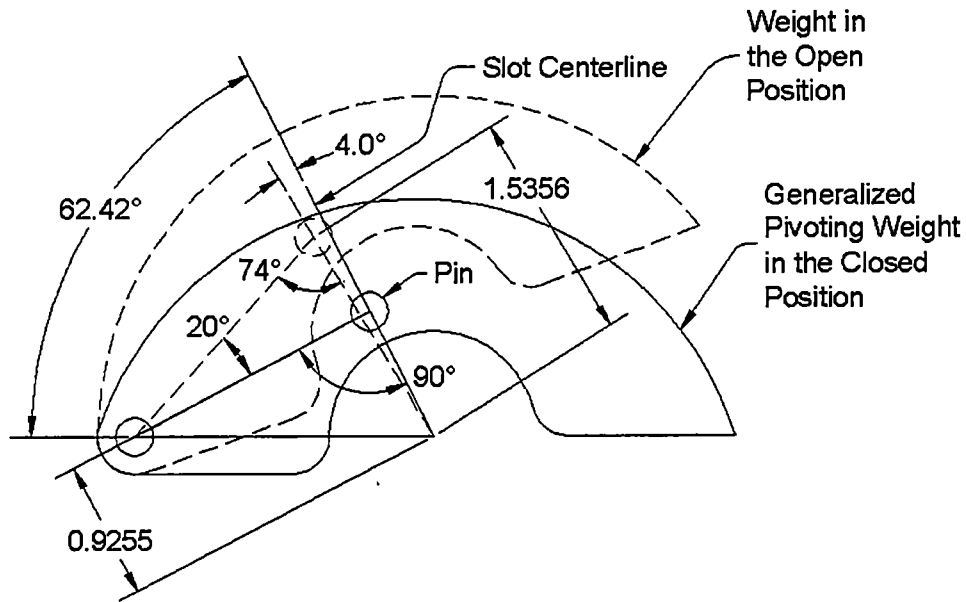


Figure 15 – Final Design Geometry

decreases as pivot angle decreases. Therefore, to achieve a cam retard angle of 4° and still have the mechanism fit in the space allotted to it, the weight can pivot only about 20° . Therefore 20° was chosen as the pivot angle.

The critical dimensions of this geometry are shown in figure 15. This configuration was superior to other geometries for two reasons. First, in the closed or initial position the system is non-backdrivable because the working angle between the slot and pin (the angle between a line connecting the pivot point of the weight and the pin and a line connecting the center of camshaft rotation and the pin) is 90° . Secondly, the slot is along a radius line meaning that during manufacture, both slots can be cut along the same line thus avoiding time-consuming re-alignment.

The retard angle versus the centrifugal weight pivot angle is shown in figure 16. It shows that the retard angle is approximately cubic with pivot angle of the centrifugal weights.

The torque dependency curve for this geometry is given in figure 17. It shows that 0% of the torque required to drive the valve train is transmitted to the centrifugal weight when the weights are closed. The backdriving percentage rises non-linearly until, at full rotation, 31.8% of the torque required to drive the valve train backdrives the mechanism.

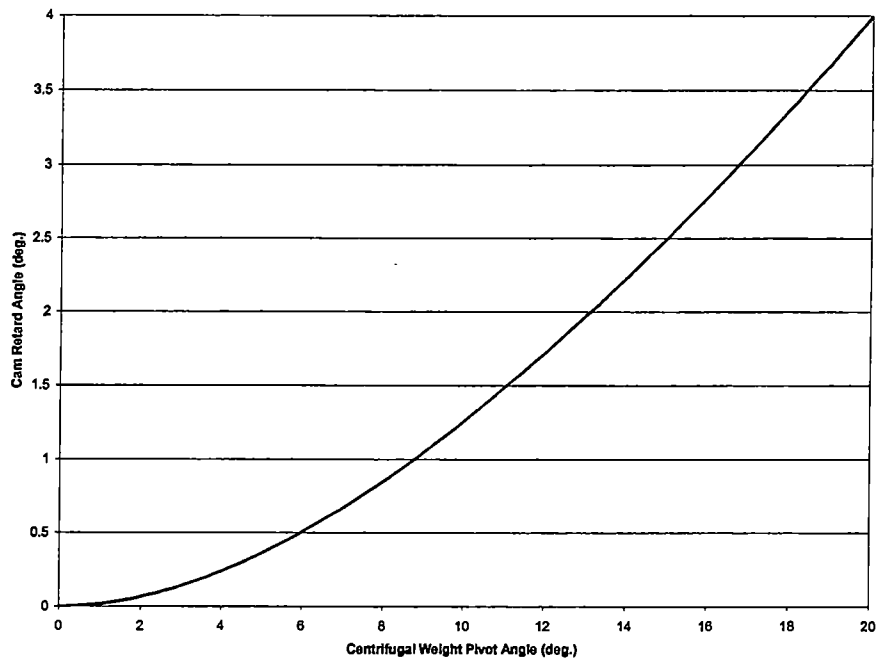


Figure 16 – Camshaft Retard Angle vs. Centrifugal Weight Pivot Angle

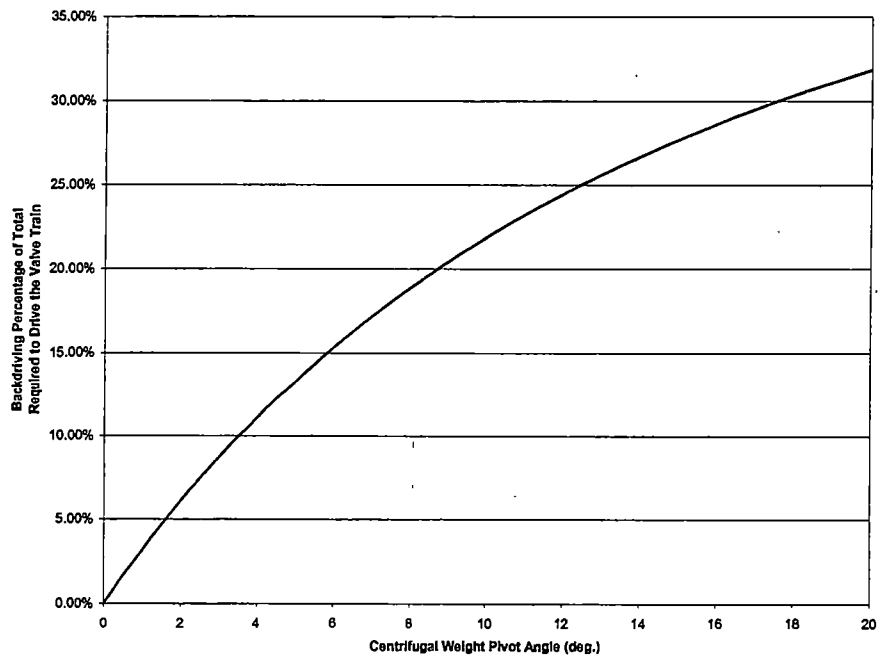


Figure 17 – Percentage of Torque Required to Drive the Valve Train That Backdrives the Mechanism versus Centrifugal Weight Rotation Angle

It should be noted that for any geometry that has an initial working angle between the pin and slot of 90° , the minimum backdriving percentage achievable would be 31.8% for 4° of cam rotation. This is because the working angle between the slot and pin always approaches 74° (see Appendix A4 for mathematical proof).

Finalizing the Design Concept

As mentioned earlier, space is at a premium since the mechanism is limited to the interior and close proximity of a stock timing gear. One major fault was found with the three previous designs, mentioned above, concerning their space inefficient methods of assembling their mechanisms. Those designs made a "sandwich" of the components by, moving from the cam outward, having a modified sprocket first, then the two centrifugal weights, and finally a "drive plate" connected to the cam via some sort of spacer or "cam extension" (see figures 1 and 4 above).

A more efficient use of the limited space available was to include the "drive plate" and "cam extension" into one part and, instead of placing it at the last level, placing it and the sprocket on the same level (see figure 18). This allowed the weights to be more massive thus reducing hysteresis. However, it likely required more machine work than the previous designs in that this method required a completely new sprocket whereas the previous designs were able to machine an existing sprocket to their specifications.

The torque "flow" to the camshaft would originate with the sprocket being driven via a chain drive. The sprocket drives the centrifugal weights by the pins on which they rotate (not shown in figure 18). The centrifugal weights drive the cam extension / drive plate through the pins and slots, and the cam extension / drive plate is rigidly connected to the camshaft.

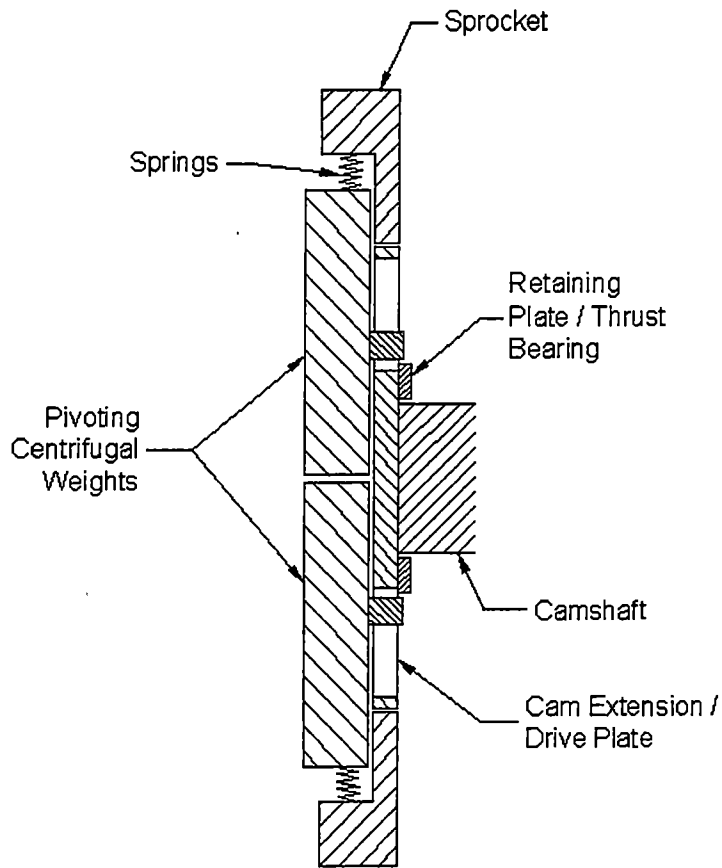


Figure 18 – Schematic of the Final Design Concept

CHAPTER 4

COMPONENT DESIGN

As in most large design projects, the individual parts cannot be designed independently. The components must be designed to interact correctly with each other to accomplish the specified task. In this chapter, individual parts are discussed separately, but they were designed with the others in mind and were designed in an iterative fashion. That is, one change was made to a part and then sympathetic changes were made to the other parts. This was repeated until a satisfactory design was reached. The drawings for all of the parts are included in Appendix D.

Stock Timing Gear

Since this design is limited to the interior and close proximity of the stock timing gear, this design began with a study of a stock timing gear. Following a similar line of thought, the discussion of the various components should be preceded by a review of the original equipment. Figure 19 is a dimensioned drawing of a double-roller stock timing gear that is used on late-model (1987-present) Chevrolet small-block engines. Early model (1955-1987) timing sets differ from late-model sets in only two ways. One, the bolt circle of the retaining screws is $\varnothing 1.360$ -inches versus the late-model's $\varnothing 1.160$ -inches. Two, the spacer or bearing is integral to the sprocket in the early-model timing sets.

This design is only for a late-model applications. As previously shown, the slot centerline begins at a radius of 0.9255-inches from the cam center and, at a minimum, a $\frac{1}{4}$ -inch pin must be used. This means that a working slot and pin arrangement must begin at a distance no greater than 0.8-inches from the cam center. The portion of the cam that inserts into the timing gear barely fits with a radius of 0.78-inches. Late-model cams have an insert radius of 0.93-inches, at least 0.13-inches too large.

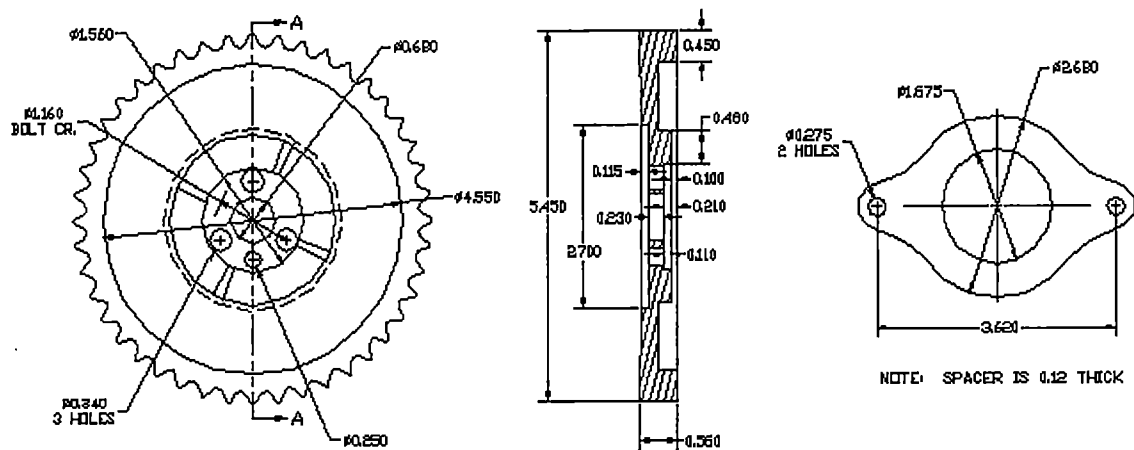


Figure 19 – Chevrolet Small-Block Timing Sprocket, 1987 to Present

Cam Extension Design

The essence of the final design concept is the joining of the cam extension and drive plate and placing this as a part of the sprocket instead of separate from it. Therefore, as the heart of the device, it will be discussed first.

The cam extension (shown in figure 20, see Appendix D for the machine drawings of all of the parts) is rigidly attached to the camshaft by three low-profile 5/16-18 socket-head cap screws. It is designed to "float" in relationship to the sprocket thus allowing the cam to rotate relative to the sprocket. The screw thread and bolt pattern is the same as that of a stock cam thus the cam requires no modification. The low-profile socket-head cap screws are due to space limitation, a shorter screw allows for thicker and more massive centrifugal weights. The indentation on the back of the object is for a positive fit on the cam and is the same dimensions as the indentation found on stock timing gears. This insures that the device will install the same distance from the block as a stock gear, therefore the stock retainer plate found on late-model engines will fit.

The grooves on the outside edge of the cam extension restrict the sprocket from sliding backward into the engine block. Matching grooves are cut into the sprocket so that these two parts fit together and can rotate relative to one another. The cutouts along the periphery of the part, along with the eight tapped holes, are for the balancing springs - a concept that will be discussed in a later section. The hole in the center of the cam extension is threaded for the

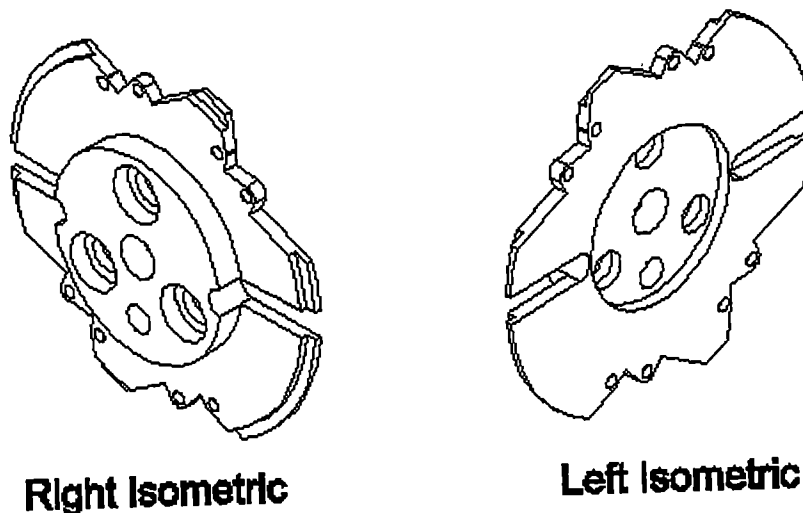


Figure 20 – Isometric Drawing of the Cam Extension

"cam button" part. Lastly, the slots are of the same centerline dimensions as that outlined above and have a width of 0.252-inches to allow 1/4-inch dowel pins to slide in them freely.

Balancing Springs

The concept of balancing springs is used in an effort to minimize the backdriving torque that the valve train exerts on the weights by having springs "carry" the cam. The balancing spring system is comprised of springs anchored to the cam extension and to the sprocket (see figure 21). As the cam extension rotates relative to the sprocket, the springs stretch inducing a torque that acts in the opposite direction as that of the valve train torque. Ideally, the torque created by the balancing springs would be equal and opposite to the torque required to drive the valve train at all times. This was not practical, so it was deemed optimal to have the balancing spring torque to be opposite and equal to the valve train torque at full deflection. At small camshaft retard angles, however, the torque generated by the balancing springs is small. This, however, is acceptable because the torque dependency of the device increases from 0% to 31.8% as the centrifugal weights rotate (see figure 17). The net effect, then, is that the torque dependency is reduced over the entire operating range and it is a minimum at or near the endpoints.

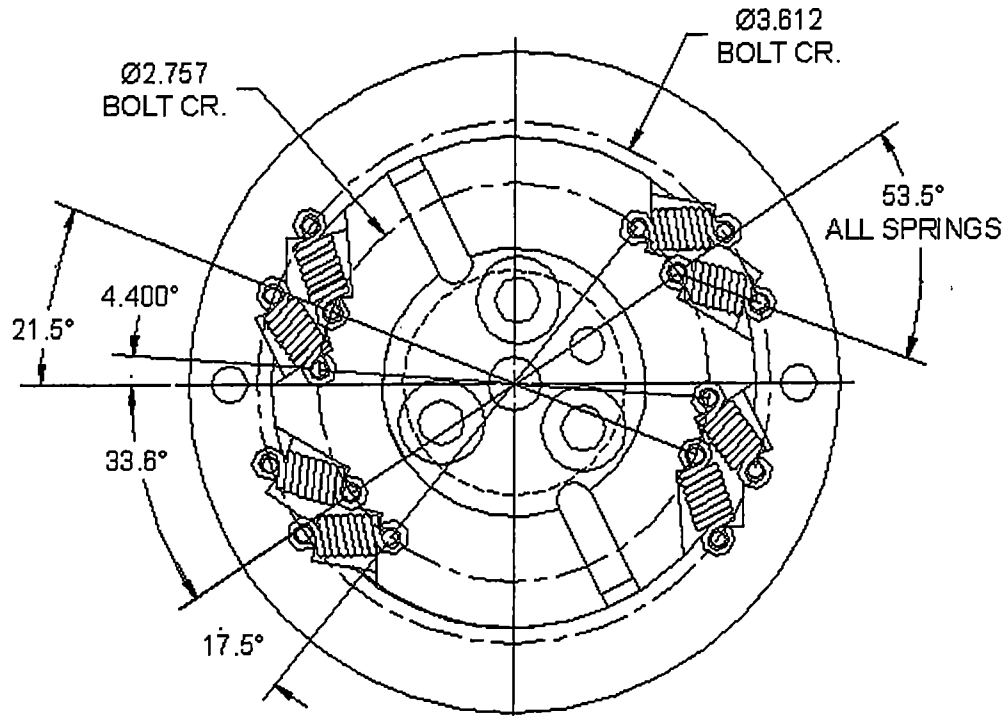


Figure 21 - Balancing Spring Geometry

The balancing springs are extension springs from Century Spring Corp. in Los Angeles, CA [8]. They have a spring constant of 314-lb/in with 10-lb of pre-wound tension, have an outside diameter of 0.281-inches, and have a wire diameter of 0.060-inches (see figure 22). According to the Century Spring catalog, the springs can withstand a maximum repeatable deflection, based on a 1,000,000-cycle life, of 0.090-inches. This design has a maximum deflection of 0.077-inches at 4° of cam extension rotation; therefore these springs should have a fatigue life well in excess of 1,000,000 cycles.

Figure 21 illustrates that up to eight balancing springs can be used yielding a maximum balancing torque of over 340-in-lb. Six springs have over 255-in-lb of torque, four springs generate about 170 in-lb, and two springs yield over 85-in-lb of torque. The idea was that the system could be "tunable" to the valve-train on which they would operate.

The balancing spring system, however, does not completely eliminate backdriving torque and, in certain configurations can actually be a detriment. Figure 23 illustrates that, if the torque generated by the balancing springs at maximum deflection closely coincides with the torque required to drive the valve

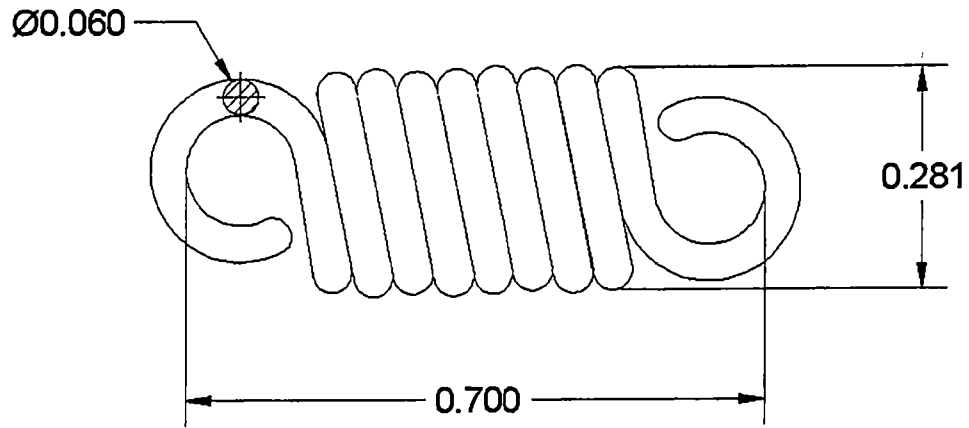


Figure 22 – Balancing Spring Dimensions (Inches)

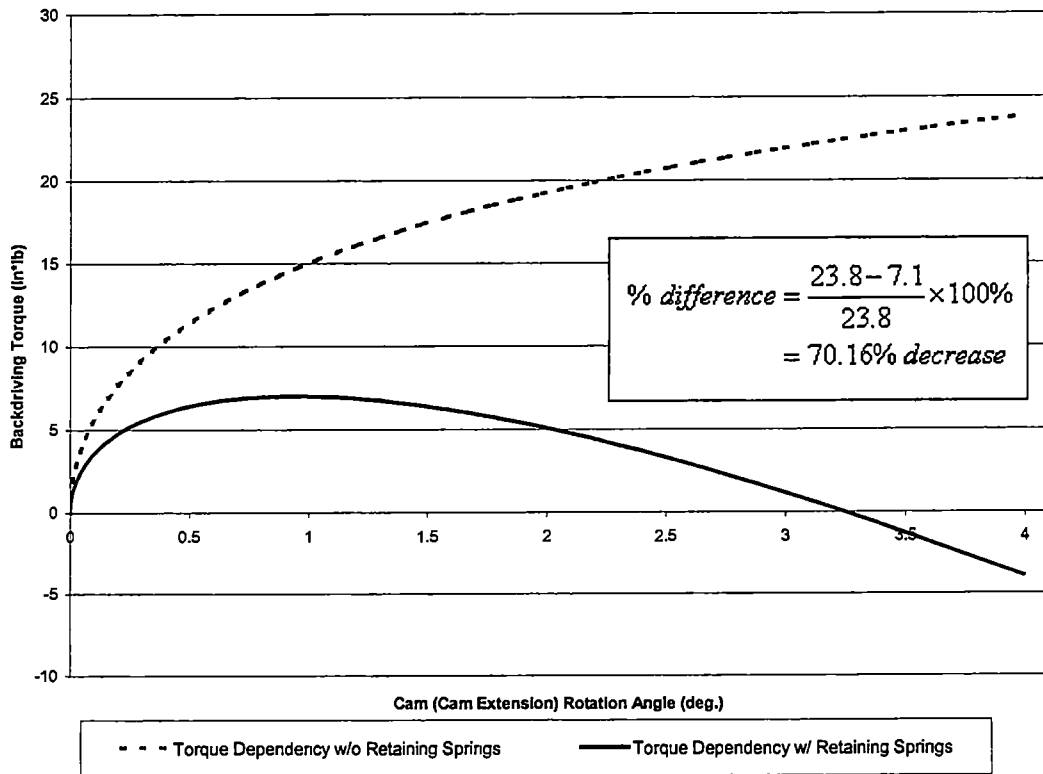


Figure 23 – Theoretical Torque Dependency Curves with and without Four Balancing Springs

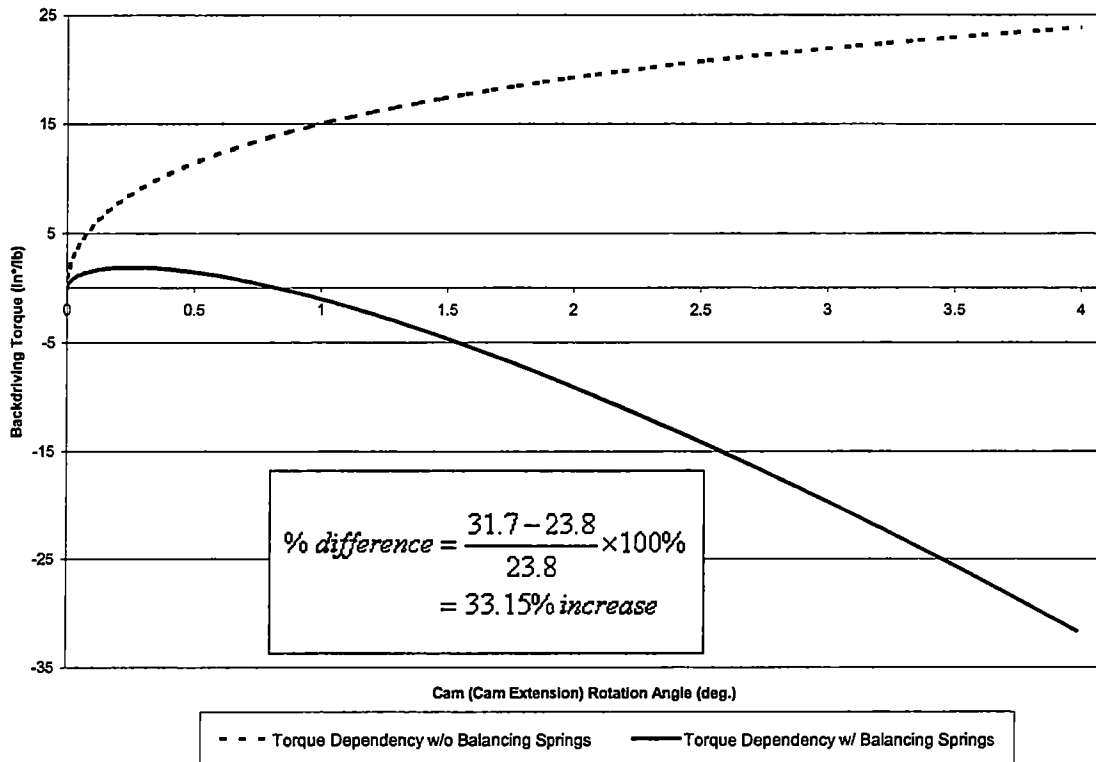


Figure 24 – Theoretical Torque Dependency Curves with and without Eight Balancing Springs

train, while the torque dependency is not eliminated, it is reduced significantly. However, if the torque generated by the balancing springs is much greater or much less than the valve train torque, then the torque dependency of the centrifugal weights is worse than that of a system using no balancing springs (see figure 24). Both of the latter figures are based on the assumption that the torque required to drive valve train torque is 150-in-lbs [9]. In figure 232, four balancing springs were used while eight balancing springs were used in figure 24.

A negative backdriving torque, in figures 23 and 24, indicates that the centrifugal weights are reverse-backdriven. This means that the balancing spring torque has overcome the torque required to drive the valve train and acts to keep the centrifugal weights closed. Thus, if the torque generated by the balancing springs is not matched to the valve train torque, the device's torque dependency can be worse than that with no balancing springs at all. The effects of this mismatch can be that the centrifugal weights do not completely open, thus restricting the retard angle, or that the centrifugal weights open too quickly.

Figure 26 is the detail drawing of the exterior or teeth portion of the sprocket. The lip shown in the section view is a positive stop that insures that the interior will not become skewed during the pressing operation of assembly. Note that to get sufficient space, the wall thickness of the sprocket must be turned very thin, 0.077-inches was used. For strength and safety reasons a steel sprocket machined from billet rather than the cast variety was used. A steel sprocket is considerably more expensive but is much less brittle.

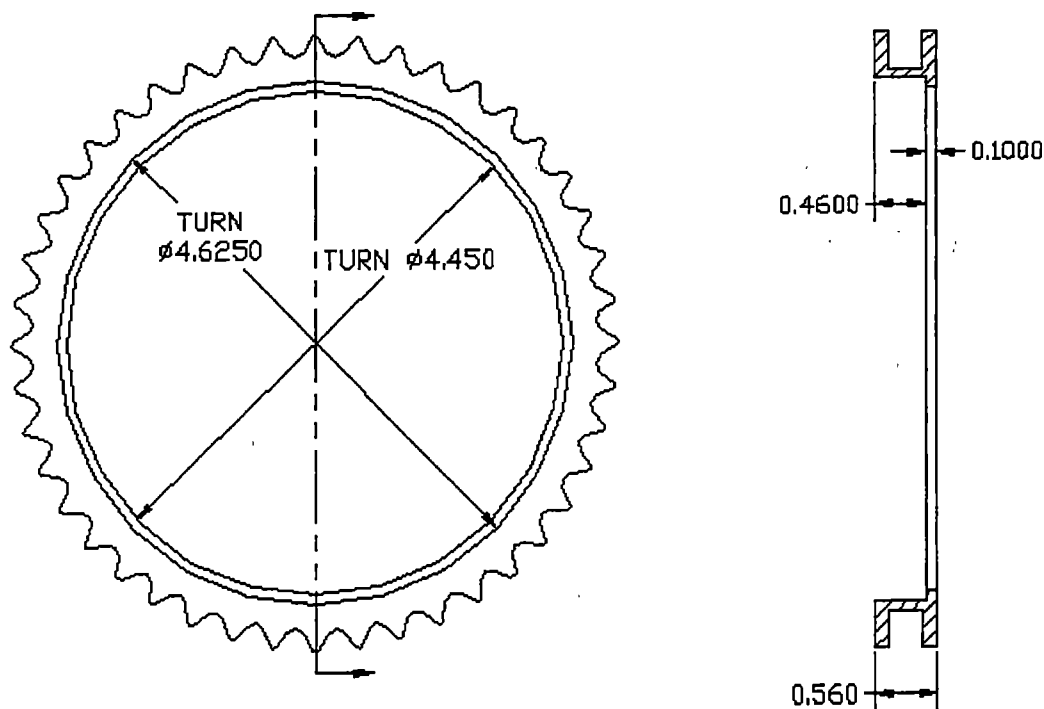


Figure 26 - Sprocket Exterior

All timing sets have a mark on both the cam and crank sprockets that must be aligned. The interior and exterior parts of the sprocket must, therefore, be aligned correctly. It was found that on a stock timing sprocket a line passing through the center of the sprocket and the timing mark and a line passing through the center of the sprocket and the alignment pin on the camshaft make an angle of 86°. To figure the alignment angles necessary for assembly, the configuration of the cam extension within the sprocket had to be considered. Figure 27 is a detail drawing showing the relative angles that the various parts should be configured in when the sprocket is assembled with cam extension.

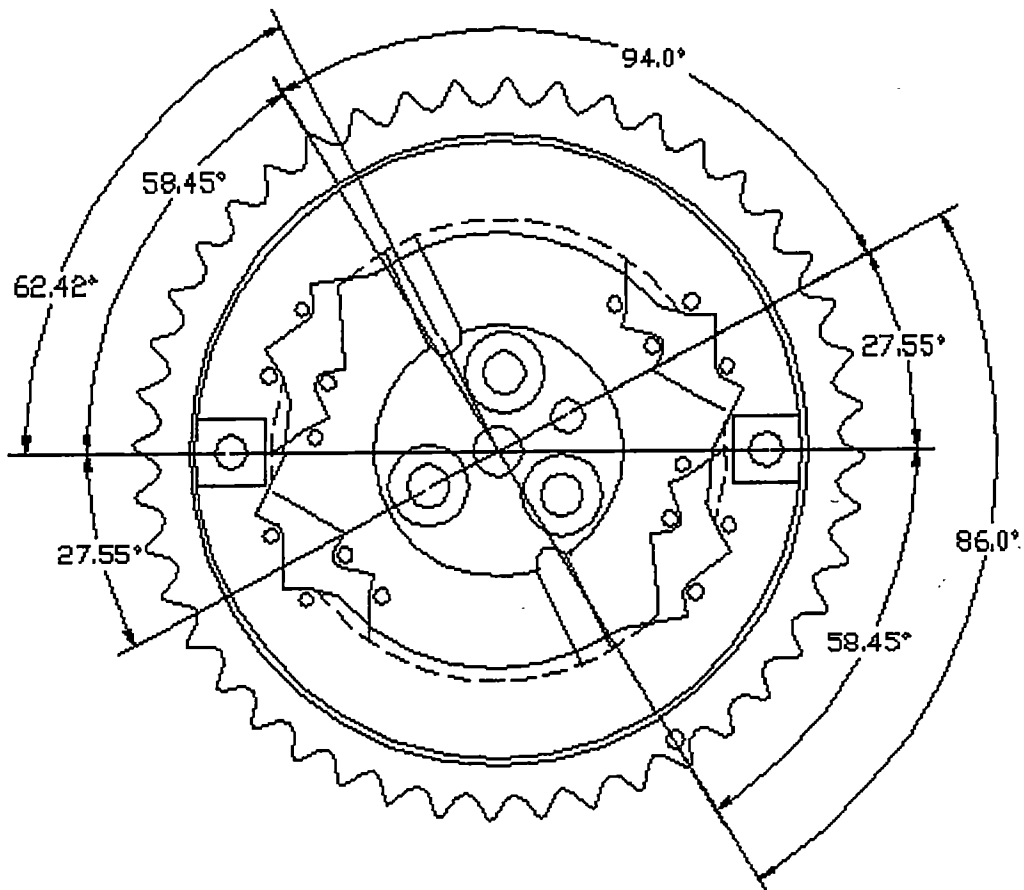


Figure 27 – Alignment Angles of the Two Sprocket Components and the Cam Extension

Centrifugal Weight Design

The controlling components of the device are its two centrifugal weights (see figure 28). Centrifugal force acting on these weights is opposed by spring force and provides the control to accurately change the phase angle relationship between the cam and crank. As such, this part demanded the most thought, consumed the most time, and underwent the most revisions of any of the components.

The challenge in designing the centrifugal weights was to maximize the moment induced by centrifugal acceleration while creating a design that would fit and be able to rotate freely within the confines of the sprocket and cam extension. First, from the mathematical model of the weights, maximizing the distance from the center of rotation (camshaft center) to the pivot point of the weight is advantageous because any increase in this distance correspondingly increases the torque generated by centrifugal force. A distance of 2.0-inches,

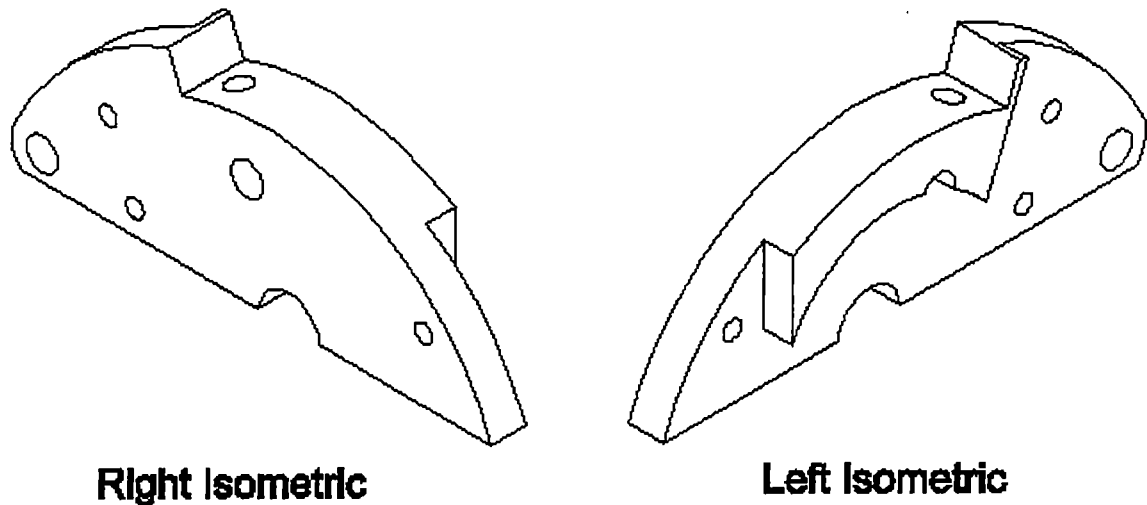


Figure 28 - Isometric Drawing of the Centrifugal Weight

which was the maximum amount available due to space and strength limitations, was chosen.

Unlike the pivot pin, the location of the slot pin was pre-determined. It also had to transmit the force required to drive the valve-train, and it had sufficient material surrounding it to give it strength. The cutouts on the back of the weight were designed to give the weights clearance to move freely over the balancing springs and cam extension.

Arguably, the most critical aspect of the centrifugal weights are the springs. Much deliberation went into a design that would allow the leaf springs to provide the necessary forces to counteract centrifugal forces and do this in a manner that would not overstress and, therefore, fatigue the springs. The maximum radius deemed acceptable to space and strength constraints is 1.945-inches. This value was chosen because the space available had to contain enough leaf springs to generate the torque and their securing screw. Eleven 0.020-inch thick leaf springs and a screw head of 0.080-inch were deemed acceptable. 0.020-inch spring stock was chosen because the maximum stress allowed in the springs is 150,000-psi. By equation 2, given above, this configuration creates a maximum stress of 154,000-psi in the bottom leaf that should give the bottom leaf a fatigue life close to the 1,000,000-cycles desired

(see table 2). The position of the anchor point of the leaf springs was determined experimentally to be near optimal.

The width of the centrifugal weights, 0.500-inch, was chosen because the leaf springs were made from feeler-gage stock that came in strips that were 0.500-inches wide. The springs are fastened to the weights by a #10-32 machine screw that, as mentioned, has a head height not greater than 0.080-inches.

The overall thickness of the device at this point was such that an additional 0.125-inches could be added and still meet the first requirement of a successful design stating that a modified timing cover was acceptable. The solution was to design a "weight cap," see figure 29, that would be 0.125-inches thick and would have the added benefit of increasing the mass of the centrifugal weights by 45%!

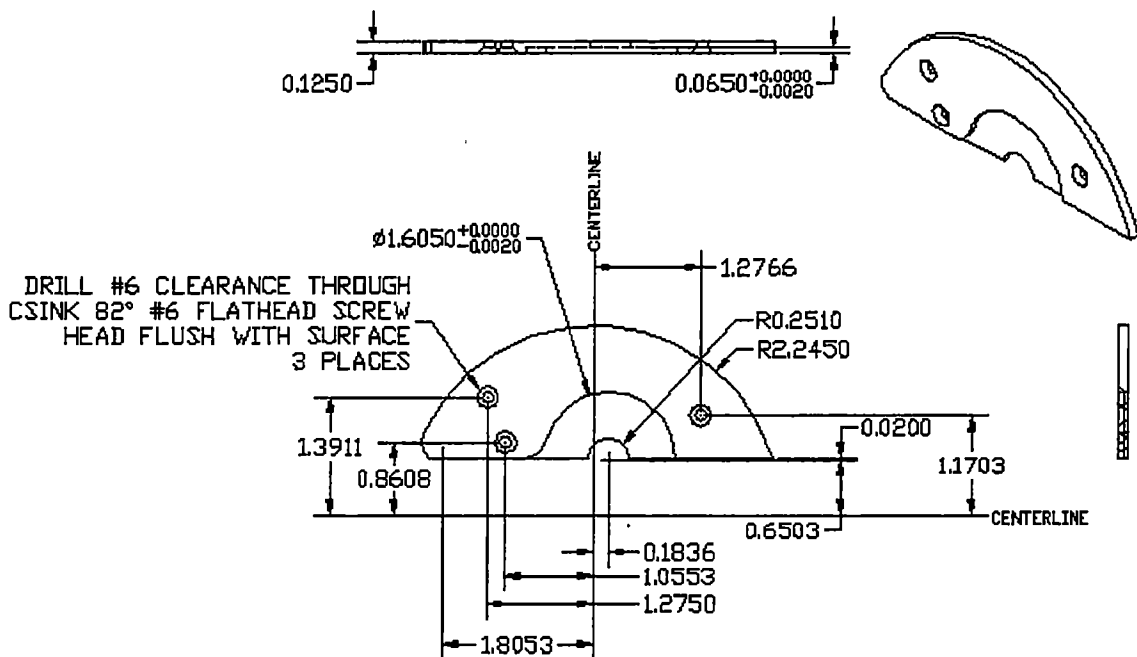


Figure 29 - Detail Drawing of Weight Cap

The weight cap's outline matches that of the centrifugal weight and is secured to the centrifugal weight by three #6 - 32 flat-head machine screws that correspond to three countersunk clearance holes on the weight cap. The 0.251-inch radius at the bottom, center of both the centrifugal weight and the weight cap and the 1.605-inch radius in the weight cap are for the "cam button" part.

Cam Button

A property of pins is that they can move axially as well as rotate, meaning that the centrifugal weights are free to slide axially outward thus disengaging themselves from the mechanism. Also, the sprocket, though constrained so that it could not move axially into the block, could move axially away from the block thus disengaging itself from the cam extension. Therefore the only part that was rigidly fixed to the engine was the cam extension.

The solution to this problem is the cam button (see figure 30). It is threaded into the cam, and, if necessary, it can act as a traditional cam button by utilizing a threaded insert that is screwed into the 1/4 - 20 hole. It restrains the centrifugal weights from sliding out of their pivot holes by $\varnothing 1.600$ -inch surface that corresponds to the $\varnothing 1.605$ -inch diameter cutout in the weight cap. The sprocket is constrained by limiting the axial freedom of the centrifugal weights. This means that just as the weights cannot move axially forward, the sprocket cannot either. The six 0.1875-inch holes arrayed on the constraining surface are to allow tightening of the part via a spanner wrench.

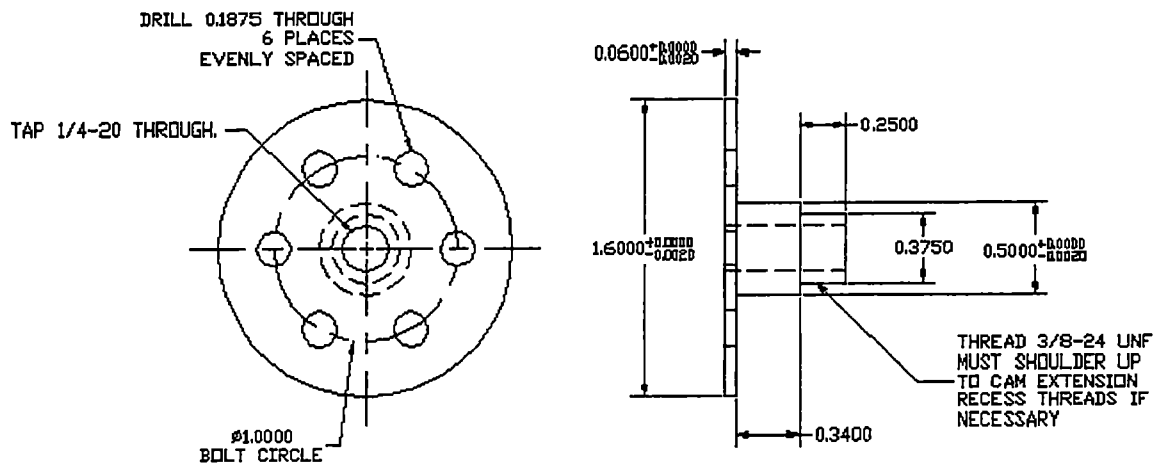


Figure 30 – Detail Drawing of Cam Button

CHAPTER 5

PROTOTYPE DESIGN

The prototype variable camshaft-phasing device consists of the parts listed in the previous chapter and the accompanying fasteners, springs, and pins. The assembly and bill of materials for each centrifugal weight is given in figure 31 and table 3, respectively. Figure 32 and table 4 gives the assembly and bill of materials for the complete prototype.

A few of the parts listed here have not been discussed thus far. Two would be the 0.016-inch shim washers. They are placed between the sprocket insert and the centrifugal weights and act as a bearing between the two surfaces. These are included because both the insert and the weights are made of soft material and a hardened shim washer both reduces wear and reduces friction. Other parts are the 0.005-inch liners. These two pieces are made of shim or feeler gage stock and act as a bearing surface on which the leaf springs can slide. They are deemed necessary because, as before, the insert is made of soft steel whereas the leaf springs have a Rockwell hardness of about C54. A liner, then, protects the insert and reduces friction.

Recall that one of the requirements of the design is that it must fit an unmodified Chevrolet engine block with the standard accessories but can include a modified timing cover if necessary. The assembled prototype device requires an extra axial clearance of approximately 0.125-inches and no additional space is required in the radial direction. This clearance is easily achievable by flattening the indentions that appear on a stock timing cover. For testing purposes, a 4.5-inch hole was cut into the center of the timing cover and a Plexiglas cover was fabricated to view the working of the mechanism. This cover gives ample clearance since it gives a material thickness in addition to removing the recesses on the cover face. Figure 33 is a photograph of the timing cover used for prototype testing.

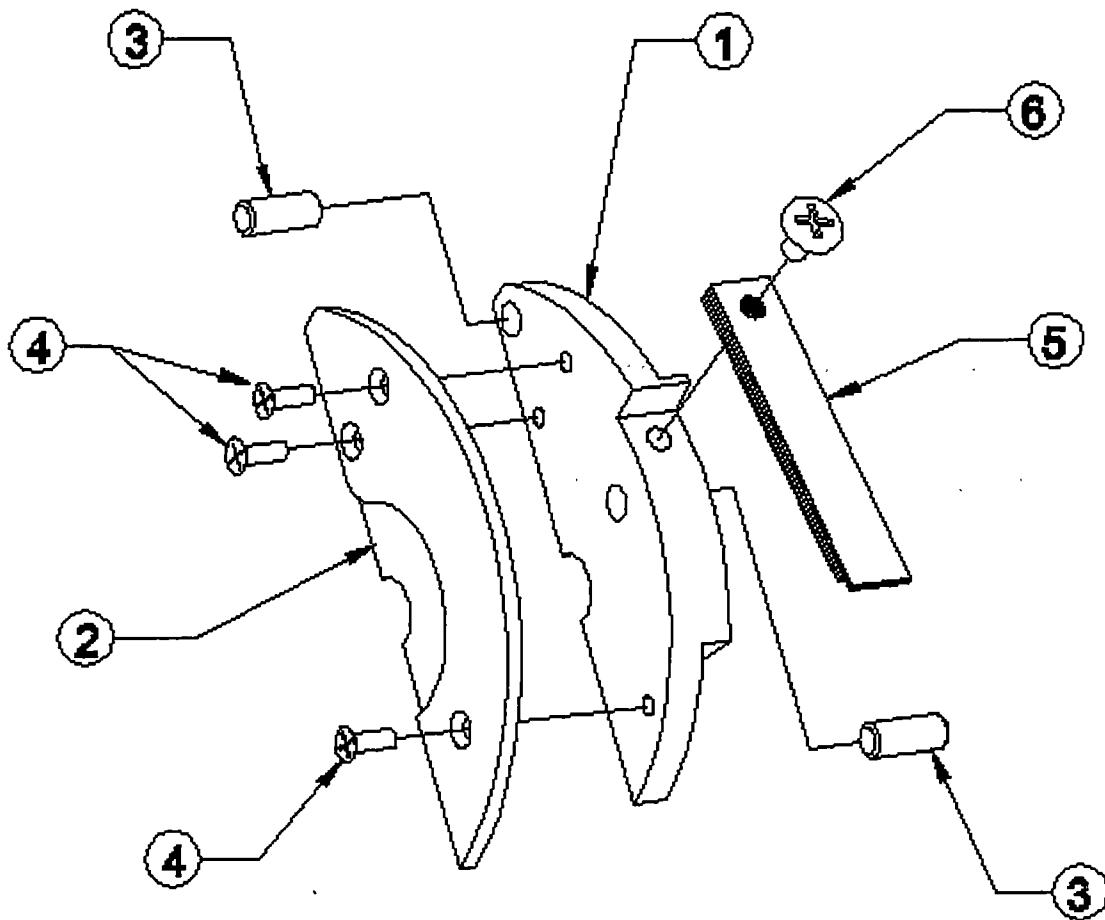


Figure 31 – Exploded Assembly View of the Centrifugal Weight

Table 3 – Bill of Materials for Centrifugal Weight Assembly		
Part No.	Quantity	Description / Specification
1	1	Centrifugal Weight
2	1	Centrifugal Weight Cap
3	2	0.250 x 0.625 Dowel Pin
4	3	6 – 32 x 0.625 Flathead Machine Screw
5	1	Leaf Spring Pack (Number and length of springs may vary)
6	1	10 – 32 x 0.250 Pan Head Machine Screw

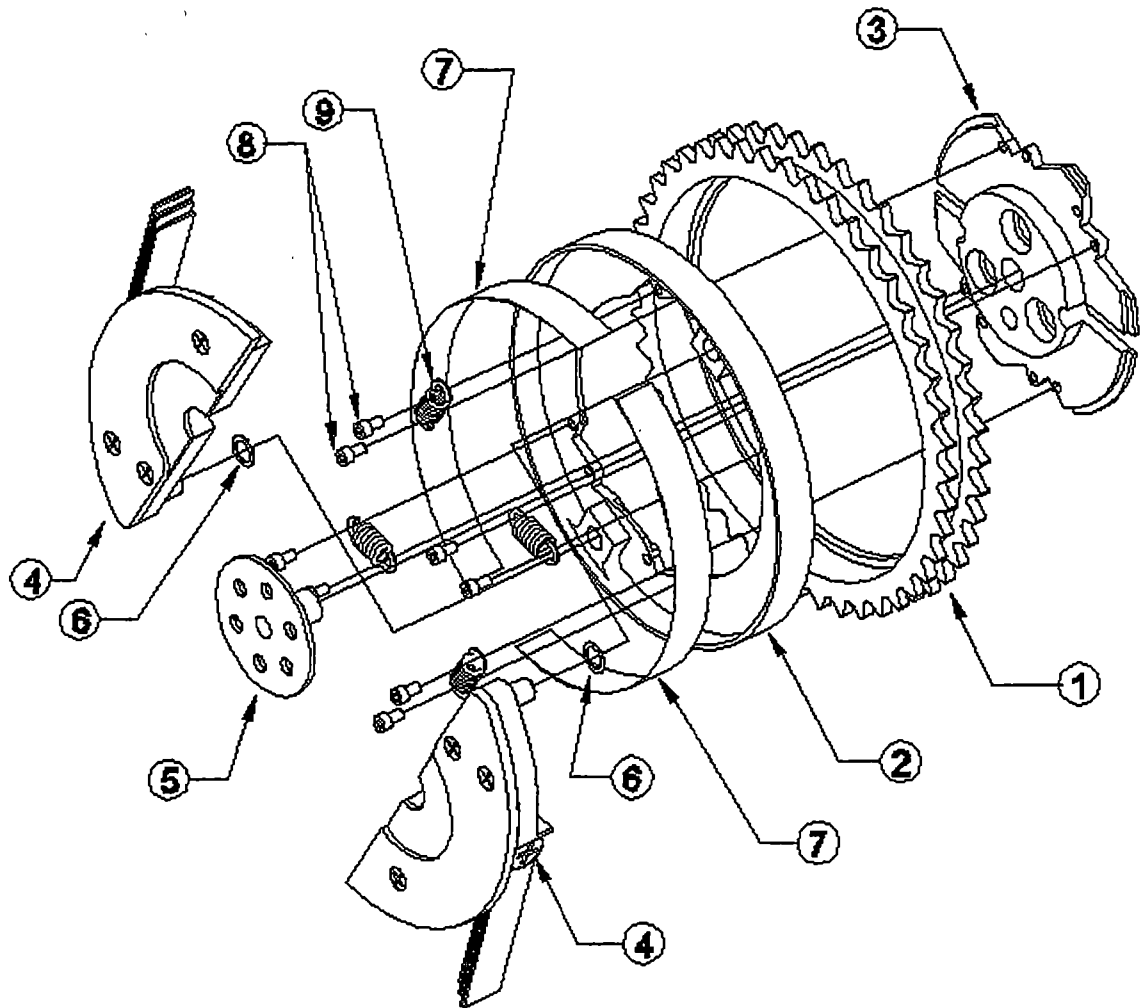


Figure 32 – Exploded Assembly View of the Prototype VCP Mechanism

Table 4 – Bill of Materials for Prototype VCP Mechanism		
Part No.	Quantity	Description / Specification
1	1	Sprocket Teeth
2	1	Sprocket Interior (Press-fit Insert)
3	1	Cam Extension
4	2	Centrifugal Weight Assembly
5	1	Cam Button
6	2	0.016-inch Shim Washer
7	2	0.005" x 0.500" Shim Stock Liner
8	4 – 16	#4-40 x 0.20" Socket Head Cap Screw
9	2 – 8	Balancing Spring



Figure 33 – Timing Cover Used in Prototype Testing

CHAPTER 6

DEVICE TESTING AND RESULTS

Analytical tools such as programming languages and CAD programs are invaluable during the design process, but they do have their limitations. Nothing can substitute actual, real-world testing and, almost always, a design subjected to actual testing will immediately illuminate areas where improvements can and/or should be made.

Static Testing and Results

Static testing was used to validate some of the assumptions made during mathematical modeling of certain components of the device and evaluate those models. It was also used to explore aspects of the device that would be critical to operation or were too complex to model.

The first part to undergo testing was the centrifugal weights and the leaf springs. Both components went through several design iterations because of lessons learned during testing. Figure 34 is a photograph of the test centrifugal weight and a leaf spring pack that was used in static testing. This testing model had the same constant radius for leaf spring deflection as that of the design and had a nut welded to the weight at the pivot point. The nut was used for verifying the torque generated by the leaf springs on the weight. Note that an additional leaf spring attachment point is available on this test weight that was used to investigate how altering the attachment point of the springs affected the torque generated by the springs.

Figure 35 is a photograph of the static-testing fixture. It consisted of a machined steel cylinder that simulates the sprocket and engine block. The large cavity was of the same diameter as that of the inside of the actual sprocket, the large hole in the middle represents the first cam bearing, and the turned cavity around it is for the cam extension. Note that a 0.005-inch liner was also used in static testing.

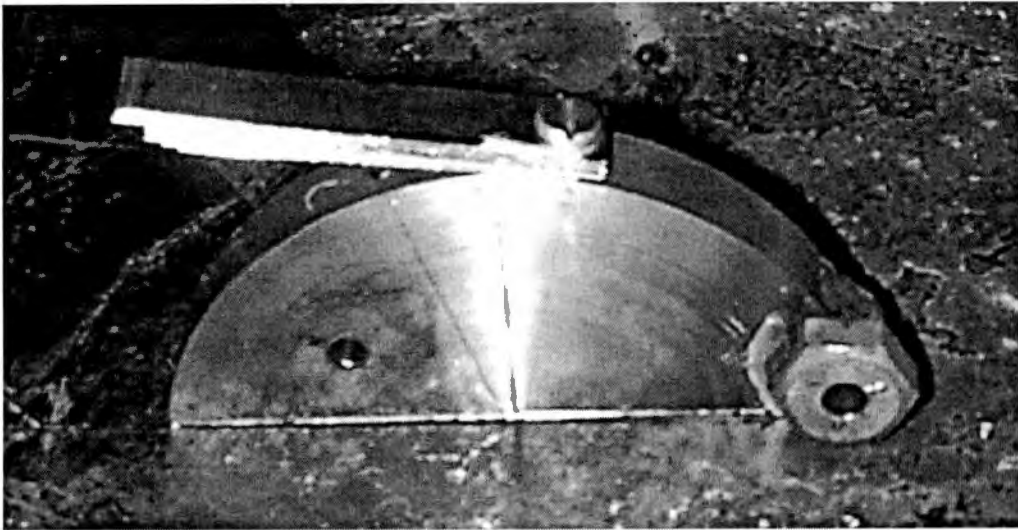


Figure 34 – Static Testing Weight

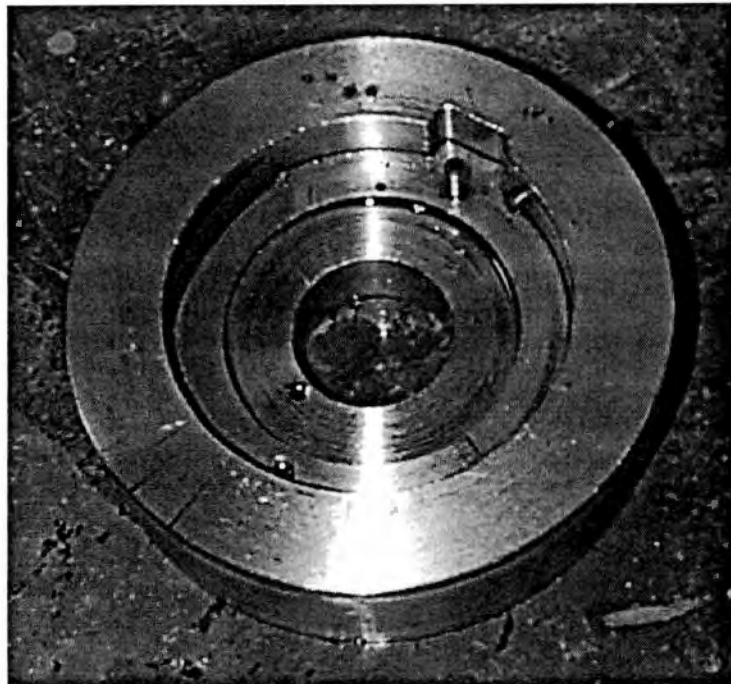


Figure 35 – Static Testing Fixture

Computer simulations predicted the torque generated by centrifugal acceleration over the device's desired operating speed range. The number and lengths of the leaf springs that would generate this torque were determined by experimentation. Note that the design of the centrifugal weight allowed for up to 11 springs. For this application (engine speed range), 8 springs were found to be sufficient. Table 5 lists the lengths of the leaf springs in the spring pack.

Table 5 – Length and Position of Spring Leaves in the Spring Pack Used in Both Static and Dynamic Testing.	
Note that spring material is 0.500 wide x 0.020 thick.	
Spring	Length (Inches)
1 (Bottom Leaf)	2.25
2	2.25
3	2.375
4	2.5
5	2.5
6	2.5
7	2.625
8 (Top Leaf)	2.625

Figure 36 is a plot of the torque generated by the leaf spring pack about the pivot point of the centrifugal weight. The least squares curve fit of the data is also included on this plot and was used for simulating the operation of the mechanism using this spring pack.

Computer simulations, using this spring pack, predicted the operation of the device giving, among other things, the camshaft retard angle as a function of engine rpm. Figures 37, 38, 39, and 40 are plots showing the predicted operation of the device with a system of 8, 6, 4, and 2 balancing springs, respectively, and assuming a coefficient of friction between the pin and slot of 0.1 [10].

The vertical portion in each curve represents an area where the operation of the device is unstable. The explanation is that, in the closed position, the weights are non-backdriven, but, at the onset of motion (centrifugal torque equals the torque generated by the leaf springs), the torque dependency of the weights increase rapidly thus the device moves a portion of its motion all at

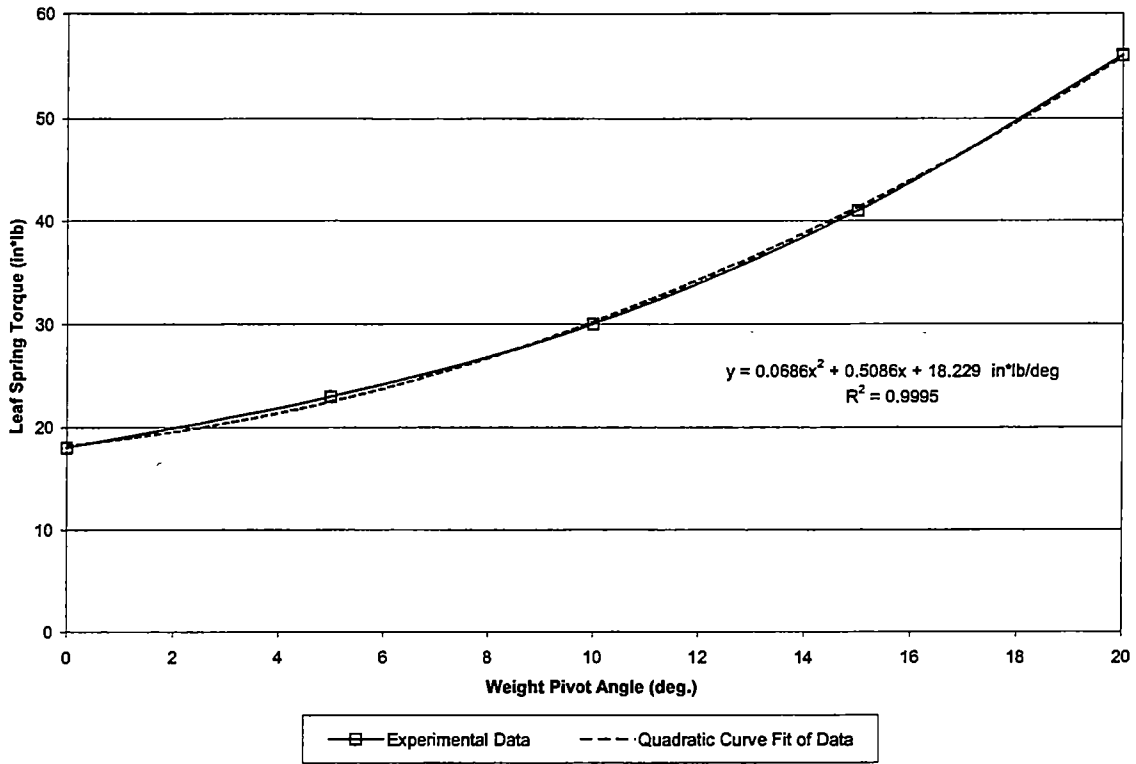


Figure 36 – Experimental Leaf Spring Torque Data and Curve Fit

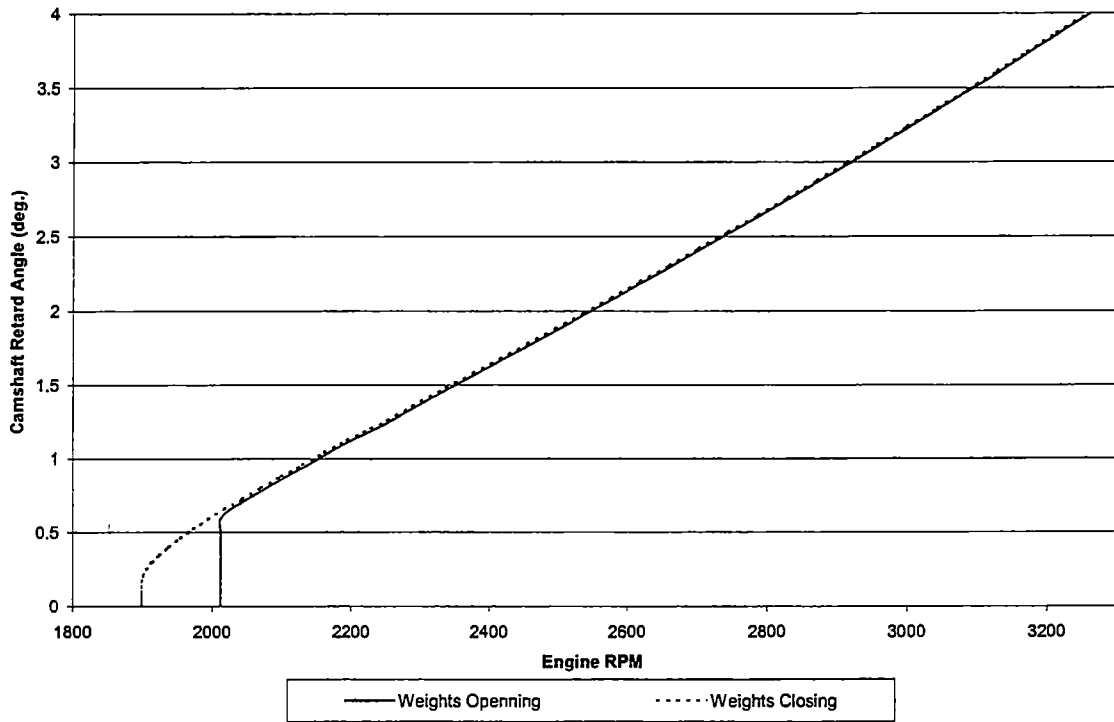


Figure 37 – Predicted Operation Curves for a System Using 8 Balancing Springs

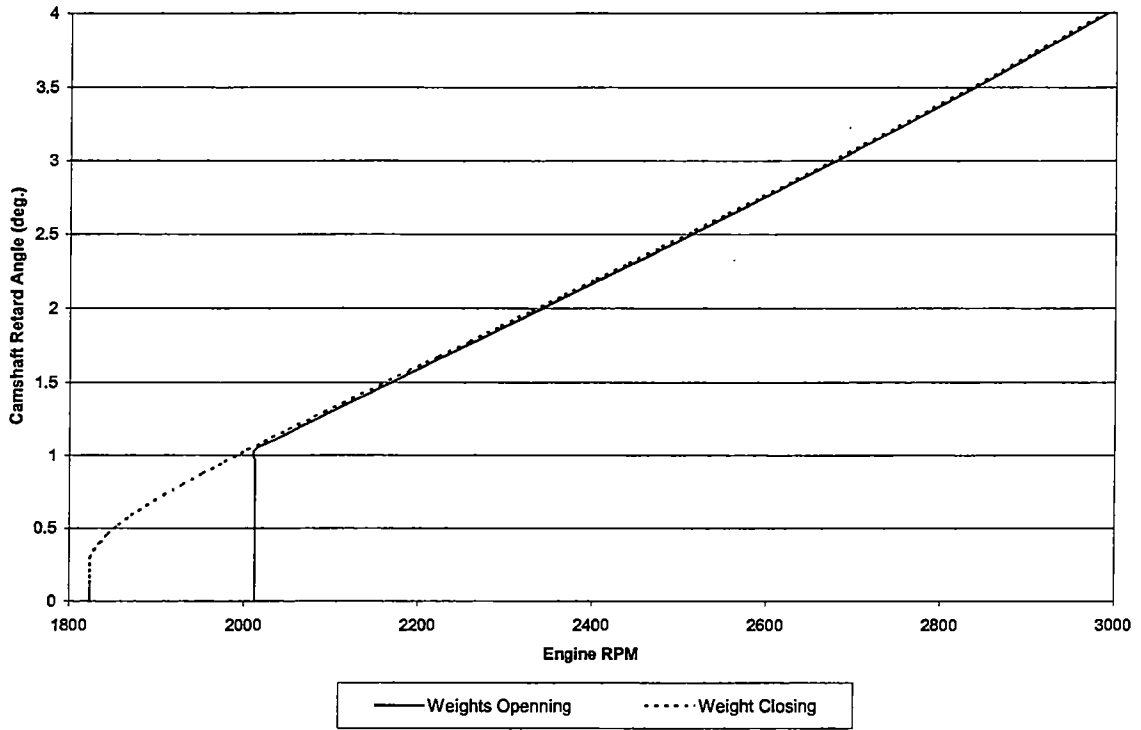


Figure 38 – Predicted Operation Curves for a System Using 6 Balancing Springs

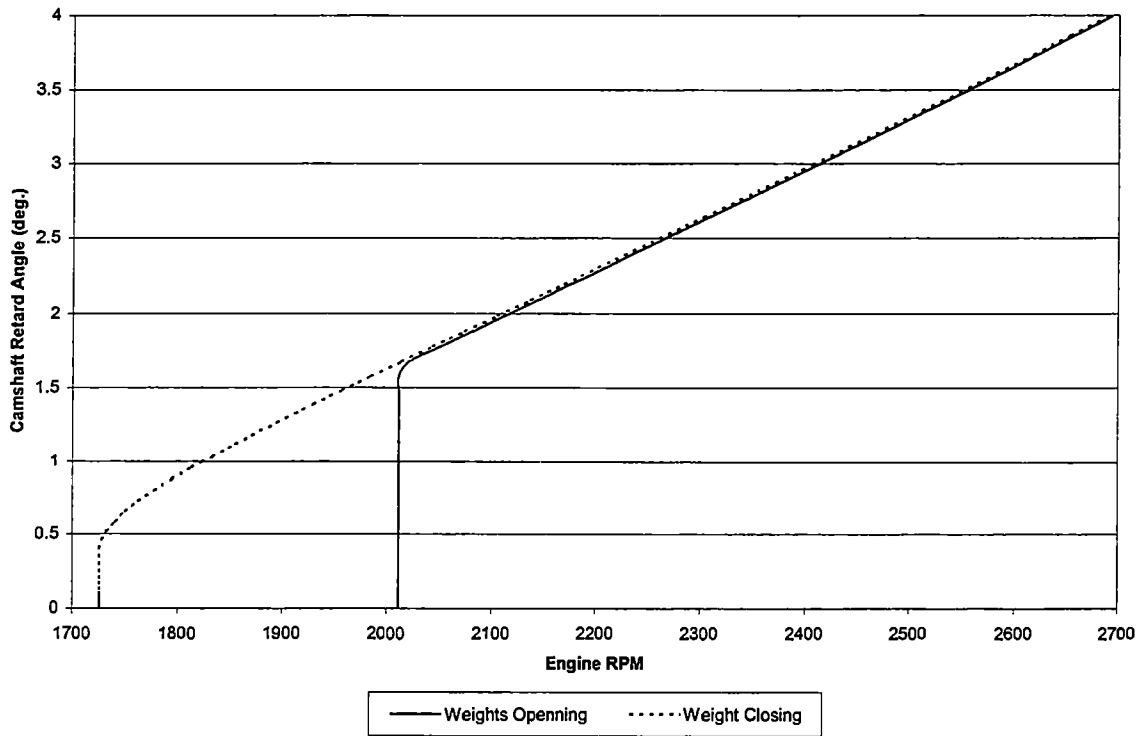


Figure 39 - Predicted Operation Curves for a System Using 4 Balancing Springs

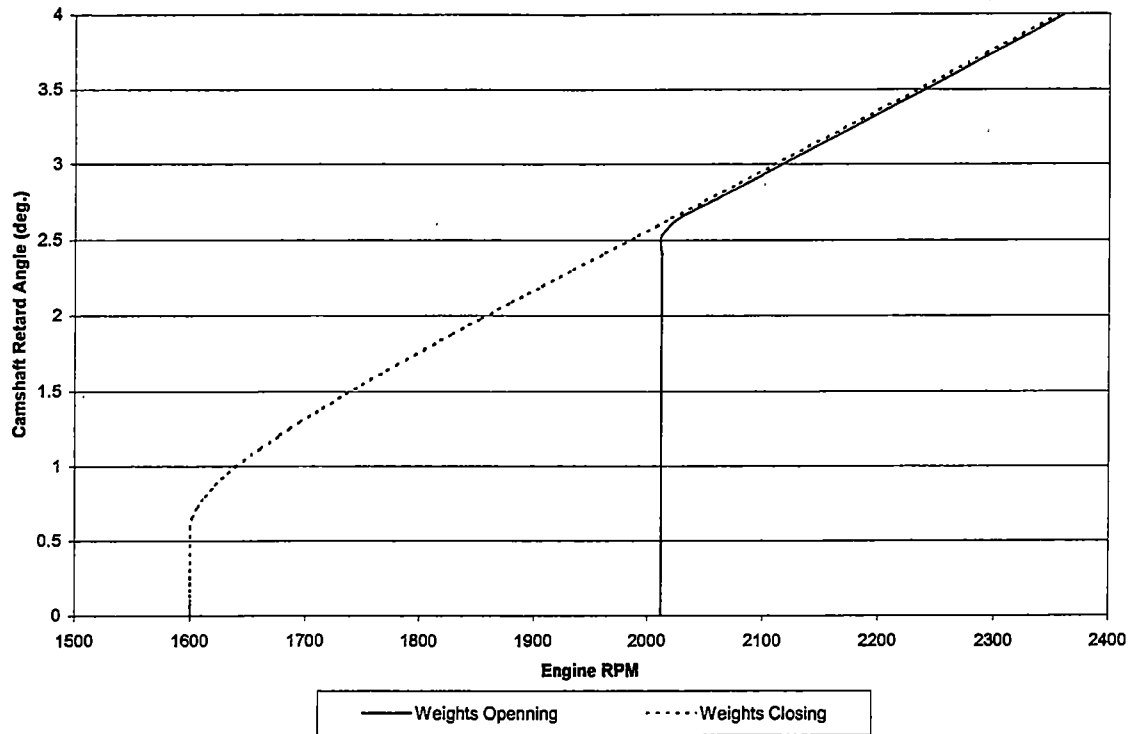


Figure 40 - Predicted Operation Curves for a System Using 2 Balancing Springs

once. The difference between the engine speed at which the weights begin to open and the speed at which the weights finish closing is a result of the same phenomenon.

Except for the unstable portion of the curves, camshaft retard was predicted to be linear with engine RPM. Hysteresis, except in the unstable region of operation, was predicted to be small; however, note that friction was only considered in the region of the slot and pin. There is friction throughout the mechanism, but the friction in this area was thought to contribute the most to hysteresis. Also note that the configuration using 6 balancing springs was predicted to give an operating speed range that most closely matches the desired range of 2000 to 3000 engine RPM.

The design stresses imposed on the leaf springs were acceptable if the spring stock had a Rockwell hardness of C54. However, the range of hardnesses that the distributor quoted (C48 – C61) was large and left some uncertainty. Cyclical testing was performed to determine if the fatigue life of the springs was satisfactory. Figure 41 is a photograph of the fatigue testing setup that consisted of the test weight, test fixture, and a pneumatic cylinder controlled via a programmable logic controller (PLC). This testing apparatus cycled the leaf

springs over 600,000 times without a detectable loss in spring force. The spring force was measured by stopping the testing and using a torque wrench to measure the torque generated by the leaf springs at two weight pivot angles, in this case at an arbitrary point at the start of rotation and another at full deflection.

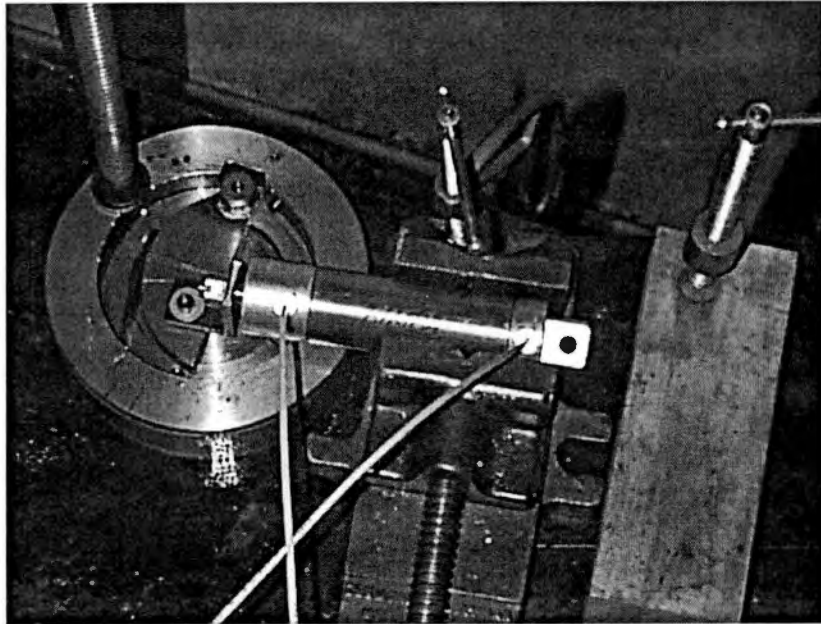


Figure 41 – Setup for Fatigue Testing Leaf Springs

Dynamic Testing

Verification and evaluation of the prototype design could only be accomplished through dynamic testing of the device. The best platform for dynamic testing would be an actual engine in which the device was designed to operate. Several options were considered including testing the device in a running automobile, testing in a running engine on some sort of engine test stand or dynamometer, or testing in a non-running engine driven by an electric motor. The latter option was selected for three reasons. First, the Mechanical Engineering Department had an engine dynamometer available consisting of an electric motor that can be driven by or drive an engine. Secondly, a driven engine allowed more freedom of observation in that the normal accessories like a water pump, belts, and pulleys were unnecessary. Lastly, since the engine was not required to run, any failures that the device might experience would be easier and more quickly fixed.

Dynamic Testing Procedure

The test bed selected was a mid-1970's Chevrolet 350. The valve-train was retrofitted with a late-model roller camshaft and hydraulic, roller lifters because, because, as mentioned earlier, the device cannot be used on pre-1987 camshafts because of the cam extension design. The camshaft used was a stock LT1 cam that appeared in mid-1990's Corvettes and Z28s. Relative cam rotation was measured using timing a light, a fixed-timing distributor (the centrifugal advance in this distributor was disabled), and the stock timing markers. Figures 42, 43, and 44 are photographs of the test facility and the test engine with the device installed.

Several tests were run to explore the operation of the device, most of which were not data-collecting tests but visual tests to verify that the device was functioning properly. There were six data-gathering tests taken between December 30, 1998 and January 3, 1999. One of these tests verified that a maximum of 4° of cam rotation occurred by running the device without any leaf springs and another the estimated the amount of torque required to drive the valve train by running the device without the centrifugal weights. The final four tests explored the effects of changing the number of balancing springs used (2, 4, 6, and 8) on the operation of the mechanism.

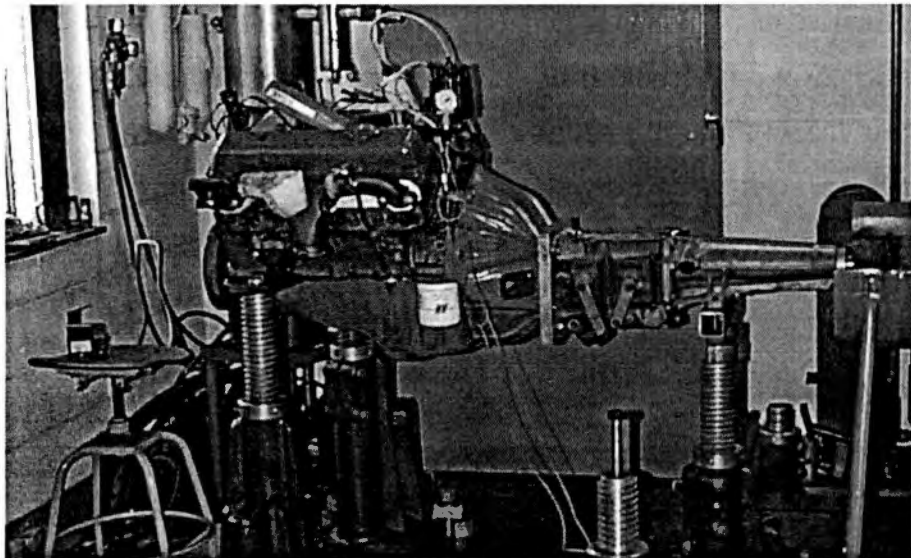


Figure 42 – Dynamic Testing, Engine on Test Stand

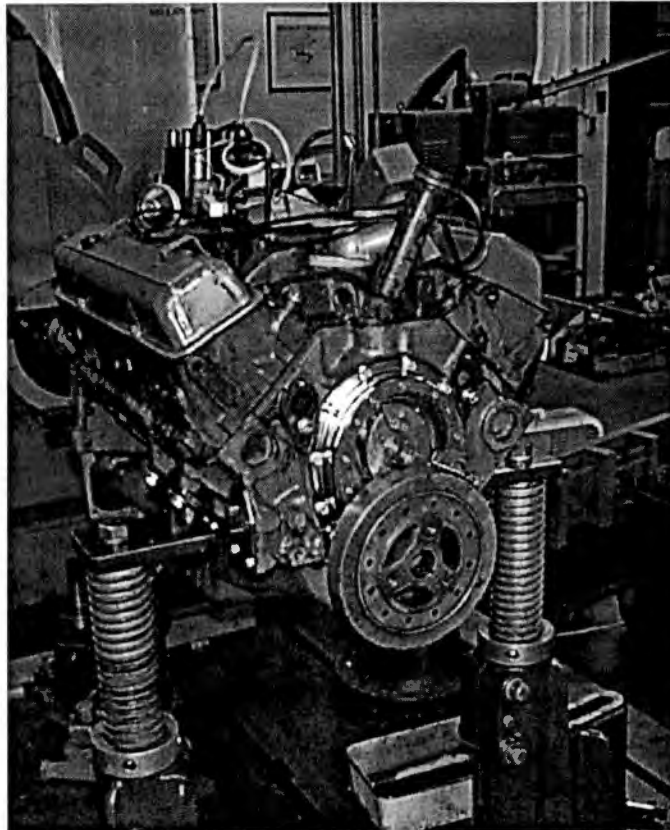


Figure 43 – Dynamic Testing, Device and Modified Timing Cover Installed on Test Engine

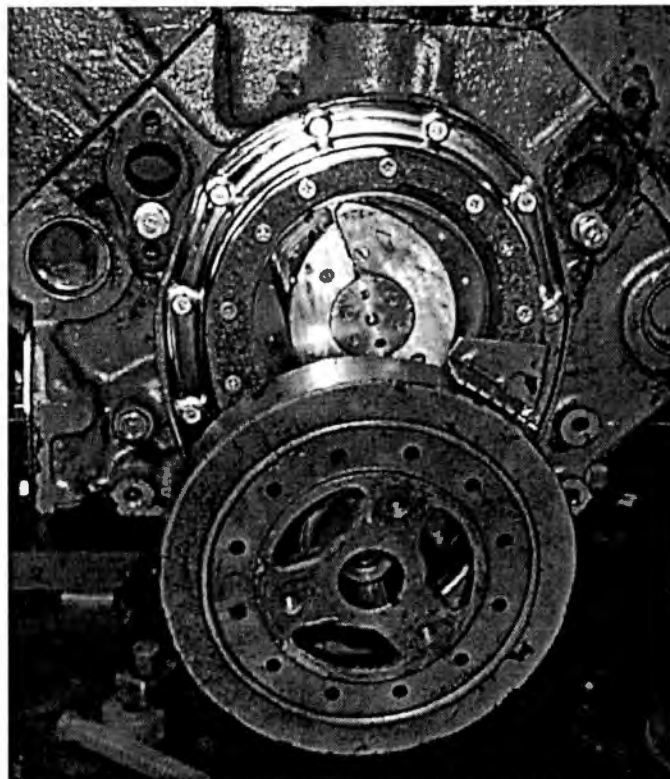


Figure 44 – Dynamic Testing, Close-up of Device and Modified Timing Cover Installed on Test Engine

Testing the effects of altering the number and length of the leaf springs was not performed during this time. Changing these parameters would allow "tuning" of the retard curve and would help to validate computer models and static testing findings.

Dynamic Testing Results and Analysis

The first test concerned with verifying that the device did in fact retard the camshaft 4° was disappointing because it did not retard 4° . The reason was found to be an error made during the design phase: the radius of the pin that slides in the slot was not taken into account! This limited the angle through which the weights rotate to about 17° . Consequently the camshaft was allowed only to retard approximately 3° .

The second test outlined above attempted to estimate the valve train torque by running the device without the centrifugal weights. Four springs proved to be the best number of balancing springs because the camshaft lagged behind the timing sprocket by 3.5° to 4° . Note that this test also proved the device to be robust in that it can still drive the valve train without the aid of the centrifugal weights.

The next set of tests examined the operation of the device with different numbers of balancing springs. These tests were very encouraging because the device worked as planned (with the exception of the fault found during the first test) and experienced very little hysteresis. Figures 45, 46, 47, and 48 are plots of the experimental data for eight, six, four, and two balancing springs respectively compared with the simulation predictions.

Note that the first two dynamic tests did not achieve the theoretical limit of about 3° of cam retard. This is because the balancing springs conspired to keep the weights from opening because the torque that they exerted on the device was much greater than the opposite torque that the valve train required. If the engine speed had been increased to approximately 4000 RPM, the camshaft would have finished retarding the remaining 0.5° . The last test, the one utilizing

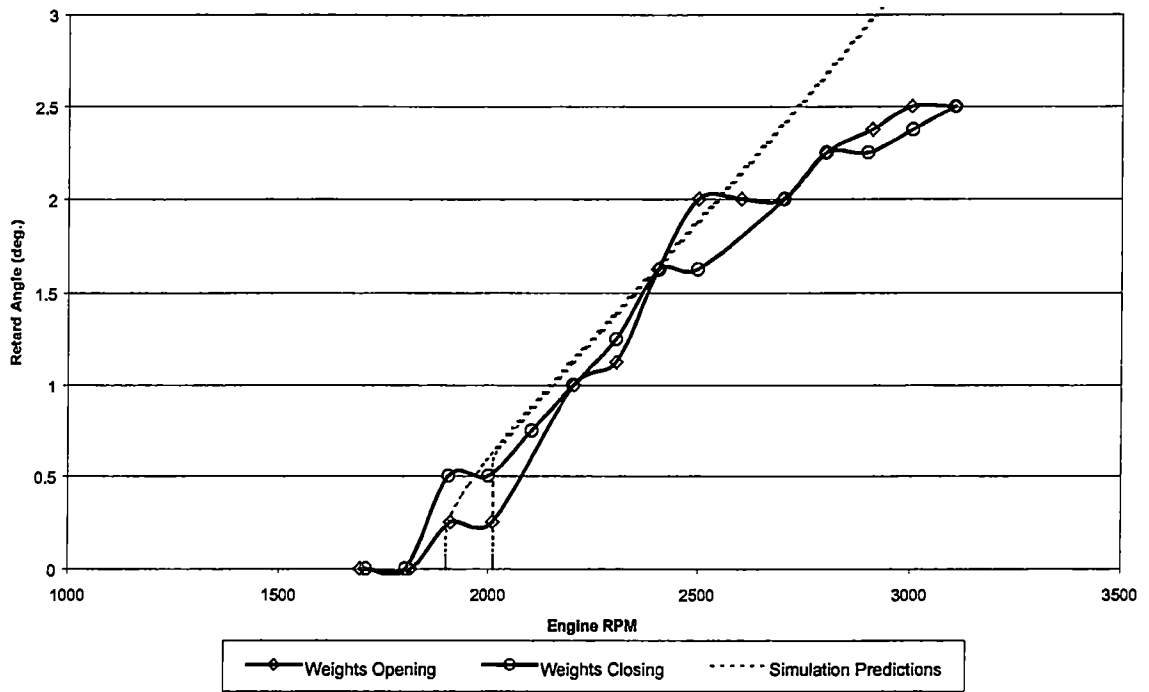


Figure 45 – Dynamic Results for a System with 8 Balancing Springs

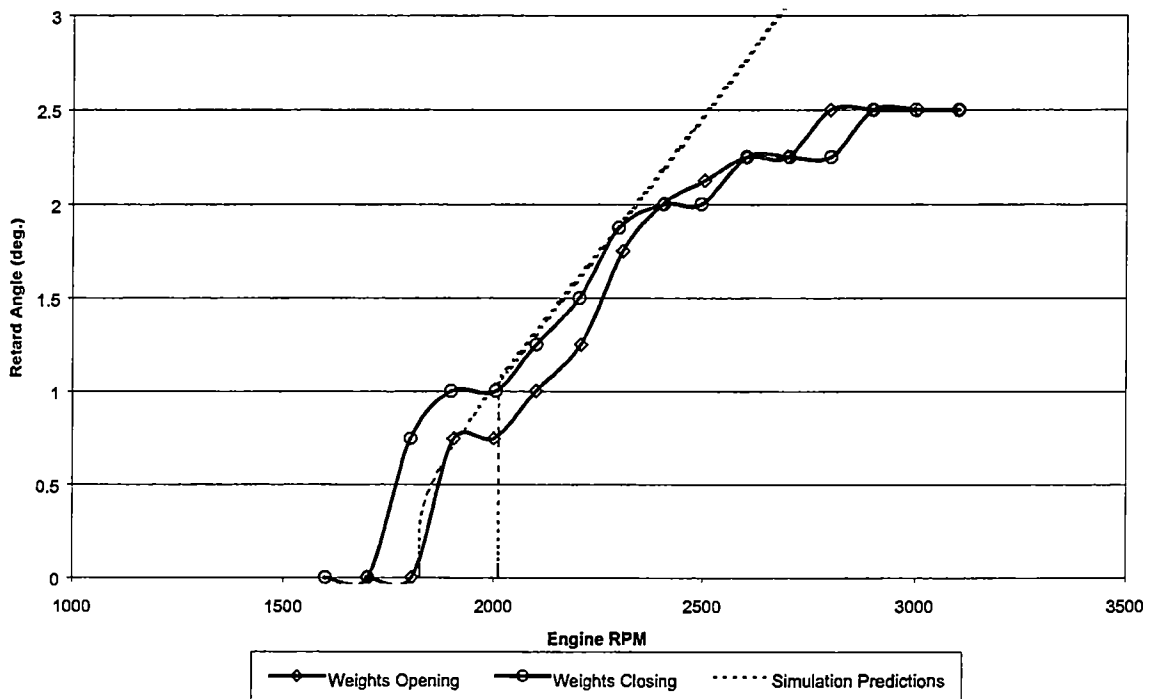


Figure 46 – Dynamic Results for a System with 6 Balancing Springs

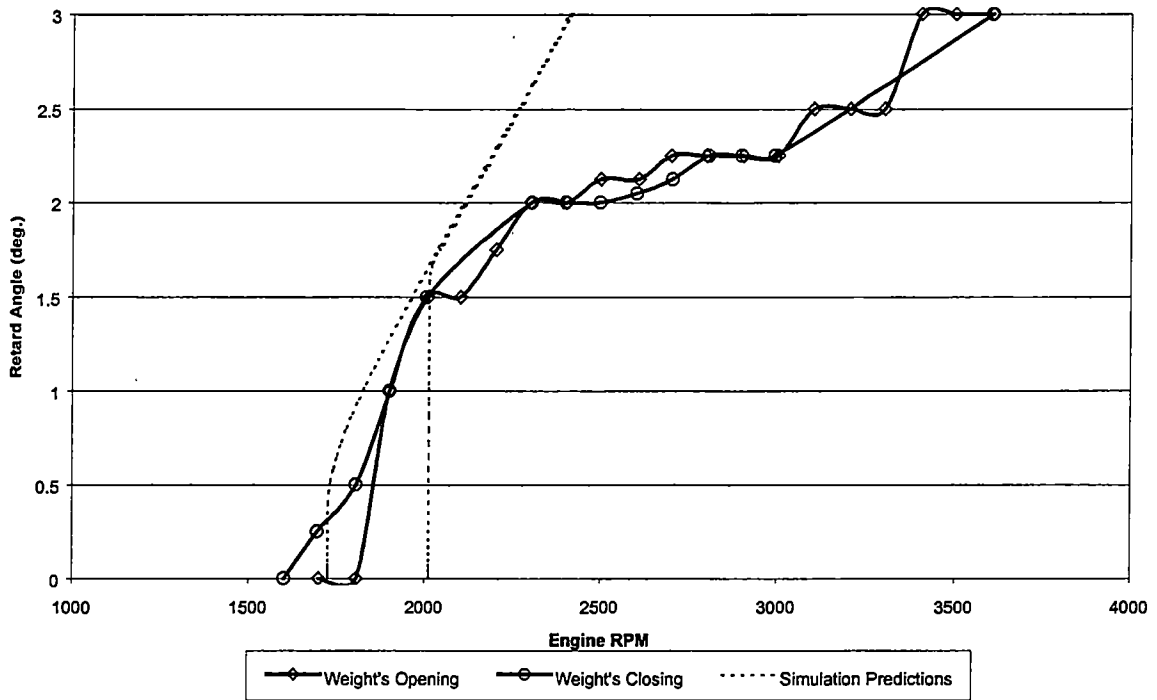


Figure 47 – Dynamic Results for a System with 4 Balancing Springs

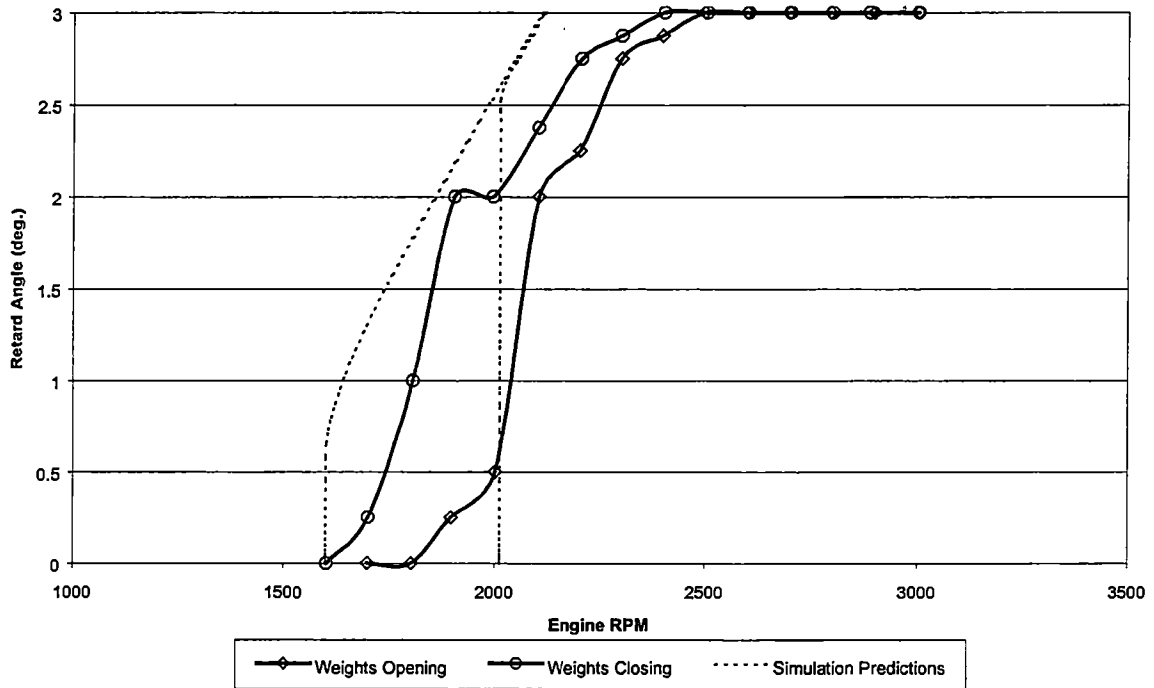


Figure 48 – Dynamic Results for a System with 2 Balancing Springs

only two balancing springs, illustrates the converse problem. Instead of restraining the weights from opening, having too few allows them to open too soon. During this test the device achieved the limit of 3° of cam retard by 2500 engine RPM. Four balancing springs proved to be the best number for this valve train and since the retard curve given in figure 47 best matches the desired operating parameters of having the retarding action occur between 2000 and 3000 engine RPM.

Uncertainties with this data arise from the method in which the data was gathered, a timing light and a person reading it. The first of which is due to the inaccuracy of the human eye; a misread of only 0.007-inch represents an error of 0.1°! This coupled with the fact that moving one's head just a little can yield a difference in measurement of more than 0.5°. During testing these facts were taken into consideration and steps were taken to avoid as much uncertainty as possible. Furthermore, each of the data gathering tests was run only once. This precluded any analysis concerning the standard deviation that would have obviated much of the uncertainty. The uncertainty in the test results, then, is estimated to be $\pm 0.5^\circ$ of cam rotation.

These results did not completely agree with those predicted by computer simulation. First, four balancing springs matched the desired operating range whereas the computer predicted six. Secondly, the dynamic results for both opening and closing better matched the simulation predictions for a closing weight. Also, the retard curves appeared to have a non-linear trend as the centrifugal weights approached full rotation whereas the predicted curves were linear.

The reasons for these discrepancies could include that the assumption that the friction in the slots represents a majority of the friction in the mechanism was false, and that the uncertainty in the data was high. Also, it can be inferred that the device was not completely backdrivable when the weights were in the closed position because of the absence of any unstable region in the curve.

Data was not the only valuable information gleaned from these tests. The

major weakness revealed in this design is the concept of having the entire device being held together by capturing or sandwiching the various components between the sprocket and cam extension on one side and the cam button on the other.

While this inadequacy was apparent, it became painfully obvious when, during testing on January 3, 1999, the device experienced a catastrophic failure. The failure resulted from under-tightening the cam button. When the cam button came out (out meaning that the part literally came through the timing cover), the weights were no longer constrained. As a result they flew out and the sprocket unseated itself from the cam extension. The device suffered a great deal of damage but was repairable and went on to perform a few more tests whose results were very similar to those outlined above. Though similar, it was deemed inappropriate to include these additional tests in any operational deviation studies because of additional uncertainties arising from the damage.

Visual inspection and comparison during and at the conclusion of testing also illuminated areas where improvements should be made in latter evolutions of the device. The region in and around the slots was found to be the area most in need of improvement. The slots showed marked wear and deformation after only a few tests from the high stresses that these areas were forced to endure.

CHAPTER 7

CONCLUSIONS AND RECOMMENDATIONS

The data and results support the conclusion that the prototype variable cam phasing device represents a viable design as it met or exceeded almost all expectations. As in all prototype designs, even those facets of its operation that did not meet the requisite requirements were learned from and illuminated areas where improvement could and should be made.

To reiterate, the device fits in an unmodified Chevrolet small-block under a slightly modified timing cover that fits under the standard engine accessories such as a water pump and a harmonic balancer. Its action occurs between 1800 and 3200 engine RPM which closely corresponded with the desired 2000 to 3000 engine RPM range desired. The torque dependency of the mechanism is reduced to a minimum, and it can be expected that this device operating on an engine with a similar valve-train will operate as expected. Also the springs have an acceptable service life with the leaf springs having a life in excess of 600,000 cycles (tested) and the extension springs expected to have a life well in excess of 1,000,000 cycles (predicted).

The biggest problem is that the device does not achieve the required 4° of camshaft retard. This problem is unlike the rest that were encountered in that it is the result of miscalculation and should have been avoided.

Other problems are in the wear and fatigue characteristics of the device. As mentioned the springs behave acceptably, but the slots wore at an unacceptably high rate. This is due in part to the material used in construction. The metal was very soft, easily machinable, low carbon steel. Had a harder grade of steel been used and/or had the material been heat treated, much of this deformation would not have occurred. Increasing the area on which the pins move by making the slots thicker and/or using a pin with a larger radius would be mandatory in any future work.

The unsatisfactory method by which the "cam button" part constrains the entire assembly is another area that merits improvement. A better way would be to have the weights bound by a shoulder bolt or a pin and snap ring.

When the "cam button" part failed and the "accident," outlined earlier, occurred, other problems or potential problems were illuminated that might or might not have otherwise surfaced. One of these is that the sprocket should be constrained from moving relative to the cam extension in both directions, not just one. Had this been so, the device would not have experienced such a catastrophic failure. This too should be a mandatory improvement should future work occur.

Future models should also have a reasonably low amount of torque dependency when the weights are in the closed position. Having a small amount of initial torque dependency likely reduces or eliminates the operating range over which the device is unstable.

Future testing should include multiple tests using the same set of variables to determine if any deviation occurs during operation. Also, data should be gathered by more accurate methods meaning that some sort of electronic sensing should be employed.

In conclusion, the device fails to meet two of the five requirements for a successful design. First, it does not retard the cam 4° , and, secondly, it does not have a satisfactory service life. However, if the prototype variable cam phasing device designed, built, and tested as part of this project is viewed as a proof of concept and a vehicle for future improvements then it is a success.

REFERENCES

REFERENCES

- [1] Demmelbauer-Ebner, W., Dachs, A., and Lenz, H. P., October, 1991, "Variable Valve Actuation", *Automotive Engineering*, pp. 12-16.
- [2] Dresner, T., and Barkan, P., (1989), "A Review and Classification of Variable Valve Timing Mechanisms", SAE Paper 890674
- [3] Speckhart, F., Professor of Mechanical Engineering, University of Tennessee, Personal Communication, 1997
- [4] Moisan, R., (1987), "Design of a Camshaft Gear for Variable Valve Timing in a 350 Cubic Inch Displacement Chevrolet High Performance Engine", Unpublished design project, The University of Tennessee, Knoxville, TN.
- [5] Conner, D. L., (1989), "The Design and Testing of a Cam Timing Delay Mechanism for High Performance Combustion Engines", Master's Thesis, The University of Tennessee, Knoxville, TN.
- [6] Griffin, T., Competition Cams, Inc., Personal Communication, 1998
- [7] Associated Spring, *Design Handbook*, Barnes Group, Inc. 1981.
- [8] Century Spring Corporation, *Stock Spring Parts Catalog*, Vol. 68.
- [9] Griffin, T., Competition Cams, Inc. *Proprietary Dynamometer Results*, 1998
- [10] T. Baumeister, L. Marks, *Standard Handbook For Mechanical Engineers*, Seventh Edition, McGraw – Hill Book Company, 1967

APPENDICES

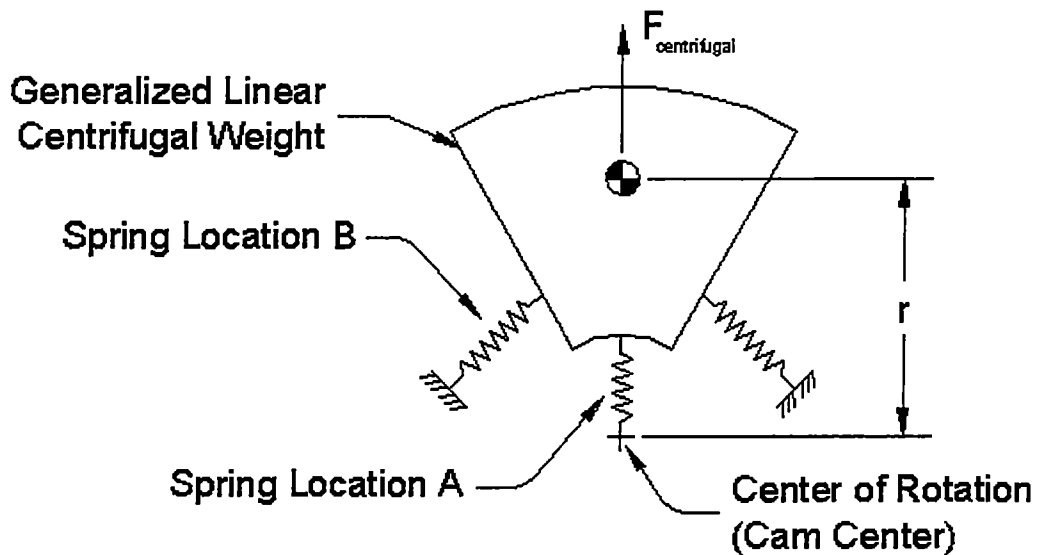
APPENDIX A

MATHEMATICAL MODELS OF THE DEVICE AND ITS SYSTEMS

CONTENTS OF APPENDIX A

A1. Linearly Translating Centrifugal Weight Calculations	61
A2. Centrifugal Torque Calculations	63
A3. Slot Analysis and Torque Dependency Calculations	64
A4. Proof that the final working angle between a line connecting the center of weight rotation and the pin, and a line connecting the center of camshaft rotation and the pin is predictable.	66
A5. Four-Bar Linkage Analysis with Torque Dependency Calculations.	67

Appendix A1
 Linearly Translating Centrifugal Weight Calculations



The differential equation governing a linearly translating centrifugal weight is given by,

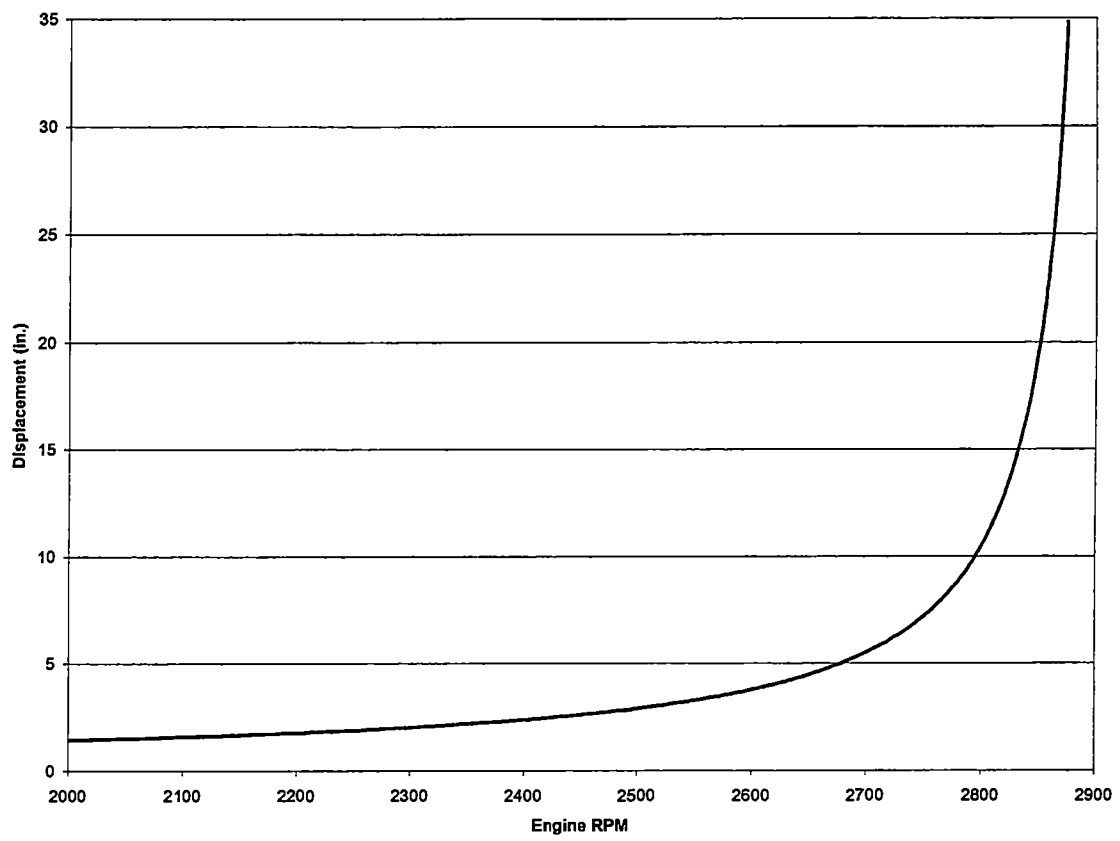
$$\Sigma F = ma = m(\ddot{r} - r\omega^2) = -c\dot{r} - k(r - r_{init})$$

$$\ddot{r} + \frac{c}{m}\dot{r} + \left(\frac{k}{m} - \omega^2\right)r = \frac{k}{m}r_{init}$$

Assuming a "quasi-static" model where the dynamic terms become zero (\ddot{r} and \dot{r} are zero), the position of the centrifugal weight reduces to the following:

$$r = \frac{\frac{k}{m}r_{init}}{\frac{k}{m} - \omega^2}$$

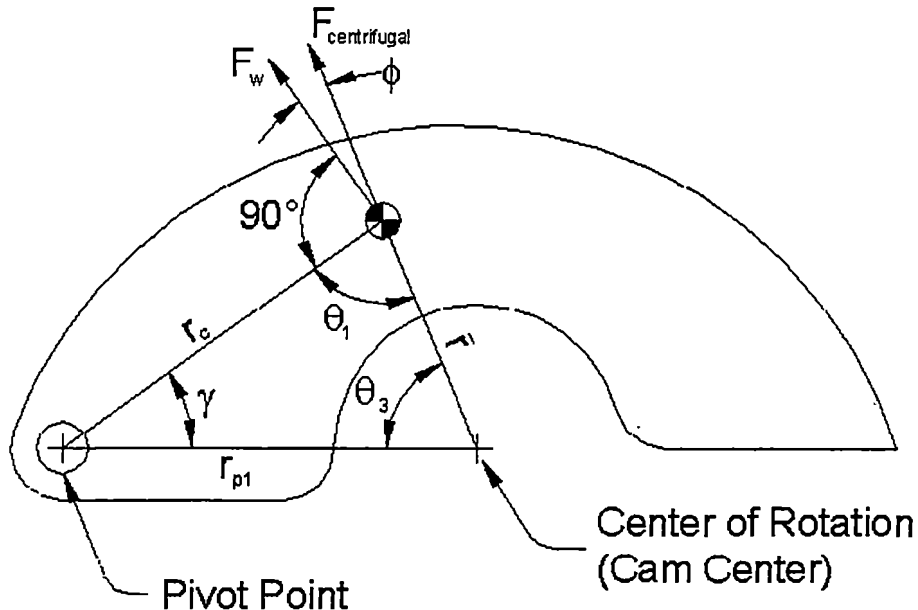
The following figure is the plot of the centrifugal weight's displacement, r , versus engine RPM (see Appendix C1 for Matlab code). Engine speed, recall, is twice the camshaft speed. It assumes a spring rate (k) of 30-in/lb, a mass of 0.5-lbm, an initial deflection (r_{init}) of 0.75-inches. Note that the movement of the centrifugal weight is predictable and that it follows an acceptable trend (small deflection for a large change in engine speed), but it rapidly degrades into an unstable system. The reason is that the spring force is linear whereas centrifugal force is quadratic.



Appendix A2

Centrifugal Torque Calculations

- Modeled to calculate the centrifugal torque of the weight for any configuration, rotation, and/or speed.
- Performed March 12, 1998



Conditions:

- r_c is known and constant
- r_{p1} is known and constant
- γ is known initially
- $\Delta\gamma$ is known

$$\gamma = \gamma_{init} + \Delta\gamma$$

$$\bar{r} = \sqrt{r_c^2 + r_{p1}^2 - 2r_c r_{p1} \cos \gamma}$$

$$\theta_1 = \sin^{-1} \left(\frac{r_{p1} \sin \gamma}{\bar{r}} \right)$$

$$\phi = 90^\circ - \theta_1$$

$$F_w = (m\bar{r}\omega^2) \cos \phi$$

$$T_w = F_w r_c$$

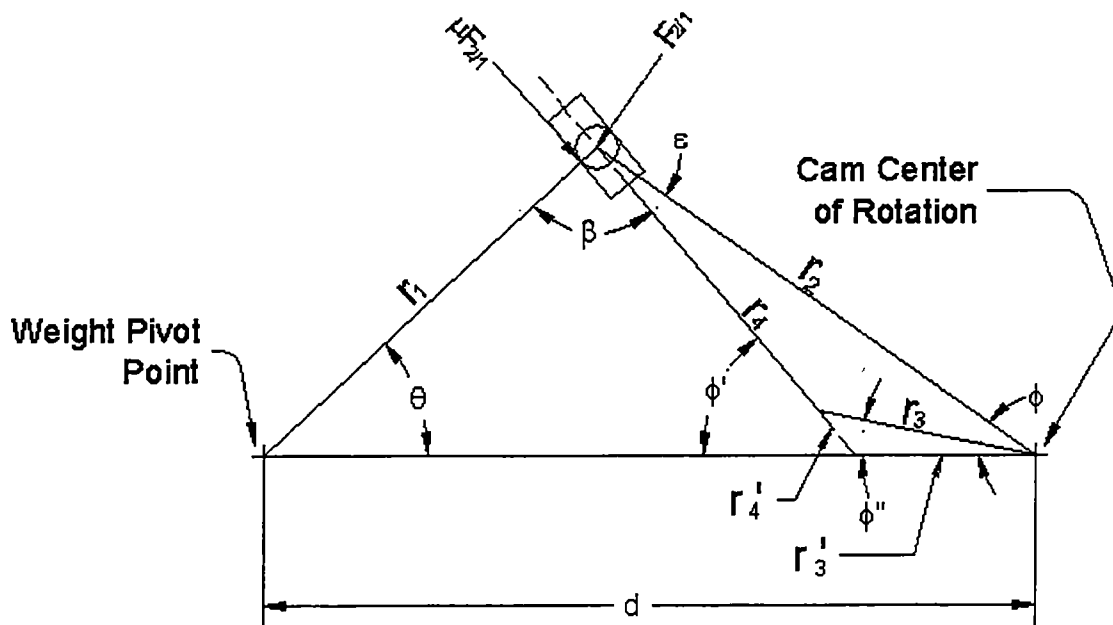
where F_w = centrifugal force along an axis from the center of rotation to the center of gravity,

T_w = torque generated by centrifugal force about the pivot of the weight.

Appendix A3

Slot Analysis and Torque Dependency Calculations

- Modeled to calculate the kinematics of the slot and pin at any time based on its initial conditions.
- Calculates the forces and torque associated with the slot's configuration based on the torque required to drive the valve train.
- Performed September 14, 1998.



Conditions:

- β is known initially.
- d is constant and known.
- r_1 is constant and known.
- $\Delta\theta$ is known.
- r_3 is constant and known.
- ϕ'' is initially 0 (zero).
- ε is unknown initially but remains constant.

Solve numerically for r_4 and then solve for the following initial and constant conditions.

$$d - r_3 = \sqrt{r_1^2 + r_4^2 - 2r_1r_4 \cos(\beta_{init})}$$

$$\phi'_{init} = \sin^{-1} \left(\frac{r_1 \sin(\beta_{init})}{d - r_3} \right)$$

$$\theta_{init} = \sin^{-1} \left(\frac{r_4 \sin(\beta_{init})}{r_1} \right)$$

$$\varepsilon = 180^\circ - \phi'_{init}$$

For each successive calculation, θ is known:

$$\theta = \theta_{init} + \Delta\theta$$

$$r_2 = \sqrt{r_1^2 + d^2 - 2r_1d \cos(\theta)}$$

$$\phi = \sin^{-1}\left(\frac{r_1 \sin(\theta)}{r_2}\right)$$

$$\varepsilon = \sin^{-1}\left(\frac{r_3 \sin(\theta)}{r_2}\right)$$

$$\phi - \phi'' = 180^\circ - \theta - \varepsilon$$

$$r_4 = \frac{r_3 \sin(\phi - \phi'')}{\sin(\varepsilon)}$$

$$\beta = 180^\circ - \theta - \phi - \varepsilon$$

$$r_4'' = \frac{r_1 \sin(\theta)}{\sin(180^\circ - \theta - \beta)} - r_4$$

$$r_3' = \sqrt{r_3^2 + r_4'^2 - 2r_3r_4' \cos(180^\circ - \varepsilon)}$$

$$\phi'' = \sin^{-1}\left(\frac{r_4' \sin(180^\circ - \varepsilon)}{r_3'}\right)$$

$\Delta\phi''$ is the cam retard angle. Forces and torques are given by,

$$F_{\frac{1}{2}} = \frac{T_{cam}}{r_2 (\cos(\varepsilon) - \mu \sin(\varepsilon))}$$

$$T_{cam/weight} = F_{\frac{1}{2}} r_1 (\sin(\beta) - \mu \cos(\beta))$$

where μ = coefficient of friction,

$T_{cam/weight}$ = backdriving torque exerted on the centrifugal weight,

T_{cam} = torque required to drive the valve train.

Appendix A4

Proof that the final working angle between the a line connecting the center of weight rotation and the pin, and a line connecting the center of camshaft rotation and the pin is predictable based on its initial angle.

- Based on the system modeled in Appendix A3; variables used in this proof are defined in Appendix A3.
- Performed September 15, 1998.

$$\theta_{init} + \beta_{init} + \phi'_{init} = 180^\circ$$

$$(\theta_{init} + \Delta\theta) + (\beta_{init} - \Delta\beta) + (\phi'_{init} + \Delta\phi') = 180^\circ$$

$$\Delta\phi' = \Delta\phi''$$

$$\beta_{init} - \Delta\beta = \beta_{end}$$

$$\beta_{end} = \beta_{init} - \Delta\theta + \Delta\phi'$$

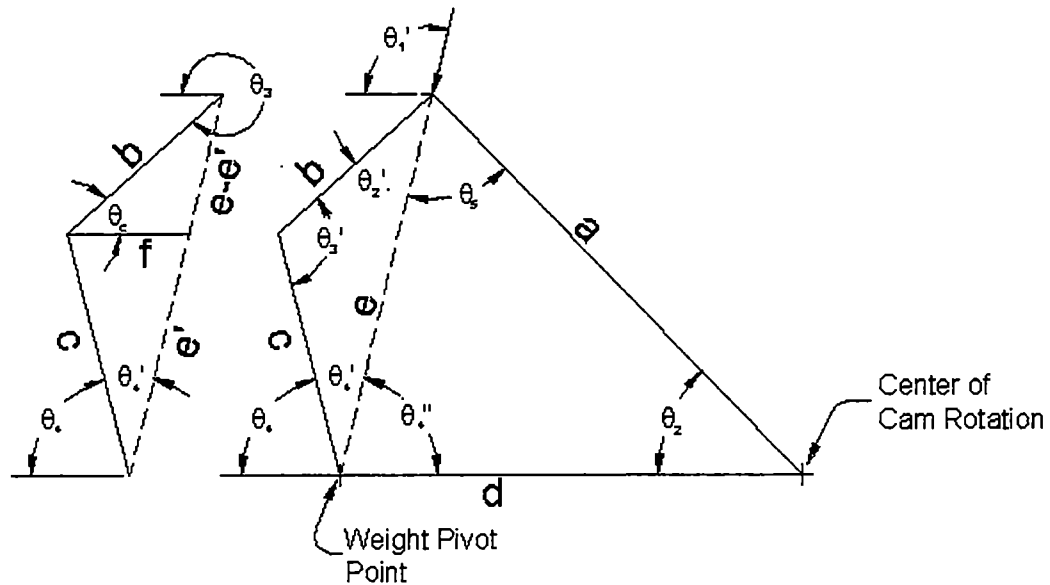
Hence, if $\beta_{init} = 90^\circ$, $\Delta\theta = 20^\circ$, $\Delta\phi' = 4^\circ$ (as it is in this design),

$$\beta_{end} = 90^\circ - 20^\circ + 4^\circ = 74^\circ.$$

Appendix A5

Four-bar Linkage Analysis

- Determines the non-crossed geometry of any four-bar linkage based on its initial conditions.
- Computes force and torque relationships.
- Performed December 23, 1997.



Conditions:

- Lengths a , b , c , and d are known and constant.
- θ_2 is known initially.
- $\Delta\theta_2$ is known.

The following equations are used to calculate the geometry of the system and are drawn from *Design of Machinery*, Robert L. Norton, 1992, McGraw-Hill Inc.

$$K_1 = d/a$$

$$K_2 = d/c$$

$$K_3 = \frac{a^2 - b^2 + c^2 + d^2}{2ac}$$

$$K_4 = d/b$$

$$K_5 = \frac{c^2 - d^2 - a^2 - b^2}{2ab}$$

$$A = \cos(\theta_2) - K_1 - K_2 \cos(\theta_2) + K_3$$

$$\begin{aligned}
B &= -2 \sin(\theta_2) \\
C &= K_1 - (K_2 + 1) \cos(\theta_2) + K_3 \\
D &= \cos(\theta_2) - K_1 + K_4 \cos(\theta_2) + K_5 \\
E &= -2 \sin(\theta_2) \\
F &= K_1 + (K_4 - 1) \cos(\theta_2) + K_5 \\
\theta_4 &= 2 \tan^{-1} \left(\frac{-B - \sqrt{B^2 - 4AC}}{2A} \right) \\
\theta_3 &= 2 \tan^{-1} \left(\frac{-E - \sqrt{E^2 - 4DF}}{2D} \right)
\end{aligned}$$

The following are the equations to determine the force/torque relationship for the system.

$$e = \sqrt{a^2 + d^2 - 2ad \cos(\theta_2)}$$

$$\theta_5 = \sin^{-1} \left(\frac{d}{e} \sin(\theta_2) \right)$$

$$\theta_4'' = 180^\circ - \theta_2 - \theta_5$$

$$\theta_4' = 180^\circ - \theta_4 - \theta_4''$$

$$\theta_2' = \frac{c}{b} \sin(\theta_4')$$

$$f = c \tan(\theta_4')$$

$$e' = \frac{f}{\sin(\theta_4')}$$

$$\theta_c = \sin^{-1} \left(\frac{e - e'}{f} \sin(\theta_2') \right)$$

$$T_{back} = \frac{T \cdot c}{a} \left(\frac{\cos(\theta_c)}{\cos(\theta_3 - \theta_2 + 90^\circ)} \right)$$

where T_{back} = backdriving torque on the centrifugal weight,
 T = torque required to drive the valve train.

APPENDIX B

SPRING ANALYSIS

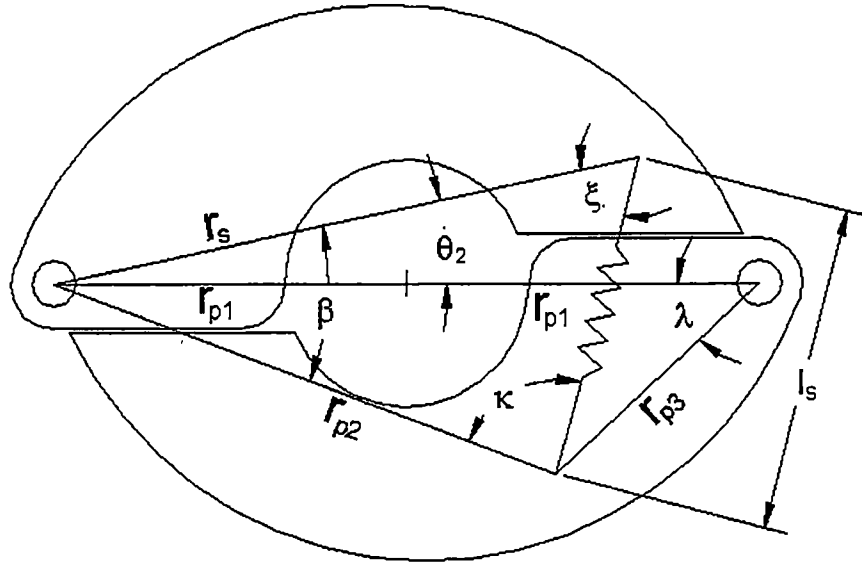
CONTENTS OF APPENDIX B

B1. Coil Spring Analysis	71
B2. Leaf Spring Analysis	73

Appendix B1

Coil spring analysis.

- Determines geometry of a coil spring system when anchored from weight to sprocket or from weight to weight at any weight rotation angle.
- Performed March 12, 1998 and March 31, 1998.



Conditions:

- r_s is known and constant.
- r_{p1} is known and constant.
- r_{p2} is known only for systems of springs anchored from weight to sprocket.
- β is known initially.
- $\Delta\beta$ is known for systems of springs anchored weight to sprocket.
- θ_2 is known, but is not necessary for systems of springs anchored weight to sprocket.
- $\Delta\theta_2$ is known, but is not necessary for systems of springs anchored weight to sprocket.
- λ is known initially, but is not necessary for systems of springs anchored weight to sprocket.
- $\Delta\lambda$ is known, but is not necessary for λ is known initially, but is not necessary for systems of springs anchored weight to sprocket.

For systems of coil springs anchored weight to sprocket:

$$\beta = \beta_{init} + \Delta\beta$$

$$l_s = \sqrt{r_s^2 + r_{p2}^2 - 2r_s r_{p2} \cos(\beta)}$$

$$\xi = \sin^{-1}\left(\frac{r_s \sin(\beta)}{l_s}\right)$$

$$T_{spring/weight} = \{F_{spring,initial} + k(l_s - l_{s,initial})\} r_s \sin(\xi)$$

where k = spring constant of the spring(s),

$$F_{spring,initial} = \frac{T_{weight,start}}{r_s \sin(\xi_{init})}$$

For systems of coil springs anchored weight to weight,

$$\theta_2 = \theta_{2,initial} + \Delta\theta_2$$

$$\lambda = \lambda_{initial} + \Delta\lambda$$

$$r_{p2} = \sqrt{(2r_{p1})^2 + r_{p3}^2 - 4r_{p1}r_{p3} \cos(\lambda)}$$

$$\beta = \sin^{-1}\left(\frac{r_s \sin(\lambda)}{r_{p2}}\right) + \theta_2$$

$$l_s = \sqrt{r_s^2 + r_{p2}^2 - 2r_s r_{p2} \cos(\beta)}$$

$$\kappa = \sin^{-1}\left(\frac{r_s \sin(\beta)}{l_s}\right)$$

$$\Omega = \sin^{-1}\left(\frac{2r_{p1} \sin(\lambda)}{r_{p2}}\right)$$

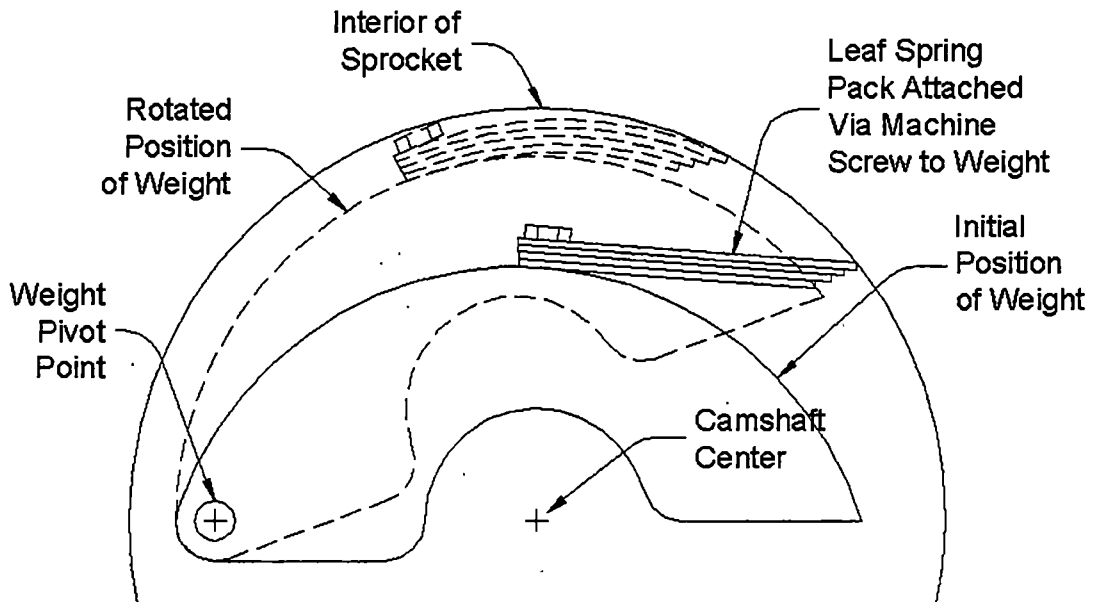
$$T_{spring/weight} = \{F_{spring,initial} + k(l_s - l_{s,initial})\}r_s \sin(\xi) + \{F_{spring,initial} + k(l_s - l_{s,initial})\}r_{p3} \sin(\Omega - \kappa)$$

where k = spring constant of the spring(s),

$$F_{spring,initial} = \frac{T_{weight,start}}{r_s \sin(\xi_{initial}) + r_{p3} \sin(\Omega_{init} - \kappa_{initial})}$$

Appendix B2
Leaf spring analysis.

The parameters of the leaf spring pack (see following figure) were chosen through a process of both theoretical and analytical analysis. It was deemed optimal to have a constant radius of curvature thus ensuring that stress is constant along the length of a spring leaf. The radius of curvature and the maximum stress in the bottom leaf were the most critical parameters. Concurrent to this analysis was determining the length and number of spring leaves that were required to generate a given amount of torque. The torque that that was required of the leaf springs was equal to the torque generated by centrifugal acceleration.



The spring rate of cantilever springs is proportional to the cube of the spring's thickness times the width:

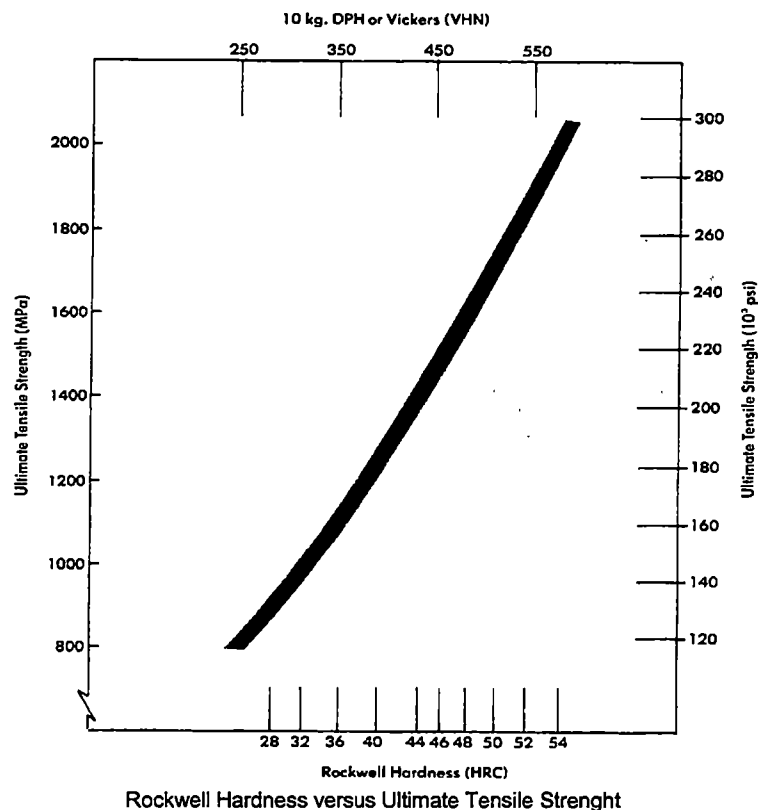
$$k \propto b \cdot t^3$$

This means that, holding the width of the spring constant, a change in thickness of 0.005-inches increased the spring rate by,

$$\begin{aligned}
 \text{difference} &= \frac{|b(t_1^3 - t_s^3)|}{bt_1^3} \times 100\% = \frac{|t_1^3 - t_s^3|}{t_1^3} \times 100\% \\
 &= \frac{|0.020^3 - 0.025^3|}{0.020^3} \times 100\% = 95.3\%
 \end{aligned}$$

Therefore, an increase in the spring thickness means that the radius of curvature over which the springs deflect can be increased. This is because it requires fewer springs to generate the same torque, even though they are slightly thicker.

However, the constrictive space requirements became the deciding factor because of stress. The spring material was feeler gage stock and was assumed to have a Rockwell hardness of C54 which corresponds to an ultimate tensile strength of 300,000-psi (see figure below). To achieve a fatigue life of 1,000,000-cycles, the repetitive stress cannot exceed 50% of the ultimate tensile stress, in this case 150,000-psi.



The stress in the bottom spring is given by,

$$\sigma = \frac{E \cdot y}{r}$$

where σ is stress,

E is the modulus of elasticity,

y is half of the thickness of the leaf,

r is the radius of curvature.

A leaf spring pack consisting of 0.025-inch thick material would require 5 leaves to produce the desired torque. Allow for seven springs (for future tunability) and screw with a 0.080-inch head height. The radius of curvature was found by subtracting material thickness from the maximum radius of 2.245-inches to give,

$$2.245 - 7 \cdot 0.025 - 0.80 = 1.99\text{-inches.}$$

This gave a maximum stress of,

$$\frac{30E6 \cdot 0.025 / 2}{1.99} = 188,400\text{-psi.}$$

This number is much too high.

A leaf spring pack consisting of 0.020-inch thick material would require 8 spring leaves to generate the desired torque. Allow for 11 spring leaves (again, for future tunability) and a screw with a 0.080-inch head height. The radius of curvature was given by,

$$2.245 - 11 \cdot 0.020 - 0.080 = 1.945\text{-inches.}$$

This gave a maximum stress of,

$$\frac{30E6 \cdot 0.020 / 2}{1.945} = 154,200\text{-psi.}$$

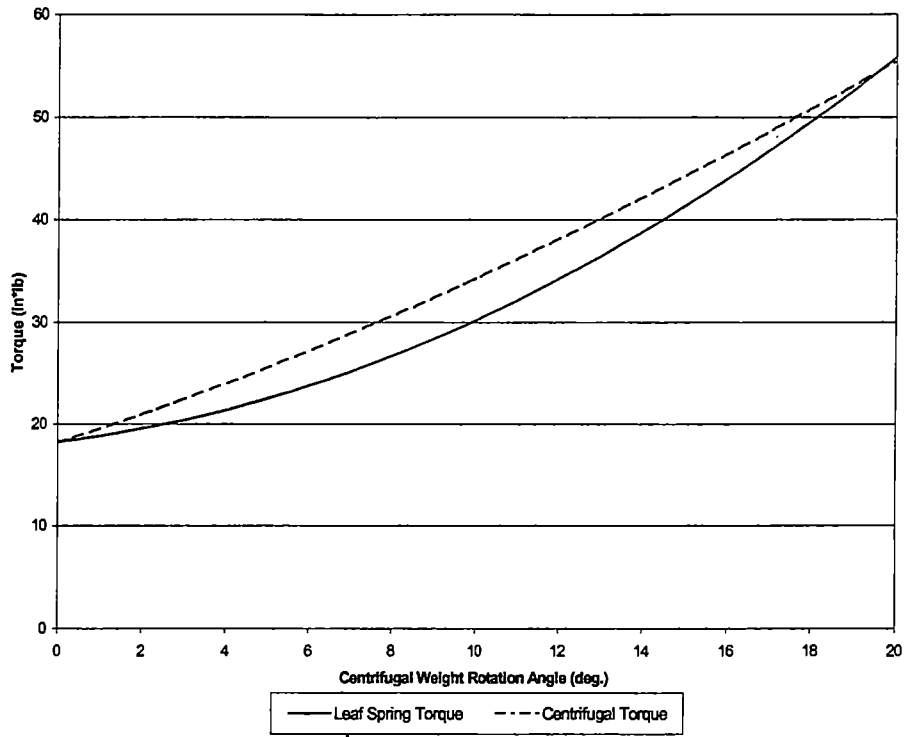
This amount was deemed to be satisfactory by cyclically testing the spring pack to more than 600,000-cycles with no discernable loss. Note that one cycle is having the centrifugal weight open completely and then close completely.

The following table is a listing of the length and order of each spring leaf. The lengths were determined experimentally. A longer spring had a higher initial torque because it had a higher initial deflection; a shorter spring had a lower initial torque. Conversely, the torque generated by a longer spring at full deflection is less than that of a shorter spring. If the springs are stacked such

that the spring leaves are shorter as the distance from the center increases, the total torque generated by the spring pack is the sum of the torque generated by the individual springs. However, if the springs are inverted, meaning that a longer spring is on top of a shorter one, then the total torque is not additive. The effects of this type of arrangement are such that the initial torque is considerably higher (because the shorter springs are deflecting more, initially, under the longer springs) and that the final torque is about the same.

Leaf Spring Pack Used in both Static and Dynamic Testing.	
Note that spring material is 0.500 wide x 0.020 thick.	
Spring	Length (Inches)
1 (Bottom Leaf)	2.25
2	2.25
3	2.375
4	2.5
5	2.5
6	2.5
7	2.625
8 (Top Leaf)	2.625

The following figure is a plot of the theoretical torque generated by centrifugal acceleration and the torque generated by the leaf spring pack used during testing. Note that while both curves are quadratic, the centrifugal torque is more linear than the leaf spring torque thus the leaf spring torque is equal to centrifugal torque only at the endpoints. This means that, if the balancing spring torque is closely matched with the torque required to drive the valve train, the device will always begin and end at the correct engine speed.



APPENDIX C

COMPUTER PROGRAMS

CONTENTS OF APPENDIX C

C1. Linearly Translating Centrifugal Weight Program	80
C2. Centrifugal Torque of the Centrifugal Weight Program	81
C3. Slot Analysis Program with Backdriving Torque Calculations	82
C4. Four-Bar Linkage Program with Backdriving Torque Calculations	84
C5. Coil Spring Program to Compute Deflection and Stress	86
C6. Total Mechanism Simulation	89

Appendix C1 Linearly Translating Centrifugal Weight Program

The purpose of this program was to predict the position of a linearly translating centrifugal weight based on its conditions including spring rate, mass, and the initial stretch of the spring.

```

%%%%%%%%%%%%%%%%%%%%%%%%%%%%%%%%%%%%%%%%%%%%%%%%%%%%%%%%%%%%%%%%%%%%%%%%%%
%LINEAR.M
%
%Program to solve for the position of a linearly
%translating centrifugal weight based on engine
%RPM. Uses a quasi-static model.
%%%%%%%%%%%%%%%%%%%%%%%%%%%%%%%%%%%%%%%%%%%%%%%%%%%%%%%%%%%%%%%%%%%%%%%%%%

rpm=2000:5:2875; %range of engine RPM
w=(rpm/120)*2*pi; %converts to cam speed (rad/s)

k=30; %spring rate (lb/in)
m=0.5/386; %mass of weight (blobs)
r_init=0.75; %initial spring stretch (in)

for i=1:length(rpm),
    r(i)=((k/m)*r_init)/((k/m)-w(i)^2);
end

```

Appendix C2 Centrifugal Torque of the Centrifugal Weight Program

The purpose of this program was to predict the torque generated by the centrifugal acceleration of the weight about its pivot point.

```

%%%%%%%%%%%%%%%%%%%%%%%%%%%%%%%%%%%%%%%%%%%%%%%%%%%%%%%%%%%%%%%%%%%%%%%%
%WEIGHT.M
%
%Program calculates centrifugal torque of the
%weight based on the dimensions and properties of
%the weight.
%
%Assumes that weight is a rigid body.
%
%John C. McCracken - March 14, 1998
%Contains elements of calculations dated:
%   March 12,1998
%%%%%%%%%%%%%%%%%%%%%%%%%%%%%%%%%%%%%%%%%%%%%%%%%%%%%%%%%%%%%%%%%%%%%%%%

del_weight=20;           %pivot angle in degrees
m=.5076/386;           %in blobs
rpm_start=2000;        %in engine rpm
rpm_end=3000;          %in engine rpm
r_p1=2;                %d from cam center to weight hub
rc=1.7354;             %d from hub to cg (inches)
gamma=21.217;          %angle rc makes with r_p1 (degrees)
N=100;                 %number of points to calculate

%Calculations follow
GAMMA=gamma*pi/180;
DEL_WEIGHT=linspace(0,(del_weight*pi/180),N);
rpm=linspace(rpm_start,rpm_end,N);
for i=1:N,
    w(i)=((rpm(i)/60)/2)*2*pi;
    r_bar(i)=sqrt(rc^2+r_p1^2-(2*rc*r_p1*cos(GAMMA)));
    theta1(i)=asin(r_p1*sin(GAMMA)/r_bar(1,i));
    phi_w(i)=(pi/2)-theta1(1,i);
    Tw(i)=m*r_bar(i)*w(i)^2*rc*cos(phi_w(i));
end

```

Appendix C3 Slot Analysis Program with Backdriving Torque Calculations

This program computes the geometry of the slot and pin as a function of centrifugal weight rotation angle. From the geometry, the camshaft retard angle as a function of weight rotation is calculated. The backdriving torque as a function of either is calculated based on the torque required to drive the valve train.

```

%%%%%%%%%%%%%%%%%%%%%%%%%%%%%%%%%%%%%%%%%%%%%%%%%%%%%%%%%%%%%%%%%%%%%%%%
% SLOT.M
%
% Slot analysis program that computes the geometry
% of a slot and pin mechanism. Calculates the retard
% and backdriving torque curves taking friction into
% account.
%
% John McCracken - September 18, 1998
% Contains elements of calculations dated:
%     September 14, 1998
%%%%%%%%%%%%%%%%%%%%%%%%%%%%%%%%%%%%%%%%%%%%%%%%%%%%%%%%%%%%%%%%%%%%%%%%

% Constants used throughout model
T=150;                % torque require to drive cam
                    (in*lbf)
del_weight=20*pi/180; % in radians
mu=0.075;            % friction coefficient between slot
                    and pin
r_p1=2.0;            % d from cam center to weight hub
beta_init=90*pi/180; % in radians
r1=1.773;           % in inches (1.773)
r3=0.000001;       % in inches
rp=0.125;          % in inches, radius of pin
d=r_p1;            % d and r_p1 must be the same

%%%%%%%%%%%%%%%%%%%%%%%%%%%%%%%%%%%%%%%%%%%%%%%%%%%%%%%%%%%%%%%%%%%%%%%%
% Bisection routine numerically solves for initial
% conditions.
%%%%%%%%%%%%%%%%%%%%%%%%%%%%%%%%%%%%%%%%%%%%%%%%%%%%%%%%%%%%%%%%%%%%%%%%
dl=5;
r4bis=0;
while abs(dl)>0.00001
    dl=dl/2;
    if sqrt(r1^2+r4bis^2-2*r1*r4bis*cos(beta_init))<(r_p1-
r3),
        r4bis=r4bis+dl;

```

```

elseif sqrt(r1^2+r4bis^2-
2*r1*r4bis*cos(beta_init))>(r_p1-r3),
    r4bis=r4bis-dl;
end
end
r4_init=r4bis;
theta_init=asin(r4_init*sin(beta_init)/(r_p1-r3));
phip_init=asin(r1*sin(beta_init)/(d-r3));
zeta=pi-hiph_init;

%%%%%%%%%%%%%%%%%%%%%%%%%%%%%%%%%%%%%%%%%%%%%%%%%%%%%%%%%%%%%%%%%%%%%%%%
%Loop computes the configuration of the slot,      %
%the backdriving torque, and the rotation of the %
%cam as the weight opens.                        %
%%%%%%%%%%%%%%%%%%%%%%%%%%%%%%%%%%%%%%%%%%%%%%%%%%%%%%%%%%%%%%%%%%%%%%%%
i=1;
for th=theta_init:(del_weight/49):(theta_init+del_weight),
    theta(i)=th;
    r2(i)=sqrt(r1^2+d^2-2*r1*d*cos(theta(i)));
    phi(i)=asin(r1*sin(theta(i))/r2(i));
    E(i)=asin(r3*sin(zeta)/r2(i));
    phiminushiph(i)=pi-E(i)-zeta;
    r4(i)=r3*sin(phiminushiph(i))/sin(E(i));
    beta(i)=pi-phi(i)-theta(i)-E(i);
    r4p(i)=(r1*sin(theta(i))/sin(pi-theta(i)-beta(i)))-
r4(i);
    r3p(i)=sqrt(r3^2+r4p(i)^2-2*r3*r4p(i)*cos(pi-zeta));
    phipp(i)=asin(r4p(i)*sin(pi-zeta)/r3p(i));

    F21(i)=1/(r2(i)*(cos(E(i))-mu*sin(E(i))));
    Tc(i)=F21(i)*r1*(sin(beta(i))-pi/2);
    T_open(i)=Tc(i)+mu*sin(beta(i));
    T_close(i)=-Tc(i)+mu*sin(beta(i));

    i=i+1;
end
del_cam=(phipp-phipp(1))*180/pi;

```

Appendix C4 Four-Bar Linkage Program with Backdriving Torque Calculations

The purpose of this program was to calculate the geometry of a four-bar linkage retard mechanism as a function of camshaft retard angle. The geometry of the linkage gives the rotation angle of the centrifugal weight as a function of camshaft retard angle and is used to compute the backdriving torque.

```

%%%%%%%%%%%%%%%%%%%%%%%%%%%%%%%%%%%%%%%%%%%%%%%%%%%%%%%%%%%%%%%%%%%%%%%%
%FOURBAR.M
%
%Fourbar linkage analysis program that computes the
%geometry of the linkage as a function of camshaft
%retard angle and computes the backdriving torque
%exerted on the cam based on the total valve train
%torque.
%
%Equations derived from those in "Design of
%Machinery" by R.L. Norton

%Assumes links are rigid bodies.
%
%John McCracken - December 24, 1997
%Contains elements of calculations dated:
%    December 23, 1997
%%%%%%%%%%%%%%%%%%%%%%%%%%%%%%%%%%%%%%%%%%%%%%%%%%%%%%%%%%%%%%%%%%%%%%%%

T=1;           %torque (in/lbf) required to drive cam
theta=37       %maximum angle of theta2 in degrees
del=4;

a=2.5;        %length of first 1 DOF link
d=2;          %length of stationary link
b=0.5454;     % length of second 1 DOF link

%Calculates last length based on other lengths
bc=sqrt(a^2+d^2-(2*a*d*cos((theta)*(pi/180)));
c=bc-b;       %calculates last link

i=1;
for theta2=((theta-del)*pi/180):0.001:(theta*pi/180),
    x(1,i)=theta2;
    e=sqrt(a^2+d^2-(2*a*d*cos(theta2)));

    K1=d/a;
    K2=d/c;

```



```

K3=(a^2-b^2+c^2+d^2)/(2*a*c);
K4=d/b;
K5=(c^2-d^2-a^2-b^2)/(2*a*b);

A=cos(theta2)-K1-(K2*cos(theta2))+K3;
B=-2*sin(theta2);
C=K1-((K2+1)*cos(theta2))+K3;
D=cos(theta2)-K1+(K4*cos(theta2))+K5;
E=-2*sin(theta2);
F=K1+((K4-1)*cos(theta2))+K5;

theta4(1,i)=(2*atan((-B-sqrt(B^2-
4*A*C))/(2*A)))*(180/pi);
theta3(1,i)=(2*atan((-E-sqrt(E^2-
4*D*F))/(2*D)))*(180/pi);
theta4(1,i)=theta4(1,i)*(pi/180);
theta3(1,i)=theta3(1,i)*(pi/180);
theta5(1,i)=asin((d/e)*sin(theta2));
theta4pp(1,i)=pi-theta2-theta5(1,i);
theta4p=pi-theta4(1,i)-theta4pp(1,i);
theta2p=(c/b)*sin(theta4p);

f=c*tan(theta4p);
ep=f/sin(theta4p);
thetac=asin(((e-ep)/f)*sin(theta2p));

thetab=theta3(1,i)-theta2+(pi/2);

Tc(1,i)=((T*c)/a)*(cos(thetac)/cos(thetab));

i=i+1;
end
X=x*(180/pi);
plot(X,Tc)

```

Appendix C5 Coil Spring Program to Computing Deflection and Stress

The following program computes the total deflection, initial deflection, and stress in a helical, compression spring based on the springs dimensions and spring rate. This program is indicative of many and could include loops to search for optimal dimensions, be modified for extension springs, or be used for nested spring combinations.

```

%%%%%%%%%%%%%%%%%%%%%%%%%%%%%%%%%%%%%%%%%%%%%%%%%%%%%%%%%%%%%%%%%%%%%%%%
%COIL1.M
%
%This program determines the total deflection,
%initial deflection, and stress in a coil,
%compression spring of given size and rate.
%
%John McCracken - September 25, 1998
%Contains elements of calculations dated:
%   March 12,1998
%%%%%%%%%%%%%%%%%%%%%%%%%%%%%%%%%%%%%%%%%%%%%%%%%%%%%%%%%%%%%%%%%%%%%%%%

%dimensions (in.) and angles (deg.)
r_p1=2.0;
rc=2.521;
rs=3.25;
r_p2=3.617;
gamma=36.509;
beta=13.889;

%mass and starting, radial displacement, and ending rpm
rpm_start=2000;      %in engine rpm
delta=20;            %weight rotation (degrees)

%spring constants
k=173.56;            %spring constant
wire_d=0.04;        %wire diameter (in.)
N=10.2;             %number of turns
OD1=0.7;            %outside dia of spring (in.)
Compress_L=1.3;     %compressed length of spring (in.)
S_max=150E3;        %maximum stress spring can handle
                    (psi)
G=11.5E6;           %Young's modulus (psi)

%convert anglular measurements to radians
gamma_r=gamma*(pi/180);
beta_r=beta*(pi/180);

```

```

w_start=((rpm_start/2)/60)*2*pi;    %in cam rad/sec

%stepsize is the step size in loops
stepsize=0.000698132;

%loop to compute centripetal torque; angles and lengths
that change
i=1;
for DELTA=0:stepsize:(delta*pi/180),
    %changing angles
    GAMMA(1,i)=gamma_r+DELTA;
    BETA(1,i)=beta_r+DELTA;

    %compute lengths that change and angles that change with
lengths
    r_bar(1,i)=sqrt(rc^2+r_p1^2-
(2*rc*r_p1*cos(GAMMA(1,i))));
    ls(1,i)=sqrt(rs^2+r_p2^2-(2*rs*r_p2*cos(BETA(1,i))));
    xi(1,i)=asin(r_p2*sin(BETA(1,i))/ls(1,i));
    theta1(1,i)=asin(r_p1*sin(GAMMA(1,i))/r_bar(1,i));
    phi(1,i)=(pi/2)-theta1(1,i);

    i=i+1;
end

del_spring=ls(end)-ls(1);
Tw_start=m*r_bar(1,1)*w_start^2*rc*cos(phi(1,1));
F_init=Tw_start/(rs*sin(xi(1,1)));

%loop to compute initial deflection
Tw_start=m*r_bar(1,1)*w_start^2*rc*cos(phi(1,1));
F_init=Tw_start/(rs*sin(xi(1,1)));
del_init=F_init/k;
del=del_init+del_spring;

%convert some radian measurements to degrees for plotting
purposes
GAMMA_d=GAMMA*(180/pi);
BETA_d=BETA*(180/pi);
DELTA_d=(0:stepsize:delta*(pi/180))*180/pi;

%spring calculations to arrive at stress
D1(i)=OD1-wire_d;
C1(i)=D1(i)/wire_d;
d1(i)=wire_d;
Na1(i)=N;

```

```
k(i)=G*d1(i)^4/(8*D1(i)^3*Na1(i));  
P(i)=k(i)*del_spring;  
Kw1_1(i)=(4*C1(i)-1)/(4*C1(i)-4)+0.615/C1(i);  
S1(i)=8*P1(i)*D1(i)*Kw1_1(i)/(pi*d1(i)^3);
```

Appendix C6
Total Mechanism Simulation

The program simulates the mechanism in its entirety. It combines the programs listed above and incorporates and analysis of the balancing springs similar and the analytical leaf spring data to compute the retard curves as a function of engine RPM. It does this for circumstances both when the weights are opening and closing and can thus predict hysteresis. This model is a "quasi-static" simulation meaning that dynamic effects and damping are either negligible or that there is not enough information is available to be predicted.

```
%%%%%%%%%%%%%%%%%%%%%%%%%%%%%%%%%%%%%%%%%%%%%%%%%%%%%%%%%%%%%%%%%%%%%%%%%  
%CAM.M                                                                    %  
%                                                                    %  
%Complete cam retarder simulation including back- %  
%driving and friction. Computes slot configuration, %  
%backdriving torque curves, and retard curves for %  
%all engine speeds. %  
%                                                                    %  
%Lumped type model that employs quasi-static type %  
%(dynamic approximation) modeling. %  
%                                                                    %  
%John McCracken - September 25, 1998 %  
%Contains elements of calculations dated: %  
%   March 12,1998 %  
%   March 31,1998 %  
%   April 27,1998 %  
%   August 31,1998 %  
%   September 14, 1998 %  
%%%%%%%%%%%%%%%%%%%%%%%%%%%%%%%%%%%%%%%%%%%%%%%%%%%%%%%%%%%%%%%%%%%%%%%%%  
  
%%%%%%%%%%%%%%%%%%%%%%%%%%%%%%%%%%%%%%%%%%%%%%%%%%%%%%%%%%%%%%%%%%%%%%%%%  
%Fixed variables and initial conditions. %  
%%%%%%%%%%%%%%%%%%%%%%%%%%%%%%%%%%%%%%%%%%%%%%%%%%%%%%%%%%%%%%%%%%%%%%%%%  
%Torque required to drive cam  
T=150; %in in*lbF  
%Variables used throughout model  
del_weight=20*pi/180; %in radians  
m=.5076/386; %in blobs  
mu=0.1; %friction coefficient  
r_p1=2; %d from cam center to weight hub  
%Variables used in slot calculations  
beta_init=90*pi/180; %in radians  
r1=1.773; %in inches (1.773)  
r3=0.000001; %in inches  
rp=0.125; %in inches, radius of pin
```

```

d=r_p1; %d and r_p1 must be the same
%Balancing spring constants
k=314; %in lbf/in
F_init=10; %in lbf
r_sp_pin=1.8062; %in inches
r_sp=1.320; %in inches
Free_L=0.7; %in inches
ls_init=0.705; %in inches
angle1_init=19.031; %in degrees
N=2; %number of retaining springs
%Variables used in centrifugal calculations
rc=1.7354; %d from hub to cg, inches
gamma=21.217*pi/180; %angle rc makes with r_p1 (radians)
%Leaf spring torque vs. rotation angle (enter as two row
vectors)
measured_T=[18 23 30 41 56];
measured_angle=[0 5 10 15 20];

%%%%%%%%%%%%%%%%%%%%%%%%%%%%%%%%%%%%%%%%%%%%%%%%%%%%%%%%%%%%%%%%%%%%%%%%
%Following routine solves for initial conditions of %
%slot necessary to complete slot computations. %
%Numerical solution for r4 and closed-form solution %
%for theta and zeta. %
%%%%%%%%%%%%%%%%%%%%%%%%%%%%%%%%%%%%%%%%%%%%%%%%%%%%%%%%%%%%%%%%%%%%%%%%
dl=5;
r4bis=0;
%bisection routine
while abs(dl)>0.00001
    dl=dl/2;
    if sqrt(r1^2+r4bis^2-2*r1*r4bis*cos(beta_init))<(r_p1-
r3),
        r4bis=r4bis+dl;
    elseif sqrt(r1^2+r4bis^2-
2*r1*r4bis*cos(beta_init))>(r_p1-r3),
        r4bis=r4bis-dl;
    end
end
r4_init=r4bis;
theta_init=asin(r4_init*sin(beta_init)/(r_p1-r3));
hip_init=asin(r1*sin(beta_init)/(d-r3));
zeta=pi-hip_init;

%%%%%%%%%%%%%%%%%%%%%%%%%%%%%%%%%%%%%%%%%%%%%%%%%%%%%%%%%%%%%%%%%%%%%%%%
%Loop computes the configuration of the slot, %
%the backdriving torque fraction, and the rotation %
%of the cam as the weight opens. %

```

```

%%%%%%%%%%%%%%%%%%%%%%%%%%%%%%%%%%%%%%%%%%%%%%%%%%%%%%%%%%%%%%%%%%%%%%%%
i=1;
for th=theta_init:(del_weight/49):(theta_init+del_weight),
    theta(i)=th;
    r2(i)=sqrt(r1^2+d^2-2*r1*d*cos(theta(i)));
    phi(i)=asin(r1*sin(theta(i))/r2(i));
    E(i)=asin(r3*sin(zeta)/r2(i));
    phiminushipp(i)=pi-E(i)-zeta;
    r4(i)=r3*sin(phiminushipp(i))/sin(E(i));
    beta(i)=pi-phi(i)-theta(i)-E(i);
    r4p(i)=(r1*sin(theta(i))/sin(pi-theta(i)-beta(i)))-
r4(i);
    r3p(i)=sqrt(r3^2+r4p(i)^2-2*r3*r4p(i)*cos(pi-zeta));
    phipp(i)=asin(r4p(i)*sin(pi-zeta)/r3p(i));

    F21(i)=1/(r2(i)*(cos(E(i))-mu*sin(E(i))));
    Tc(i)=F21(i)*r1*(sin(beta(i)-pi/2));
    T_open(i)=Tc(i)+mu*sin(beta(i));
    T_close(i)=-Tc(i)+mu*sin(beta(i));

    i=i+1;
end
del_cam=(phipp-phipp(1))*180/pi;

```

```

%%%%%%%%%%%%%%%%%%%%%%%%%%%%%%%%%%%%%%%%%%%%%%%%%%%%%%%%%%%%%%%%%%%%%%%%
%Backdriving curves are plotted, frictionless curve%
%and the friction curve for both the weight opening%
%and closing. These plots are the fraction of cam %
%torque that the cam exerts on the weight. %
%%%%%%%%%%%%%%%%%%%%%%%%%%%%%%%%%%%%%%%%%%%%%%%%%%%%%%%%%%%%%%%%%%%%%%%%
plot(-del_cam,-Tc,-del_cam,-T_open,-del_cam,-T_close);
ylabel('Fraction of cam torque that is backdriving');
xlabel('Cam rotation angle (degrees)');
legend('Frictionless','Opening','Closing');
disp('Press any key to continue')
pause
clf

```

```

%%%%%%%%%%%%%%%%%%%%%%%%%%%%%%%%%%%%%%%%%%%%%%%%%%%%%%%%%%%%%%%%%%%%%%%%
%Backdriving curves are plotted, frictionless curve%
%and the friction curve for both the weight opening%
%and closing. These plots are the actual torque %
%exerted by the cam on each weight. %
%%%%%%%%%%%%%%%%%%%%%%%%%%%%%%%%%%%%%%%%%%%%%%%%%%%%%%%%%%%%%%%%%%%%%%%%
for i=1:50,

```

```

Tc_total(i)=0.5*(T*F21(i)*r1*(sin(beta(i)-pi/2))); %0.5
because there are two weights
T_open_total(i)=Tc_total(i)+mu*sin(beta(i));
T_close_total(i)=-Tc_total(i)+mu*sin(beta(i));
end
plot(-del_cam,-Tc_total,-del_cam,-T_open_total,-del_cam,-
T_close_total);
ylabel('Backdriving Torque per weight(in*lbF)');
xlabel('Cam rotation angle (degrees)');
legend('Frictionless','Opening','Closing');
disp('Press any key to continue')
pause
clf

```

```

%%%%%%%%%%%%%%%%%%%%%%%%%%%%%%%%%%%%%%%%%%%%%%%%%%%%%%%%%%%%%%%%%%%%%%%%
%Calculations pertaining to the torque being %
%generated by the balancing springs and the torque %
%the resulting influence on the backdriving torque %
%on each centrifugal weight. %
%%%%%%%%%%%%%%%%%%%%%%%%%%%%%%%%%%%%%%%%%%%%%%%%%%%%%%%%%%%%%%%%%%%%%%%%
def_init=ls_init-Free_L;
for i=1:50,
    angle1(i)=(angle1_init*pi/180)-(del_cam(i)*pi/180);
    ls(i)=sqrt(r_sp_pin^2+r_sp^2-
2*r_sp_pin*r_sp*cos(angle1(i)));
    angle2(i)=pi-asin(r_sp_pin*sin(angle1(i))/ls(i));

    T_spring(i)=N*((k*((ls(i)-
ls_init)+def_init))+F_init)*r_sp*sin(angle2(i));
    Tc_total_retained(i)=0.5*(T-
T_spring(i))*F21(i)*r1*(sin(beta(i)-pi/2));

T_open_total_retained(i)=Tc_total_retained(i)+mu*sin(beta(i
));
T_close_total_retained(i)=-
Tc_total_retained(i)+mu*sin(beta(i));
end

```

```

%%%%%%%%%%%%%%%%%%%%%%%%%%%%%%%%%%%%%%%%%%%%%%%%%%%%%%%%%%%%%%%%%%%%%%%%
%Plots pertaining to retaining spring torque. %
%The plots are: %
%1. Torque exerted by the retaining springs as a %
% function of cam rotation. %
%2. Bacdriving torque on each of the weights with %
% the balancing springs. %
%3. Comparison of the backdriving curves with and %

```



```

%   without the balancing springs.                                     %
%%%%%%%%%%%%%%%%%%%%%%%%%%%%%%%%%%%%%%%%%%%%%%%%%%%%%%%%%%%%%%%%%%%%%%%%%
plot(-del_cam,T_spring);
xlabel('Cam rotation angle (degrees)');
ylabel('Retaining spring torque');
disp('Press any key to continue')
pause
plot(-del_cam,-Tc_total_retained,-del_cam,-
T_open_total_retained,-del_cam,-T_close_total_retained);
ylabel('Backdriving Torque per weight (in*lb)');
xlabel('Cam rotation angle (degrees)');
legend('Frictionless','Opening','Closing');
disp('Press any key to continue')
pause
plot(-del_cam,-Tc_total_retained,-del_cam,-
T_open_total_retained,-del_cam,-T_close_total_retained);
ylabel('Backdriving Torque per weight (in*lb)');
xlabel('Cam rotation angle (degrees)');
legend('Frictionless','Opening','Closing');
hold;plot(-del_cam,-Tc_total,-del_cam,-T_open_total,-
del_cam,-T_close_total);
disp('Press any key to continue')
hold off;
clf

%%%%%%%%%%%%%%%%%%%%%%%%%%%%%%%%%%%%%%%%%%%%%%%%%%%%%%%%%%%%%%%%%%%%%%%%%
%Perform calculations pertaining to cam retard          %
%angle vs. engine rpm and weight rotation vs.         %
%engine rpm. The engine rpm is calculated based on%
%a torque balance about the pivot point of the        %
%centrifugal weights. The torque balance is given %
%by sum(T)=T_springs+T_backdriving-T_weight=0        %
%%%%%%%%%%%%%%%%%%%%%%%%%%%%%%%%%%%%%%%%%%%%%%%%%%%%%%%%%%%%%%%%%%%%%%%%%
MEASURED_angle=measured_angle*pi/180;
P=polyfit(MEASURED_angle,measured_T,2); %performs quadratic
curve-fit to spring data
DEL_WEIGHT=linspace(0,del_weight,50);
GAMMA=linspace(gamma,(gamma+del_weight),50);
leaf_torque=polyval(P,DEL_WEIGHT); %expands the spring
data based on curve fit
for i=1:50,
    r_bar(i)=sqrt(rc^2+r_p1^2-(2*rc*r_p1*cos(GAMMA(i))));
    THETA1(i)=asin(r_p1*sin(GAMMA(i))/r_bar(i));
    phi_w(i)=(pi/2)-THETA1(i);
    %The following lines compute the cam speed (rad/sec) at
    which the device operates.

```

```

    %The speeds computed are, in order of appearance:
    %1. Frictionless, non-backdriven, non-balanced
operation.
    %2. Frictionless, backdriven, non-balanced operation.
    %3. Backdriven, balanced, opening operation with
friction.
    w(i)=sqrt(leaf_torque(i)/(m*r_bar(i)*rc*cos(phi_w(i))));
%frictionless operation
    if i>=2,
        if w(i)<=w(i-1),
            w(i)=w(i-1);
        end
    end
    w_not_retained(i)=sqrt((leaf_torque(i)-(-
Tc_total(i)))/(m*r_bar(i)*rc*cos(phi_w(i))));
    if i>=2,
        if w_not_retained(i)<=w_not_retained(i-1),
            w_not_retained(i)=w_not_retained(i-1);
        end
    end
    w_open(i)=sqrt((leaf_torque(i)-(-
T_open_total_retained(i)))/(m*r_bar(i)*rc*cos(phi_w(i))));
    if i>=2,
        if w_open(i)<=w_open(i-1),
            w_open(i)=w_open(i-1);
        end
    end
end
%The following loop computes the cam retard vs. engine rpm
for a closing weight
%in a system that has friction, is backdriven, and has
retaining springs. This
%curve could not be computed above because the iteration
process goes from close
%to open (i=1:50) whereas this curve needs to go from open
to close (i=50:-1:1).
for i=50:-1:1,
    w_close(i)=sqrt((leaf_torque(i)+(-
T_close_total_retained(i)))/(m*r_bar(i)*rc*cos(phi_w(i))));
    if i<=49,
        if w_close(i)>=w_close(i+1),
            w_close(i)=w_close(i+1);
        end
    end
end
end
%convert some radian measurements to degrees for analysis

```

```

gamma=GAMMA*(180/pi);
theta1=THETA1*(180/pi);
del_weight=DEL_WEIGHT*180/pi;
%determines engine rpm spread for plotting purposes
rpm=2*(w/(2*pi))*60;
rpm_not_retained=2*(w_not_retained/(2*pi))*60;
rpm_open=2*(w_open/(2*pi))*60;
rpm_close=2*(w_close/(2*pi))*60;

%%%%%%%%%%%%%%%%%%%%%%%%%%%%%%%%%%%%%%%%%%%%%%%%%%%%%%%%%%%%%%%%%%%%%%%%
%Plots predicting device operation.                                     %
%The plots are:                                                         %
%1. Cam retard angle as a function of engine rpm                       %
%   for a system that is frictionless, non-                            %
%   backdriven, and has no balancing springs.                          %
%2. Cam retard angle as a function of engine rpm                       %
%   for a system that is frictionless, backdriven,                    %
%   and has no balancing springs.                                        %
%3. Cam retard angle as a function of engine rpm                       %
%   for both weights opening and closing for a                         %
%   system that has friction, is backdriven, has                       %
%   balancing springs.                                                 %
%%%%%%%%%%%%%%%%%%%%%%%%%%%%%%%%%%%%%%%%%%%%%%%%%%%%%%%%%%%%%%%%%%%%%%%%
plot(rpm,-del_cam);
ylabel('Camshaft Retard Angle (deg.)');
xlabel('Engine RPM');
title('Frictionless, Non-Backdriven, and No Balancing
Springs');
pause
clf
plot(rpm_not_retained,-del_cam);
ylabel('Camshaft Retard Angle (deg.)');
xlabel('Engine RPM');
title('Frictionless, Backdriven, and No Balancing
Springs');
pause
clf
plot(rpm_open,-del_cam,rpm_close,-del_cam,':');
ylabel('Camshaft Retard Angle (deg.)');
xlabel('Engine RPM');
title('Friction, Backdriven, and Balancing Springs');
pause

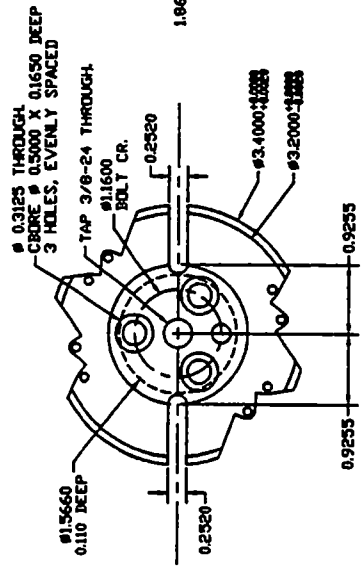
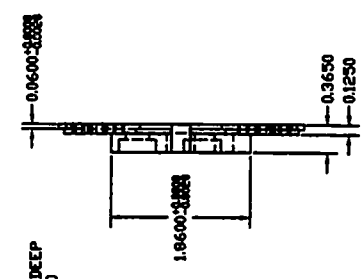
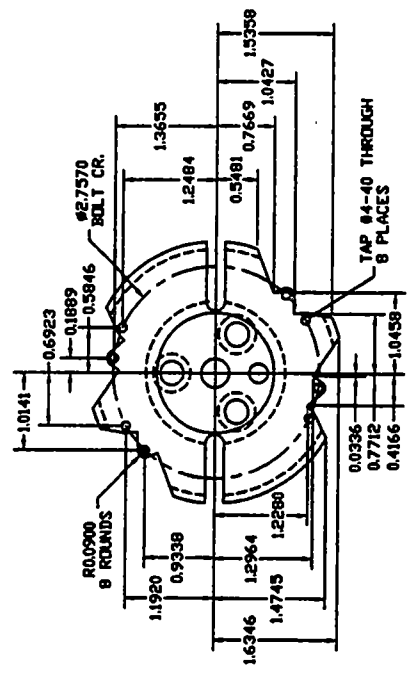
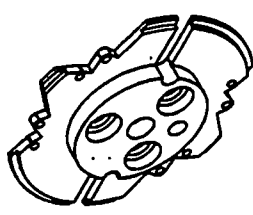
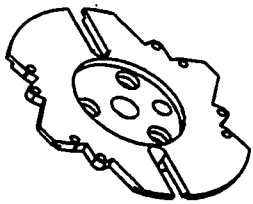
```

APPENDIX D

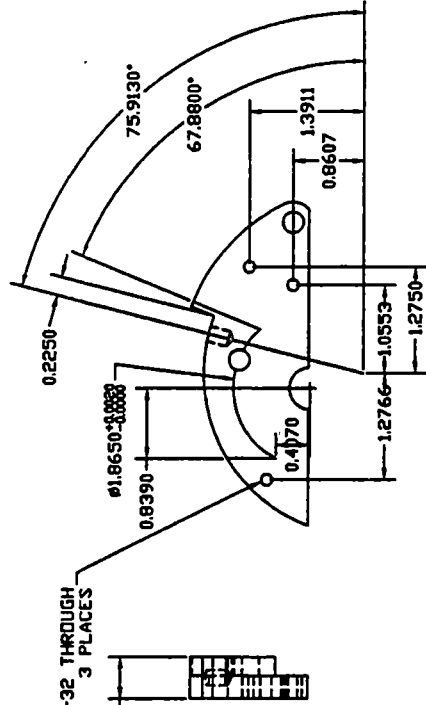
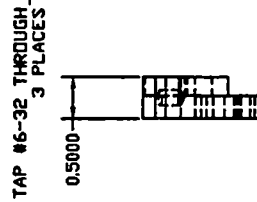
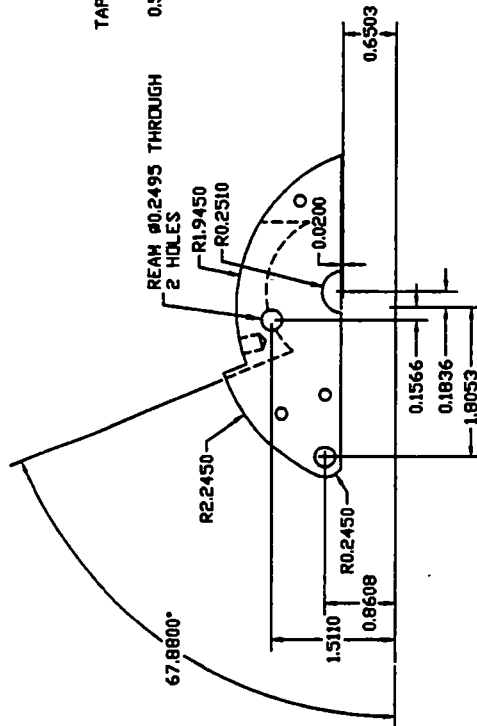
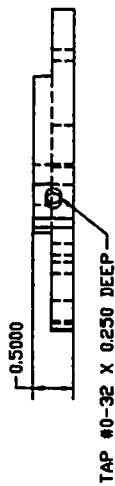
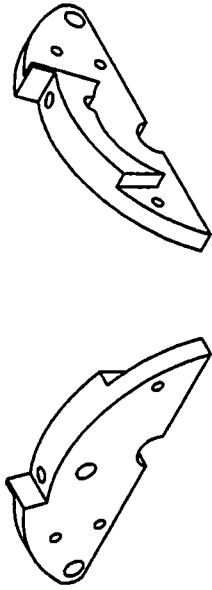
MACHINE DRAWINGS

CONTENTS OF APPENDIX D

D1. Cam Extension	98
D2. Centrifugal Weight	99
D3. Centrifugal Weight Exploded View	100
D4. Weight Cap	101
D5. Sprocket Insert	102
D6. Sprocket Exterior	103
D7. Sprocket Parts and Cam Extension Alignment Drawing	104
D8. Cam Button	105
D9. VCP Device Exploded View	106
D10. Stock Timing Gear, 1987 – Present	107



NOTES	TITLE
ONE PIECE, STEEL	CAM EXTENSION
TOLERANCES UNLESS OTHERWISE SPECIFIED	DRAWN BY
LINEAR: ±0.001	JOHN MCCrackEN
ANGULAR: ±0.01	DATE
	DEC. 1, 1998
	University of Tennessee



NOTES

TWO PIECES REQ'D, STEEL

TOLERANCES UNLESS OTHERWISE SPECIFIED

LINEAR: ±0.001

ANGULAR: ±0.01

TITLE

CENTRIFUGAL WEIGHT

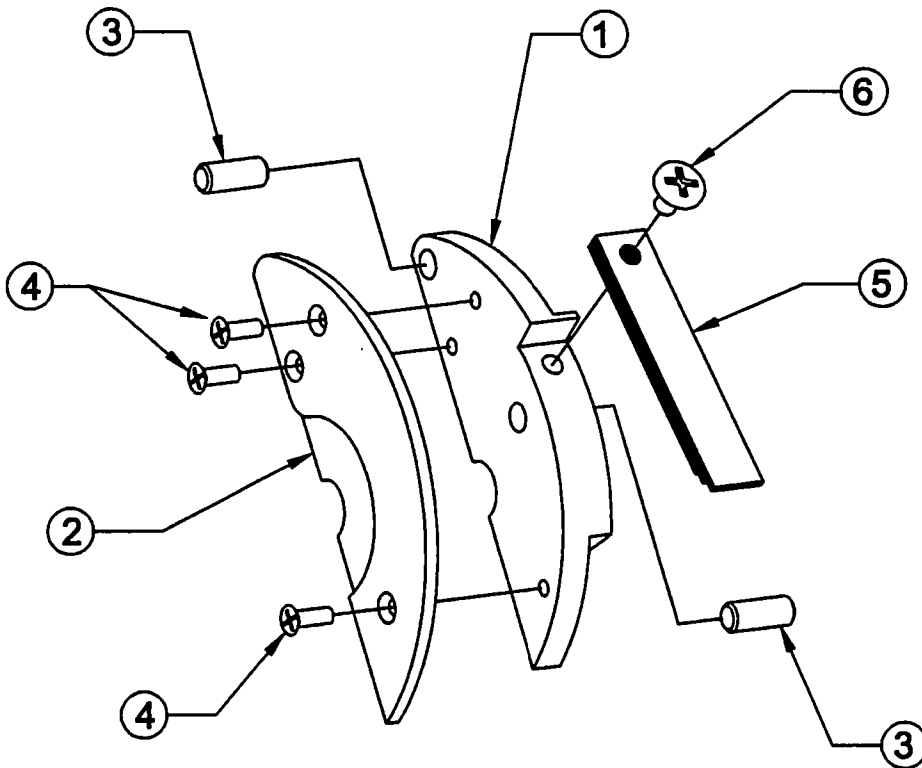
DRAWN BY

JOHN McCRACKEN

DATE

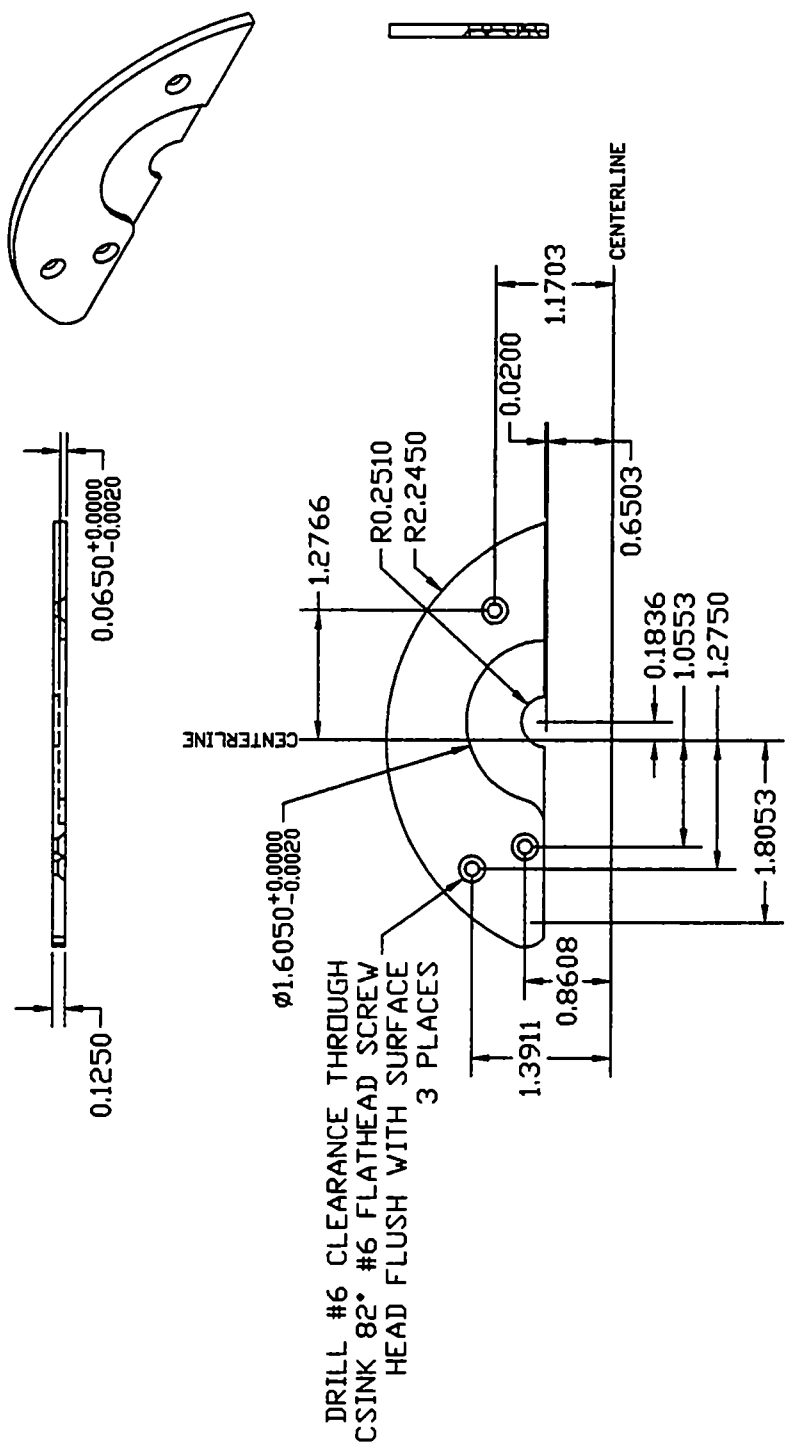
DEC. 19, 1998

University of Tennessee



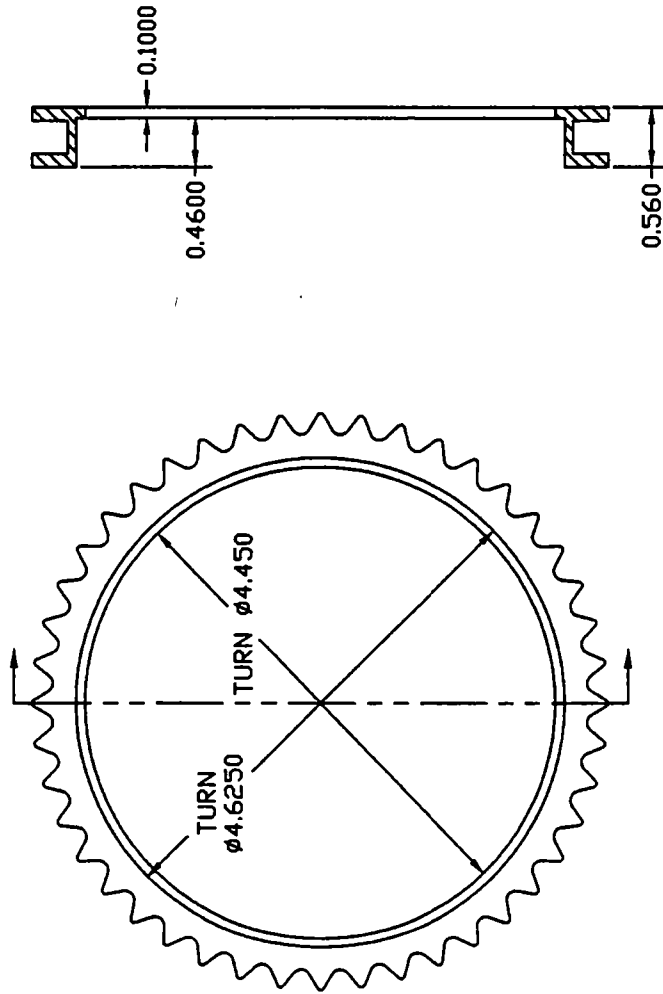
Part No.	Qty.	Description
1	1	Centrifugal Weight
2	1	Centrifugal Weight Cap
3	3	0.250 x 0.625 Dowel Pin
4	3	#6-32 x 0.625 Flathead Machine Screw
5	1	Leaf Spring Pack (Number and length may vary)
6	1	#10-32 x 0.250 Pan Head Machine Screw

NOTES	TOLERANCES UNLESS OTHERWISE SPECIFIED	TITLE
	LINEAR: ±0.001	CENTRIFUGAL WEIGHT EXPLODED VIEW
ANGULAR: ±0.01	DRAWN BY	DATE
	JOHN MCCrackEN	FEB. 25, 1999
	University of Tennessee	

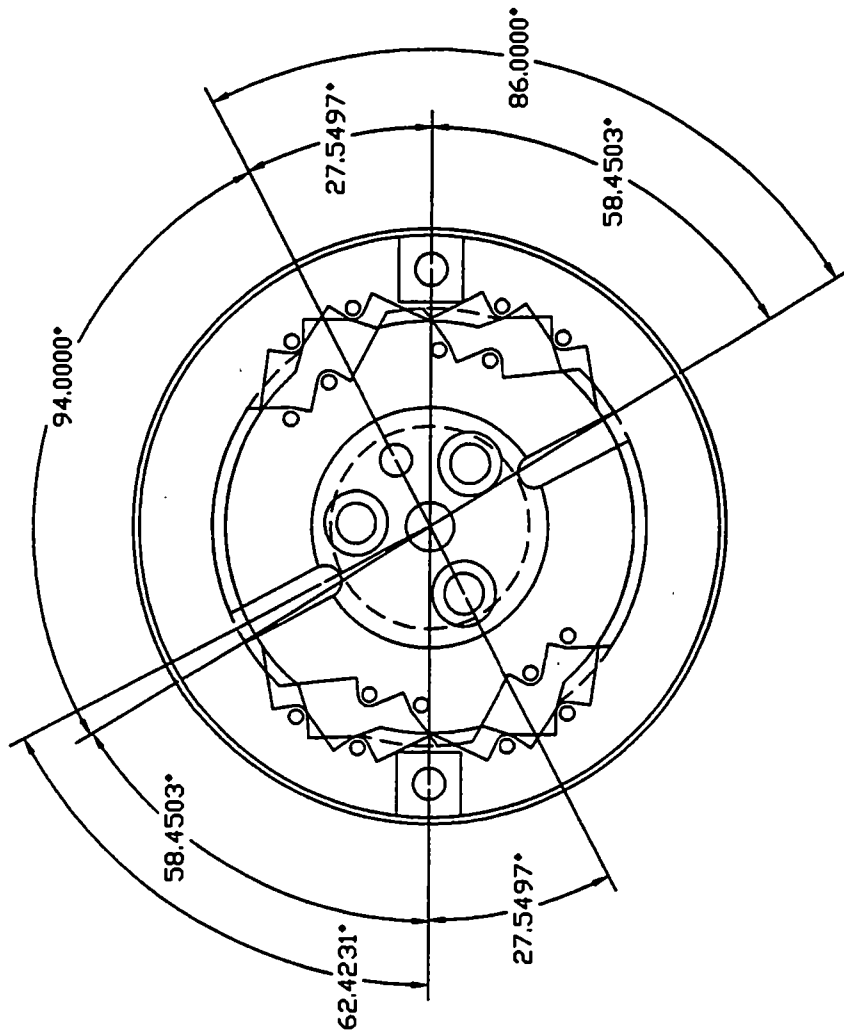


NOTE: 1) 1/8" SHEET STOCK
ACCEPTABLE
2) HAND FILE RADII

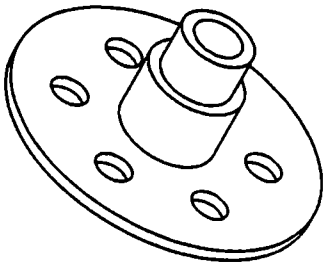
NOTES	TWO PIECES REQ'D, STEEL	TITLE	CENTRIFUGAL WEIGHT CAP	
	TOLERANCES UNLESS OTHERWISE SPECIFIED	DRAWN BY	JOHN McCracken	DATE
	LINEAR: ±0.001			DEC. 1, 1998
	ANGULAR: ±0.01		University of Tennessee	



NOTES	TITLE	
	PROTOTYPE SHRINK FIT SPROCKET TEETH	
MAKE FROM STOCK TIMING SPROCKET TOLERANCES UNLESS OTHERWISE SPECIFIED	DRAWN BY	DATE
LINEAR: ± 0.002 ANGULAR: ± 1	JOHN MCCrackEN	SEP 22, 1998
University of Tennessee		

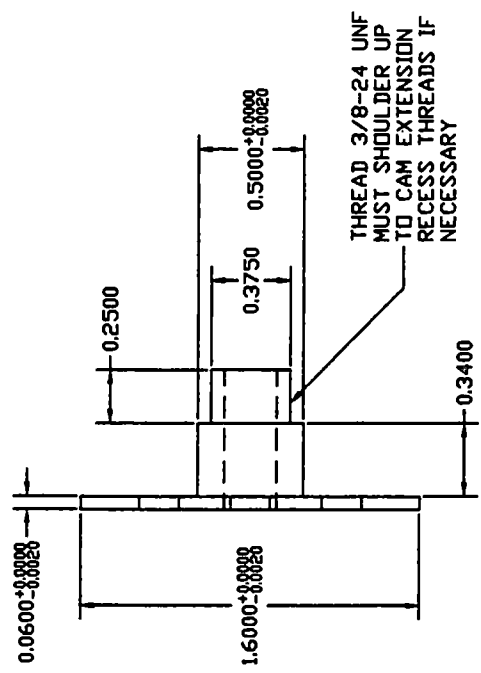
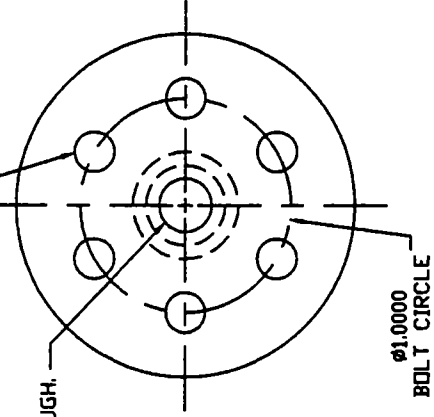


NOTES	MADE FROM STEEL	TITLE	SPROCKET ALIGNMENT
	TOLERANCES UNLESS OTHERWISE SPECIFIED	DIAGRAM	
LINEAR: ±0.001	DATE	DRAWN BY	JOHN McCracken
ANGULAR: ±1			DEC. 18, 1998
		University of Tennessee	

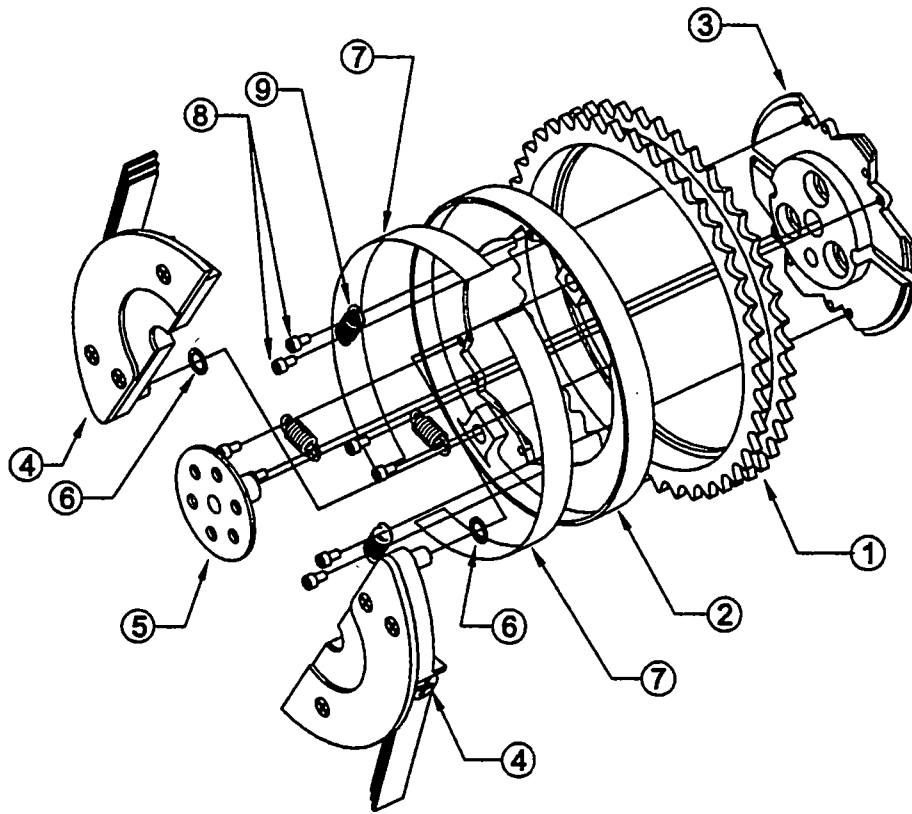


DRILL 0.1875 THROUGH
6 PLACES
EVENLY SPACED

TAP 1/4-20 THROUGH.

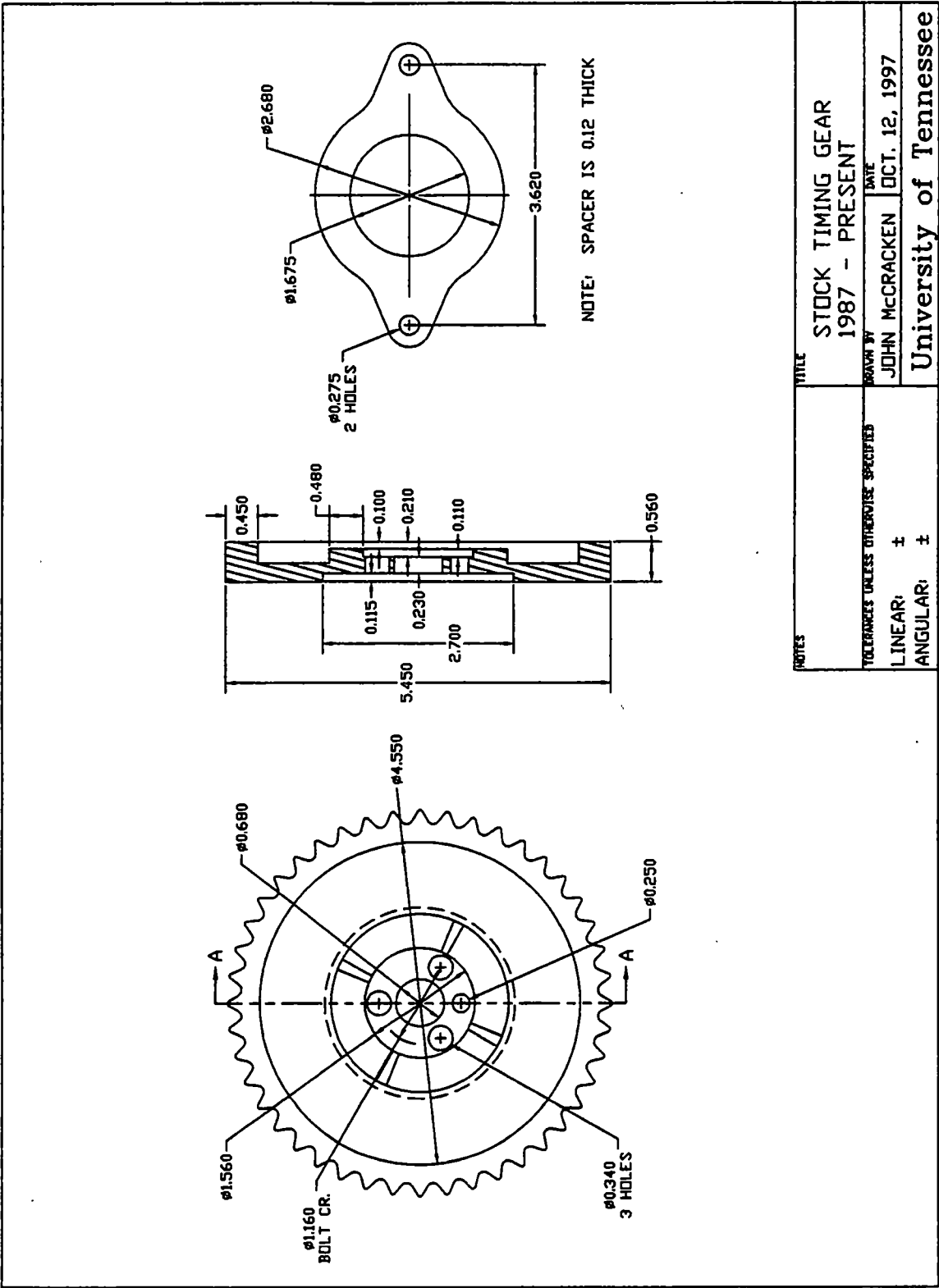


NOTES	TITLE
STEEL, ONE PIECE	CAM BUTTON
TOLERANCES UNLESS OTHERWISE SPECIFIED	DRAWN BY
LINEAR: ±0.001	JOHN McCracken
ANGULAR: ±0.01	DATE
	SEP 18, 1998
	University of Tennessee



Part No.	Qty.	Description
1	1	Sprocket Teeth
2	1	Sprocket Interior (Press-fit Insert)
3	1	Cam Extension
4	2	Centrifugal Weight Assembly
5	1	Cam Button
6	2	0.016" Thick Shim Washer
7	2	0.005" x 0.500" Shim Stock Liner
8	4-16	#4-40 x 0.20" Socket Head Cap Screws
9	2-8	Balancing Spring

TITLE		DATE	
VCP SPROCKET		MARCH 13, 1999	
DRAWN BY		REVISION	
JOHN McCracken		1	
FILENAME		SHEET	
gen2_sprocket.dwg		1 / 1	
MATERIAL / DESCRIPTION			
STEEL			
TOLERANCES UNLESS OTHERWISE SPECIFIED			
LINEAR:		±0.001	
ANGULAR:		±0.01	
NOTES			



NOTES	TOLERANCES UNLESS OTHERWISE SPECIFIED	TITLE
	LINEAR: \pm	STOCK TIMING GEAR
ANGULAR: \pm	DATE	1987 - PRESENT
	DESIGNED BY	JOHN MCCrackEN
	DATE	OCT. 12, 1997
	University of Tennessee	

VITA

John McCracken was born in Kingsport, Tennessee on December 10, 1974 and grew up on a small farm in nearby Gray, Tennessee. He attended Tri-Cities Christian School in Blountville, Tennessee until grade six when he transferred to the Washington County public school system. He graduated from Daniel Boone High School in Gray, Tennessee in 1993, third in a class of 214.

John entered the University of Tennessee in the fall semester of 1993 seeking a Bachelor of Science degree in Mechanical Engineering, which he obtained in August of 1997. He immediately resumed his studies at the University of Tennessee in the fall of that year in pursuit of a Master of Science degree in Mechanical Engineering. During his graduate work, John taught various undergraduate classes including mechanical drawing and a manufacturing process laboratory.

The author is a member of the American Society of Mechanical Engineers and the Society of Automotive Engineers. He enjoys antique automobiles and wildlife management, with his father, Larry McCracken.